OPTIMIZATION OF ASTAXANTHIN ACCUMULATION IN *Haematococcus lacustris* IN A PHOTOBIOREACTOR SYSTEM

by

Aslıhan Yesir

B.Sc. in Molecular Biology and Genetics, Istanbul Medeniyet University, 2021

Submitted to the Institute of Environmental Sciences

in partial fulfillment of the requirements for the degree of

Master of Science

in

Environmental Sciences

Boğaziçi University

2024

OPTIMIZATION OF ASTAXANTHIN ACCUMULATION IN *Haematococcus lacustris* IN A PHOTOBIOREACTOR SYSTEM

APPROVED BY:

Assist. Prof. Dr. Berat Haznedaroğlu . . . . . .
Thesis Advisor

Prof. Dr. Turgay Çakmak . . . . . .

Prof. Dr. Bahar İnce . . . . . .

DATE OF APPROVAL: 29/08/2024

ACKNOWLEDGEMENTS

Every story is unique. Even though this page is not enough, let's start anyway. First of all, I am appreciative of my esteemed advisor Assist. Prof. Dr. Berat Z. Haznedaroğlu for not only guiding my path in the thesis journey, I named "***ASH's Astax Factory***", but also for embracing my excitement every time I went to him with endless "different" ideas and so expanding his trust every time with a sweet smile. The route was more than it appeared, and I believe we will see many more lovely sites together.

I am grateful to Prof. Dr. Turgay Çakmak, who was a part of my thesis jury and more importantly, one of the most important initiators of the story, for hearing what I wanted to do and always supporting the *"**başkan**"*. I would like to thank Prof. Dr. Bahar İnce for her contributions as a thesis jury and for enlightening us despite the difficult pandemic conditions during our education period.

I would like to thank Assoc. Prof. Dr. Ulaş Tezel, one of the gifts of the institution to me, who I respect as a scientist and who consistently shares his lovely energy with me in the leadership of our *"**Wo-hoo**"* campaign. Speaking of gifts, I want to thank Dr. Havva Ateş, who is like a gift in my life and with whom I have shared a lot in a short time.

This paragraph is for the members of IMBIYOTAB: I want to thank the whole crew, especially Dr. Fahri Koray Sakarya, with whom we experienced the most intense periods and who was always there for me with a smile. Dear Duygu Özçelik, Sevda Avcı, Dila Hocaoğlu, Emren Borhan, Arca Yılmaz, Gizem Çetin, Tuna Sürmeli, Zeynep Şahin and Doğukan Parlak… Dear Dr. İrem Karamollaoğlu and Dr. Engin Bayram… I am glad you were there! I also want to thank Fatma Erkoç, who is indispensable to IMBIYOTAB and constantly supports me. I would like to thank our interns who give me hope even with their presence and give me strength by reminding me that I should be a positive role model in front of them. I am glad that you were with us!

My precious family, Nurten Yesir, Cengiz Yesir and Oğuzhan Yesir, I know I have tired you a lot with my constant enthusiasm since the first day I started primary school and my learning adventure. I know thanking you is not enough. One more time “I love you very much!”.

I would like to thank my lovely friends who understand my endless bustle, even sometimes sacrifice our memories, and whose names cannot fit on long pages. My dear Şeymanur Toktaş, you were the closest even when you were far away, you were there even when you were not there. I'm glad that you exist! Furthermore, I would like to convey my gratitude to the heroic character codenamed *"**FT-U-PR**"*, for reminding me that even a tiny candlelight may shed light on a great deal of things.

Thank you for all the challenges (yes, including Kilyos conditions and 59RK) that held my hand, insistently reminded me of who I am, and made me embrace myself with compassion once again! I am also grateful for all the details that have smiled at me even once in my life, prayed for me and added meaning to my life!

Dear me, together we have reached the end of a journey and the beginning of a new day. Thank you for seeing every day in liveable detail and for loving cells so passionately, aka *"**the mother of algae**"*. Always be your own strength before anybody and anything! Let's keep exploring!

ABSTRACT

OPTIMIZATION OF ASTAXANTHIN ACCUMULATION IN *Haematococcus lacustris* IN A PHOTOBIOREACTOR SYSTEM

Astaxanthin is a highly sought keto-carotenoid with numerous health advantages and can either be produced naturally or synthetically. Natural astaxanthin outperforms synthetic by 50-fold, coenzyme-Q10 by 100-1000, and vitamin E by 500-fold in antioxidant and anti-inflammatory properties. Thus, natural astaxanthin remains potent that can be used as a sustainable-safe substitute for synthetics in the cosmetics, nutraceutical, and functional-food industries. *Haematococcus* is one of the most preferred genus for astaxanthin accumulation. In this study, the less-studied *Haematococcus lacustris* CCAP 34/6 strain was evaluated for optimal astaxanthin accumulation, and the obtained extract was presented as the final product in encapsulated form. To achieve this, light, temperature, growth medium and sonication conditions were evaluated under titles divided into two main groups: green and red phases, considering the unique life cycle of the strain. The green phase studies demonstrated a 308.21% increase in biomass in 3N:BBM medium under gradual blue-red-light at 23°C, whereas the red phase studies showed the most rapid astaxanthin accumulation in BG11-N medium at 28°C. Following the acquired data, a biomass concentration of 2.02 g/L and an astaxanthin yield of 2.1% were achieved after large-scale-cultivation in a 6L flat panel photobioreactor. Optimum encapsulation conditions were determined and edible beads with 4 mm and 8 mm diameters containing 1 mg of pure astaxanthin were produced. Overall, the findings of this comprehensive thesis study shed light on astaxanthin production from *H. lacustris* CCAP 34/6 by creating optimal growth conditions and extended to the final encapsulated product.

ÖZET

Haematococcus lacustris'te ASTAXANTHIN BİRİKİMİNİN FOTOBİYOREAKTÖR SİSTEMİNDE OPTİMİZASYONU

Astaksantin, çok sayıda sağlık avantajı sunmasıyla günümüzde talep edilen ve doğal veya sentetik olarak üretilebilen bir keto-karotenoiddir. Doğal astaksantin, sentetik alternatifinden 50 kat, koenzim Q10'dan 100-1000 kat ve E vitamininden 500 kat daha iyi antioksidan ve anti-inflamatuar özelliklere sahiptir. Bu nedenle, doğal astaksantin, kozmetik, nutrasötik ve fonksiyonel gıda endüstrilerinde sürdürülebilir ve güvenli bir alternatif olarak ön plana çıkmaktadır. *Haematococcus*, astaksantin birikimi özelliği sayesinde en çok tercih edilen türlerden biridir. Bu çalışmada, şimdiye kadar literatürde daha az çalışılmış olan *Haematococcus lacustris* CCAP 34/6 suşu, optimum astaksantin birikimi açısından değerlendirilmiş ve elde edilen özüt, kapsüllenmiş formda son ürün olarak sunulmuştur. Bunu gerçekleştirmek üzere ışık, sıcaklık, besiyer ortamı ve sonikasyon koşulları, suşun benzersiz yaşam döngüsü göz önünde bulundurularak yeşil ve kırmızı fazlar olmak üzere iki ana gruba ayrılmış başlıklar altında değerlendirilmiştir. Yeşil faz çalışmaları, 23°C'de kademeli mavi-kırmızı ışık altında, 3N:BBM besiyerinde biyokütlede %308,21'lik bir artış olduğunu ön plana çıkarken, kırmızı faz çalışmaları 28°C'de BG11-N besiyerinde en hızlı astaksantin birikimi olduğunu gösterdi. Elde edilen verilere göre, 6L düz panelli fotobiyoreaktörde büyük ölçekli yetiştirme sonrasında 2,02 g/L'lik bir biyokütle konsantrasyonu ve %2,1'lik bir astaksantin verimi elde edildi. Optimum kapsülleme koşulları belirlendi ve 1 mg saf astaksantin içeren 4 mm ve 8 mm çapında yenilebilir boncuklar üretildi. Sonuç olarak, bu kapsamlı tez çalışmasının bulguları, *Haematococcus lacustris* CCAP 34/6'dan optimum büyüme koşulları oluşturarak ve son kapsüllenmiş ürüne kadar genişletilerek astaksantin üretiminin aydınlatılmasını sağlamıştır.

TABLE OF CONTENTS

ACKNOWLEDGEMENTS iii

ABSTRACT v

ÖZET vi

TABLE OF CONTENTS vii

LIST OF FIGURES x

LIST OF TABLES xiv

LIST OF SYMBOLS/ABBREVIATIONS xvi

1. INTRODUCTION 1

1.1. Astaxanthin 1

1.1.1. Biochemistry of Astaxanthin Molecule 1

1.2. Biological Activity of Astaxanthin from a Human Health Perspective 2

1.2.1. Antioxidant Activity of Astaxanthin 2

1.2.2. Astaxanthin in the Perspective of Diseases: Cardiovascular Disease, Diabetes, Neurodegenerative Diseases, and Cancer 4

1.3. Sources of Astaxanthin 5

1.4. Haematococcus lacustris: As the Major Natural Astaxanthin Source Perspective 7

1.5. The Objective of the Thesis 10

2. LITERATURE REVIEW 13

2.1. Microalgae Cultivation Basics (Specific to Haematococcus) 13

2.2. Astaxanthin Accumulation in Haematococcus and Its Dependence on Intracellular and Extracellular Factors 16

2.2.1. Nutrients 16

2.2.2. Sonication 17

2.2.3. Temperature 19

2.2.4. Light 19

2.3. Downstream Processing 20

2.3.1. Extraction 20

2.3.2. Encapsulation 21
3. MATERIALS AND METHODS 22
3.1. Selection of Algae Strain 22
3.2. Determination of Physiochemical Conditions for Green Phase Cultivation 23
3.2.1. Sonication Tests 23
3.2.2. Multi-Well Plate Study with Several Growth Media 25
3.2.3. Erlenmeyer Flask Study 31
3.3. Determination of Physicochemical Conditions for Red Phase Cultivation 36
3.3.1. Erlenmeyer Flask Study 37
3.4. Large Scale Cultivation 43
3.5. Dry Weight Analyses 46
3.6. Astaxanthin Extraction 48
3.7. Encapsulation 51
3.7.1. Optimization of Encapsulation 51
3.7.2. Encapsulation of Astaxanthin 52
4. RESULTS AND DISCUSSION 55
4.1. Determination of Physicochemical Conditions for Green Phase Cultivation 55
4.1.1. Sonication Tests 55
4.1.2. Multi-Well Plate Study with Several Growth Media 58
4.1.3. Erlenmeyer Flask Study 66
4.2. Determination of Physicochemical Conditions for Red Phase Cultivation 69
4.2.1. Erlenmeyer Flask Study 69
4.3. Large Scale Cultivation 71
4.4. Dry Weight Analyses 78
4.5. Astaxanthin Extraction 79
4.6. Encapsulation 81
4.6.1. Optimization of Encapsulation 81
4.6.2. Encapsulation of Astaxanthin 84

5. CONCLUSIONS AND RECOMMENDATIONS.....87

REFERENCES.....88

LIST OF FIGURES

Figure 1.1. Molecular structure of astaxanthin 1

Figure 1.2. Isomers of astaxanthin (Hinostroza et al., 2004; Bocanegra et al., 2007) (a)3S,3'S; (b)3R,3'R; (c) 3R,3'S, (d) 9-cis-astaxanthin; (e) 13-cis-astaxanthin. 2

Figure 1.3. Synthetic astaxanthin synthesis: (I) Hydroxylation; (II) Oxidation; (III) Wittig reaction 6

Figure 1.4. (A) Light Microscopy Images of the life cycle of *H. pluvialis* 8

Figure 1.4. (B) Flourecent Microscopy Images and Ilustrations of *H. pluvialis* life cycle 8

Figure 1.5. Biochemical pathway for astaxanthin production in *Haematococcus* 9

Figure 1.6. Transcriptomic shift during astaxanthin production of *Haematococcus* 10

Figure 1.7. Experimental summary of the thesis from strain selection to final product 11

Figure 1.8. Integrated Biorefinery, İstanbul Microalgae Biotechnologies Research and Development Unit 12

Figure 2.1. Open photobioreactor systems available at IMBIYOTAB 14

Figure 2.2. Closed photobioreactor systems available at IMBIYOTAB 15

Figure 2.3. Improving nutrient transport in *H. lacustris* by ultrasonication 18

Figure 2.4. An analysis of mRNA expressions in *H. lacustris* cells under ultrasonication and non-ultrasonication conditions 18

Figure 3.1. Light microscope image of *Haematococcus lacustris* CCAP 34/6 strain at different growth stages from left to right, taken at 40X. From left to right: Mature Coccoid Cell, Flagellated Cell, Intermediate Cell, and Red Mature Cyst (aplanospore).....23

Figure 3.2. *Haematococcus lacustris* in self-ventilated culture flask. 24

Figure 3.3. Sonication process of *Haematococcus lacustris* culture at 20%, 30%, 40%, 50%, 60% and 70% power levels.....24

Figure 3.4. Sonication process of *Haematococcus lacustris* culture at 20%, 30%, 40%, 50%, 60% and 70% power levels (Multiwell Plate). 25

Figure 3.5. Multiwell plate study of *Haematococcus lacustris* (CCAP 34/6) under white, blue, and red light conditions. 30

Figure 3.6. The 5L glass bottle photobioreactor (PBR) with aeration (dry air 0.5L/min) and 2000 lux white light for *Haematococcus lacustris* CCAP 34/6 cultivation. Day zero is on the left, and day 3 is on the right. 31

Figure 3.7. Erlenmeyer Flask Study of *Haematococcus lacustris* for green phase optimization. 36

Figure 3.8. The 5L glass bottle photobioreactor (PBR) with aeration for *Haematococcus lacustris* red phase cultivation.....37

Figure 3.9. Erlenmeyer Flask Study of *Haematococcus lacustris* CCAP 34/6 for red phase optimization. 38

Figure 3.10. *Haematococcus lacustris* CCAP 34/6 culture images in 6L Flat Panel PBR. From left to right: illuminated by white, red, and blue light during the green phase. 45

Figure 3.11. 6L Flat Panel PBR and sample images of *Haematococcus lacustris* CCAP 34/6.From left to right: green phase, red phase, and 16th day (the last day) sample of red phase. ..45

Figure 3.12. Stereo Microscope images of *Haematococcus lacustris* CCAP 34/6 in green and red phases (10X). 46

Figure 3.13. *Haematococcus lacustris* CCAP 34/6 harvested culture in the red phase. 47

Figure 3.14. Dry weight determination of *Haematococcus lacustris* CCAP 34/6 harvested culture in the red phase. From left to right: Vacuum filtration unit, a vacuumed sample, filters in an aluminium dish left in the desiccator. 48

Figure 3.15. Chlorophyll removal from *Haematococcus lacustris* CCAP 34/6 culture by KOH+Methanol solution treatment. 49

Figure 3.16. Extraction of astaxanthin from *Haematococcus lacustris* CCAP 34/6 culture by DMSO treatment. 50

Figure 3.17. Astaxanthin + DMSO mixture subjected to lyophilization process (left and middle). Lyophilized astaxanthin powder (right). 52

Figure 3.18. Sodium alginate + astaxanthin mixture 53

Figure 3.19. Astaxanthin+sodium alginate particles formed in 0.3 M $CaCl_2$ solution 53

Figure 3.20. Encapsulated astaxanthin extract in 4 mm and 8 mm diameters. 54

Figure 4.1. Optical density over time graph of *H. lacustris* CCAP 34/6 for four different sonication conditions. 57

Figure 4.2. Optical density over time graph of *H. lacustris* CCAP 34/6 for the conditions 20% and 30%. 57

Figure 4.3. Microscopic images of *H. lacustris* CCAP 34/6 taken at different degrees of sonication. The initial three photos in the initial row, arranged from left to right, depict the culture before sonication (at 40x magnification), the culture subjected to 20% sonication (at 40x magnification), and the culture subjected to 30% sonication (at 10x magnification). The subsequent photos in the second row depict cell bursts occurring in 40%, 50%, 60%, and 70% sonicated cultures (taken 40x) and are given out of order. 58

Figure 4.4. Time-dependent optical density graph of *H. lacustris* CCAP 34/6 strain under sonication (30%), blue+red light, and different growth media conditions. 64

Figure 4.5. Time-dependent optical density graph of *H. lacustris* CCAP 34/6 strain under blue+red light and different growth media conditions. 64

Figure 4.6. Time-dependent optical density graph of *H. lacustris* CCAP 34/6 strain under sonication (30%), white light, and different growth media conditions.....65

Figure 4.7. Time-dependent optical density graph of *H. lacustris* CCAP 34/6 strain under white light, and different growth media conditions.....65

Figure 4.8. Light microscope image of *Haematococcus lacustris* CCAP 34/6 taken at 40x. From left to right: Green Mature Coccoid Cell, Intermediate Cell (transitional cells), and Red Mature Cells. 69

Figure 4.9. Comparison of *H. lacustris* CCAP 34/6 cultures growing in BG11-N medium (front) and BBM-P medium under red phase conditions (back) on day 20.....70

Figure 4.10. Time-dependent red mature cell score graph of *H. lacustris* CCAP 34/6 strain grown under red phase conditions. 70

Figure 4.11. *H. lacustris* CCAP 34/6 strain in the green mature coccoid cell phase before and after large-scale (6L) inoculation.....74

Figure 4.12. Cell phase status of *H. lacustris* CCAP 34/6 strain under red phase stress conditions. 77

Figure 4.13. Change from Day 1 to Day 16 and astaxanthin accumulation of *Haematococcus lacustris* CCAP 34/6 strain in 6L Flat Panel PBR under red phase conditions. 78

Figure 4. 14. Encapsulated form of astaxanthin extracted from *Haematococcus lacustris* CCAP 34/6 strain in 4 mm and 8 mm diameter form 84

Figure 4.15. Instances of alternate plates using encapsulated astaxanthin beads.....85

LIST OF TABLES

Table 3.1. BG11 culture medium ingredients. 26

Table 3.2. MB3N culture medium ingredients. 27

Table 3.3. BBM culture medium ingredients. 28

Table 3.4. 3N-BBM culture medium ingredients. 29

Table 3.5. Multi-well Plate Conditions. The samples in the wells are represented by sections numbered from 1 to 12. Every triplet represents a single condition. The letter B corresponds to the BG11 Medium, the letter M corresponds to the MB3N Medium, the letter X corresponds to the BBM Medium, and the letter N corresponds to the 3N-BBM Medium. 30

Table 3.6. 3P-BBM culture medium ingredients. 32

Table 3.7. Erlenmeyer flask study conditions under 1500 lux white light (the first 18 samples). 34

Table 3.8. Erlenmeyer flask study conditions under 1500 lux blue-red light (the samples ranging 19-36). 35

Table 3.9. BG11+NaCl culture medium ingredients. 39

Table 3.10. BG11-N culture medium ingredients. 40

Table 3.11. BBM-N culture medium ingredients. 41

Table 3.12. BBM-P culture medium ingredients. 42

Table 3.13. Erlenmeyer flask study conditions under 3500 lux blue light (the samples ranging from 01 to 12). 43

Table 4.1. Optical density over time table of *H. lacustris* CCAP 34/6 for five different conditions. 56

Table 4.2. Time-dependent optical density values of *H. lacustri*s CCAP 34/6 strain under sonication (30%), blue+red light, and different growth media conditions. 60

Table 4.3. Time-dependent optical density values of *H. lacustri*s CCAP 34/6 strain under blue+red light and different growth media conditions. 61

Table 4.4. Time-dependent optical density values of *H. lacustri*s CCAP 34/6 strain under sonication (30%), white light, and different growth media conditions.....62

Table 4.5. Time-dependent optical density values of *H. lacustri*s CCAP 34/6 strain under white light, and different growth media conditions.....63

Table 4.6. Time-dependent optical density values of *H. lacustri*s CCAP 34/6 strain for the green phase study. 68

Table 4.7. Summary of red phase transformation of *H. lacustris* CCAP 34/6 strain grown under red phase conditions in different growth media conditions.....71

Table 4.8. Dry weight analysis of *H. lacustris* CCAP 34/6 harvested in the red phase.....79

Table 4.9. Astaxanthin concentration analysis of *H. lacustris* CCAP 34/6 harvested in the red phase. 80

Table 4.10. Alginate and $CaCl_2$ optimization.....82

Table 4.11. Encapsulation temperature optimization.....83

Table 4.12. Astaxanthin amount optimization 83

LIST OF SYMBOLS/ABBREVIATIONS

Symbol	**Explanation**
%	Percent
%DW	Percentage Dry Weight
°C	Degrees Celsius
µM	Micromolar
µm	Micrometer
µmol	Micromole

Abbreviations	**Explanation**
ATP	Adenosine Triphosphate
BBM	Bold's Basal Medium
BBM-N	Nitrogen deficient-Bold's Basal Medium
BBM-P	Phosphorus deficient-Bold's Basal Medium
BG11	Blue Green Medium
BG11-N	Nitrogen-deficient Blue Green Medium
BG11+NaCl	Sodium Chloride Added Blue Green Medium
BKT	β-carotene Ketolase
CAT	Catalase
CCAP	Culture Collection of Algae and Protozoa
BRN	Blue-Red Light Non-Sonicated Culture Condition
BRS	Blue-Red Light Sonicated Culture Condition
cm	Centimeter
DBW	Dry Biomass Weight
DNA	Deoxyribonucleic acid
etc.	Et Cetera
FA	Fatty Acid
g	Gram
g	Standard gravity
h	Hour
H. lacustris	*Haematococcus lacustris*
H. pluvialis	*Haematococcus pluvialis*

Hz	Hertz
IBD	Initial Biomass Density
IRC	Institute of Cancer Research
İMBİYOTAB	İstanbul Microalgae Biotechnologies Research and Development Unit
L	Liter
LDL	Low-Density Lipoprotein
LED	Light-emitting Diode
max	Maximum
MB3N	Modified Bold 3N
3N:BBM	3-Fold Nitrogen-Bold's Basal Medium
mg	Milligram
min	Minute
min	Minimum
minD	Septal Region Determining Protein
mL	Milliliter
mM	Millimolar
nm	Nanometer
OD	Optical Density
OD_{680}	Optical Density at 680 Nanometer Wavelength
3P:BBM	3-Fold Phosphorus-Bold's Basal Medium
PBR	Photobioreactor
RNA	Ribonucleic Acid
RNS	Reactive Nitrogen Species
ROS	Reactive Oxygen Species
rpm	Revolutions per Minute
s	Second
sec	Second
SOD	Superoxide Dismutase
UPW	Ultra-Pure Water
UV	Ultraviolet
v/v	Volume over Volume
w/w	Weight over Weight
WN	White Light and Non-sonicated Culture Condition

1. INTRODUCTION

1.1. Astaxanthin

1.1.1. Biochemistry of Astaxanthin Molecule

Astaxanthin, scientifically known as 3,30-dihydroxy-,-carotene−4,40-dione, is a secondary carotenoid that features an intriguing red colour and is classified as a xanthophyll keto-carotenoid (Higuera-Ciapara et al., 2006; Oslan et al., 2021). Astaxanthin, with the chemical formula C40H52O4 and a molar mass of 596.84 g/mol, is soluble in oil, exists in a solid state at the ambient temperature, and has a melting point of 182.5 ◦C (Jannel et al., 2020). The composition of the astaxanthin is 80.5% carbon, 8.78% hydrogen, and 10.72% oxygen. The molecular structure of astaxanthin is shown in Figure 1.1.

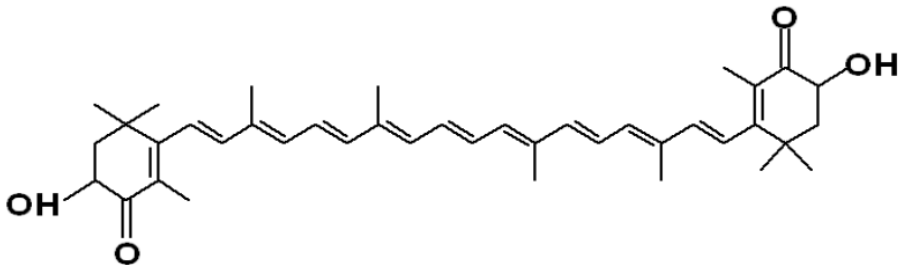


Figure 1.1. Molecular structure of astaxanthin

The tetraterpene astaxanthin is a complex molecule, which contains 40 carbon atoms, has two chirals at its core and exists in many stereoisomers, as shown in Figure 1.1. (Higuera-Ciapara et al., 2006). The presence of 13 double bonds in its structure (Figure 1.2.) enables it to effectively counteract free radicals. Consequently, it effectively eliminates reactive oxygen species (ROS), thereby establishing itself as an outstanding antioxidant compound (Miki, 199; Han et al., 2013).

The astaxanthin molecule is currently produced by either natural or synthetic methods. Multiple studies have demonstrated that the astaxanthin molecule, known for its antioxidant characteristics, has also a prophylactic impact on conditions such as diabetes, cardiovascular illnesses, and cancer, and also provides support to the immunological and neurological systems (Davinelli et al., 2018).

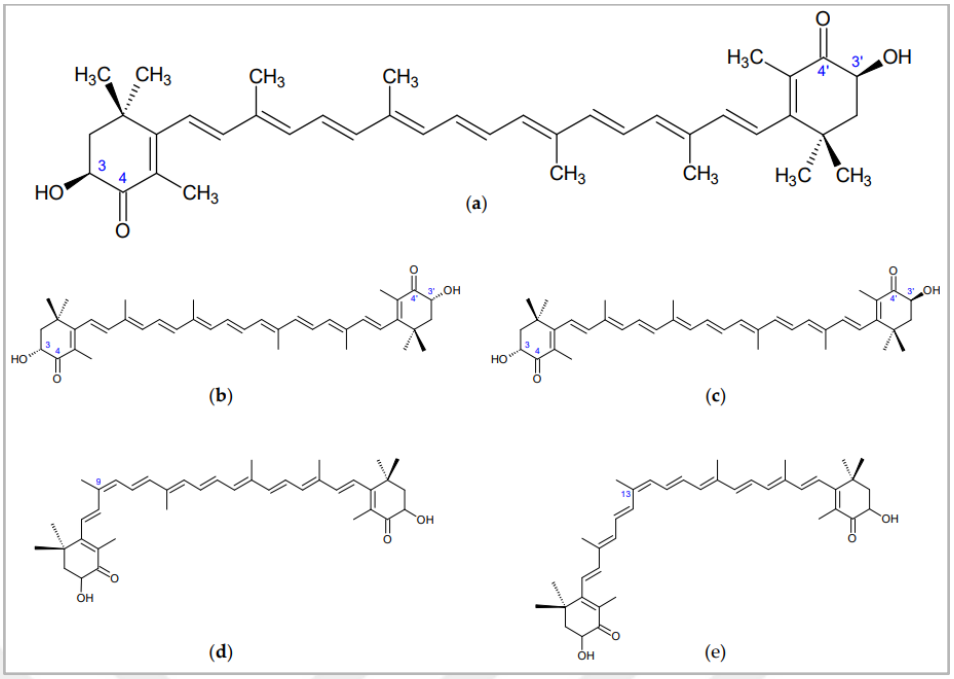


Figure 1.2. Isomers of astaxanthin (Hinostroza et al., 2004; Bocanegra et al., 2007) (a)3S,3'S; (b)3R,3'R; (c) 3R,3'S, (d) 9-cis-astaxanthin; (e) 13-cis-astaxanthin.

Nevertheless, synthetic astaxanthin is included in the diet of fish to enhance the colouration of salmon or ornamental fish, owing to its significant pigmentation characteristics (EFSA FEEDAP Panel, 2005). The astaxanthin molecule, which is produced naturally, has been refined for the food industry for consumption by humans as a dietary supplement (Davinelli et al., 2018; Kang and Sim, 2008).

1.2. Biological Activity of Astaxanthin from a Human Health Perspective

1.2.1. Antioxidant Activity of Astaxanthin

Despite its widespread application in numerous industries like cosmetics, aquaculture, and nutraceuticals, astaxanthin is well recognized for its excellent antioxidant properties. Given its prominent properties, it is also referred to in the literature as the "superstar of antioxidants." (Niizawa et al., 2018).

Astaxanthin can be derived from microalgae, yeast, fungi, certain bacteria, or flowering plants, as well as via synthetic chemical processes. Notwithstanding the prevalence of synthetic astaxanthin in the commercial market, scientific evidence has shown that naturally derived astaxanthin is up to 50 times more potent as an antioxidant than its synthetic equivalent (Capelli et al., 2013). Moreover,

natural astaxanthin demonstrates antioxidant properties that are shown to be 500 times higher than those of vitamin E and 38 times higher than those of β-carotene (Pan-utai et al., 2017). Further research has demonstrated that natural astaxanthin is up to 100 times more potent than coenzyme Q10, a widely recognized antioxidant (Zhang et al., 2018; Zhang et al., 2020).

Astaxanthin is a carotenoid that can inhibit oxidative reactions by scavenging free radicals, thanks to its electron-rich polyene chains. Additionally, since carotenoids are hydrophobic molecules, they embed themselves within the lipid bilayer of cell membranes. This embedding, coupled with the coating of the lipid layer and interaction with the membrane's polar regions, enhances the rigidity of the membrane's fluid phase and restricts the diffusion of oxygen into the hydrophobic regions (McNulty et al., 2007; 2008).

Astaxanthin has demonstrated high antioxidant activity across a broad spectrum of free radicals, reactive oxygen species (ROS), and reactive nitrogen species (RNS) in in vitro studies utilising liposomes. Notably, it has been found to be more effective than other carotenoids, such as α-tocopherol and β-carotene, in scavenging peroxyl radicals. Additionally, astaxanthin exhibits superior efficacy compared to other carotenoids in scavenging hydroxyl radicals, RO2•, and hypochlorous acid (McNulty, Jacob, & Mason, 2008; Naguib, 2000).

Research conducted with human, animal, and cell models has demonstrated that astaxanthin provides effective protective properties against various stress conditions. Studies on the biological effects of astaxanthin reveal its capacity to offer substantial protection under diverse stress scenarios. In cultured cells, astaxanthin has shown significant protective effects against oxidative stress factors such as H2O2 and MPP+(Nakajima et al., 2008; Yang et al., 2011). This protection is attributed to its ability to scavenge radicals as well as to reduce cellular oxidation and free radical production. In animal studies, astaxanthin has been observed to effectively reduce lipid peroxidation and DNA damage (Turkez et al., 2014). In apolipoprotein E-deficient mice, astaxanthin has enhanced antioxidant defence mechanisms and increased the expression of various protective genes. Human studies indicate that astaxanthin lowers LDL oxidation and 8-OHdG levels, and provides protective effects against oxidative damage associated with obesity and smoking (Choi et al., 2011; Kim et al., 2011). These findings underscore astaxanthin’s broad-spectrum antioxidant properties and its potential protective role across different health conditions.

1.2.2. Astaxanthin in the Perspective of Diseases: Cardiovascular Disease, Diabetes, Neurodegenerative Diseases, and Cancer

Astaxanthin is considered a potential therapeutic agent for the treatment of cardiovascular diseases. Supplementation with astaxanthin has been shown to help lower plasma levels by protecting LDL cholesterol from oxidation and enhancing arterial blood flow in individuals at high risk for heart attacks (Iwamoto et al., 2000; Karppi et al., 2007; Miyawaki et al., 2008). Furthermore, there is increasing evidence supporting astaxanthin's protective effects on cardiovascular diseases through its improvement of oxidative stress, inflammation, lipid, and glucose metabolism (Kishimoto, Yoshida, & Kondo, 2016).

Oxidative stress plays a critical role in the pathogenesis of neurodegenerative diseases. It has been suggested that diets rich in antioxidants may have the potential to mitigate the risk of these conditions (Ferrante et al., 1997). Astaxanthin, with its ability to cross the blood-brain barrier, possesses the capacity to attenuate the effects of neurological disorders.

Astaxanthin has the potential to support insulin secretion by reducing oxidative stress caused by hyperglycemia in pancreatic β-cells. Studies conducted with the db/db mouse model have demonstrated that astaxanthin lowers blood glucose levels and preserves the insulin production capability of β-cells (Uchiyama et al., 2002). Similarly, in alloxan-induced diabetic mice, astaxanthin has been shown to reduce hyperglycemia and alleviate oxidative stress in the kidneys (Wang, Chen, & Lu, 2012).

Astaxanthin may enhance insulin sensitivity in type 2 diabetes by reducing insulin resistance and oxidative stress. Research involving high-fructose and high-fat diet-fed mice indicates that astaxanthin reduces oxidative stress and liver inflammation while improving kidney function. Diabetes also impacts the immune system, increasing oxidative damage in neutrophils. Astaxanthin has been shown to partially reverse lipid and protein damage in neutrophils. Additionally, it may prevent diabetic nephropathy, characterized by long-term kidney damage and function loss (Bhuvaneswari, Yogalakshmi, Sreeja, & Anuradha, 2014; Naito et al., 2004; Wang, Chen, & Lu, 2012).

The antioxidant and anti-inflammatory characteristics of astaxanthin indicate its potential efficacy in the prevention of cancer. Several in vitro and in vivo experiments have shown that

astaxanthin might potentially decrease tumour formation by causing cell cycle arrest, facilitating apoptosis, or suppressing cell proliferation (Faraone et al., 2020).

The research carried out on male ICR (Institute of Cancer Research) mice revealed that the treatment of astaxanthin greatly reduced the occurrence of precancerous lesions and neoplasms in the bladder (Tanaka et al., 1994).

Astaxanthin was shown to greatly suppress the migration of breast cancer cells in mammary epithelial cells in a separate in vitro experiment. Moreover, studies have demonstrated that astaxanthin is more potent than β-carotene and lutein in suppressing the growth of breast cancers (Chew et al., 1999; Park et al., 2010).

Another study revealed that the addition of astaxanthin to the diet of BALB/c mice implanted with methylcholanthrene-induced fibrosarcoma (Meth-A tumour) cells led to a notable decrease in both tumour size and weight. Furthermore, studies conducted on F344 rats have shown that diets containing astaxanthin resulted in a decrease in the occurrence of tumours in the intestine and a decrease in cell proliferation (Tanaka et al., 1995).

1.3. Sources of Astaxanthin

As mentioned earlier, astaxanthin can be synthesised either by natural biosynthesis or synthetic methods. Despite the greater prevalence of synthetic astaxanthin in the commercial sector, it is clear that natural astaxanthin outperforms its synthetic equivalent in several dimensions. Scientific studies have demonstrated that the antioxidant potential of natural astaxanthin is up to 50 times higher than that of synthetic astaxanthin (Capelli et al., 2013). Moreover, in regards to its influence on human health, just natural astaxanthin has received approval for inclusion in the food supply (Gateau et al., 2017). As seen in Figure 1.3., the production of synthetic astaxanthin entails a sequence of chemical processes, and the resulting by-products may provide potential health hazards (Capelli et al., 2019).

Astaxanthin was first discovered by Richard Kuhn in lobsters, known scientifically as *Astacus gammarus* (Kuhn & Sörensen, 1938). Subsequent research has revealed that the astaxanthin molecule is found in various microalgae species, including *Haematococcus lacustris* (*Haematococcus pluvialis*), *Chlorella zofingiensis*, and *Chlorococcum sp.*; in the yeast *Phaffia rhodozyma*; in marine bacterial species such as *Paracoccus sp*. and *Paracoccus carotinifaciens*; as well as in flowering

plants like *Adonis aestivalis* (Becker, 2013; Cunningham & Gantt, 2005; Yuan, Peng, Yin, & Wang, 2011).

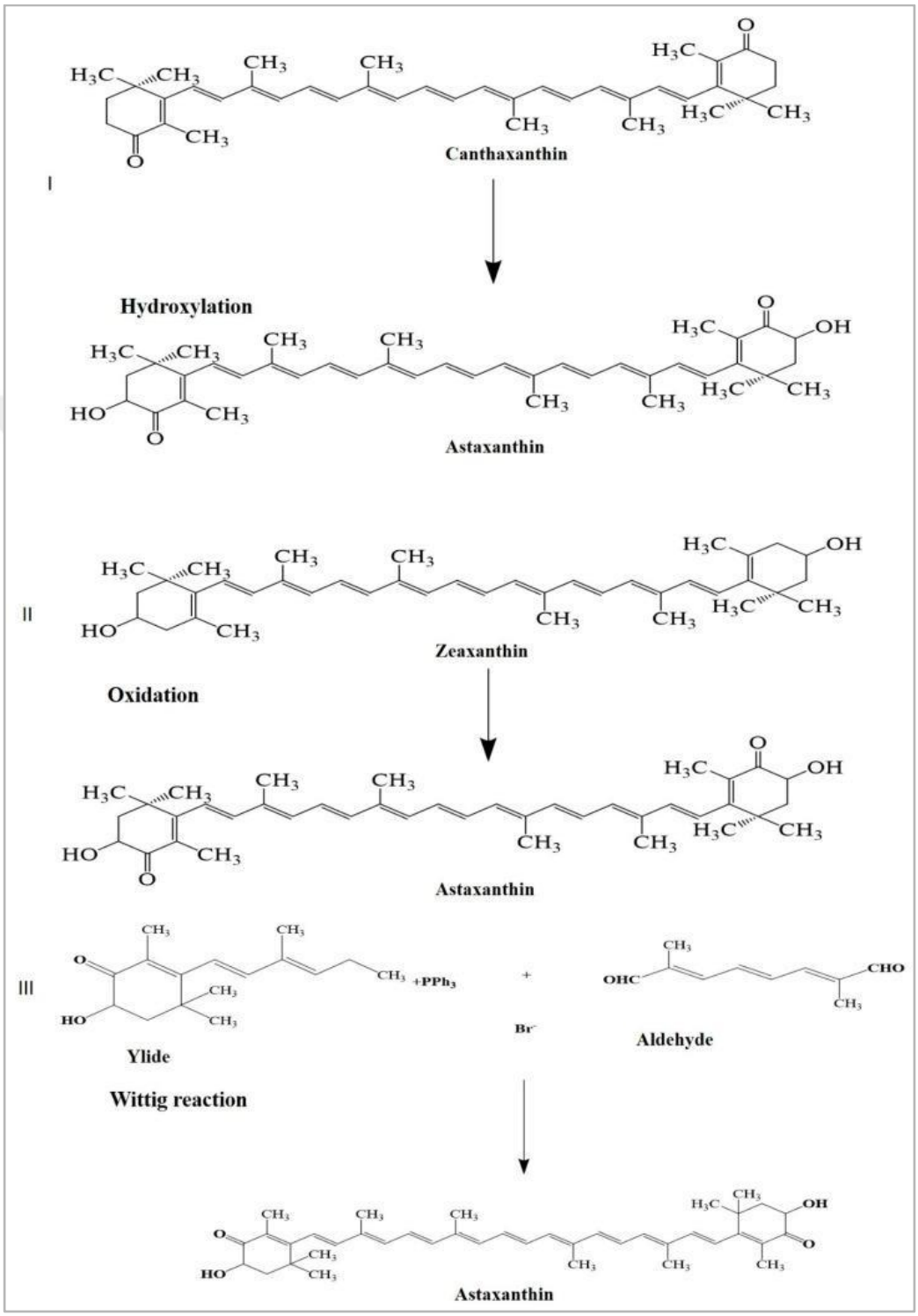


Figure 1.3. Synthetic astaxanthin synthesis: (I) Hydroxylation; (II) Oxidation; (III) Wittig reaction (Nair et al., 2023).

1.4. *Haematococcus lacustris*: As the Major Natural Astaxanthin Source Perspective

The astaxanthin molecule could be produced naturally by various microalgal species, and the manufacture of astaxanthin has been accomplished from many different microalgal species up to this point (Markou & Nerantzis, 2013). *Haematococcus*, on the other hand, has been shown to be the species that has the largest accumulation of astaxanthin and the natural source of the greatest amount of astaxanthin (Li et al., 2011; Peng et al., 2008). This was discovered by a comparison of the astaxanthin content of various species. *Haematococcus* has been steadily acknowledged as a commercial source throughout the course of time (Shah, Liang, Cheng, & Daroch, 2016). This is mostly due to the noteworthy characteristic that it possesses.

Haematococcus lacustris (formerly known as *Haematococcus pluvialis*) is a microalgal species found in temperate regions and grows in natural or artificial freshwater ponds (Nakada & Ota, 2016; Czygan, 1970). *Haematococcus lacustris* possesses a unique life cycle and is capable of synthesizing astaxanthin in response to various stress conditions such as light, temperature, and nutrient depletion (Gao et al., 2012).

J. Von Flotow first identified the *Haematococcus* in 1844, while a detailed study of its biology and life cycle was later conducted by Tracy Elliot Hazen in 1899 (Hazen, 1899; Leonardi, Popovich, & Damiani, 2011). As shown in Figure 1.4.(A-B), the life cycle progresses from the green vegetative motile cell (A) to the green vegetative palmella cell (B). The palmella cells then start accumulating astaxanthin (C) and eventually transform into aplanospores (D) (Shah et al., 2016).

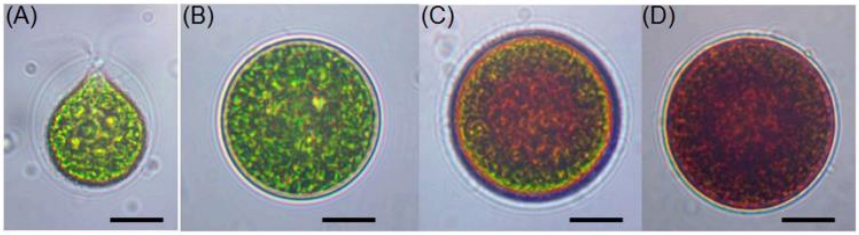


Figure 1.4. (A) Light Microscopy Images of the life cycle of *H. pluvialis* (Shah et al., 2016).

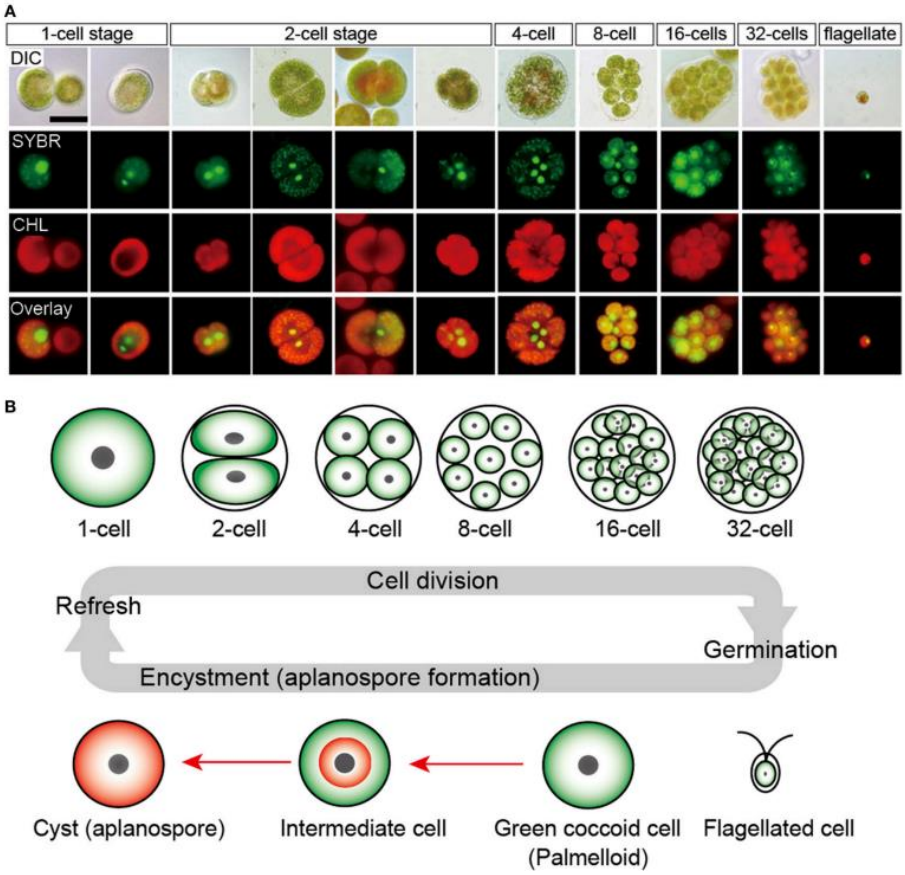


Figure 1.4. (B) Flourecent Microscopy Images and Ilustrations of *H. pluvialis* life cycle (Wayama et al., 2013).

It is possible for *Haematococcus* cells to acquire up to 1% lutein and roughly 20-25% fatty acids in their dry biomass weight (DBW) when they are in the green phase.

Between 1-5% of the dry biomass weight is comprised of astaxanthin during the transition to the red phase, whereas the accumulation of lipids can reach between 32-37% (Molino et al., 2018; Shah, Liang, Cheng, & Daroch, 2016)

In *Haematococcus lacustris*, one of the photosynthesis products is β-carotene. During the green phase, it serves as a precursor molecule for keto-carotenoids in the cytoplasm and chloroplast. The formation of canthaxanthin and echinenone occurs through the oxidation of β-carotene by the β-carotene ketolase (BKT) enzyme. Under stress conditions, β-carotene ketolase genes are upregulated. Following this stage, astaxanthin production is facilitated by the catalysis of canthaxanthin by CrtR-b, leading to its accumulation in the cell (Oslan et al., 2021). As shown in Figure 1.5., the cell follows pathways within the chloroplast and cytosol. Additionally, Figure 1.6. illustrates transcriptomic changes (Ahirwar et al., 2021).

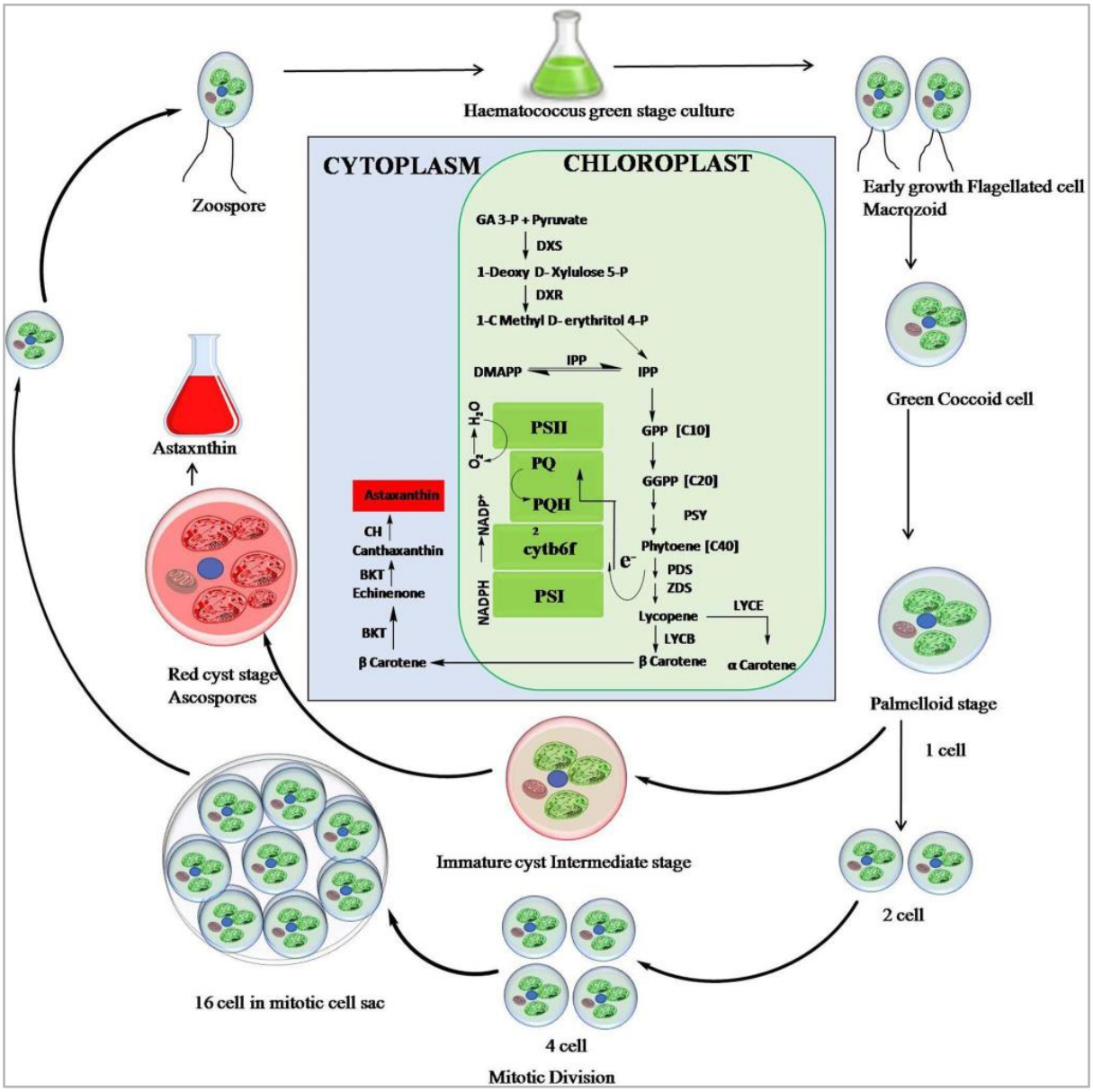


Figure 1.5. Biochemical pathway for astaxanthin production in *Haematococcus* (Ahirwar et al., 2021)

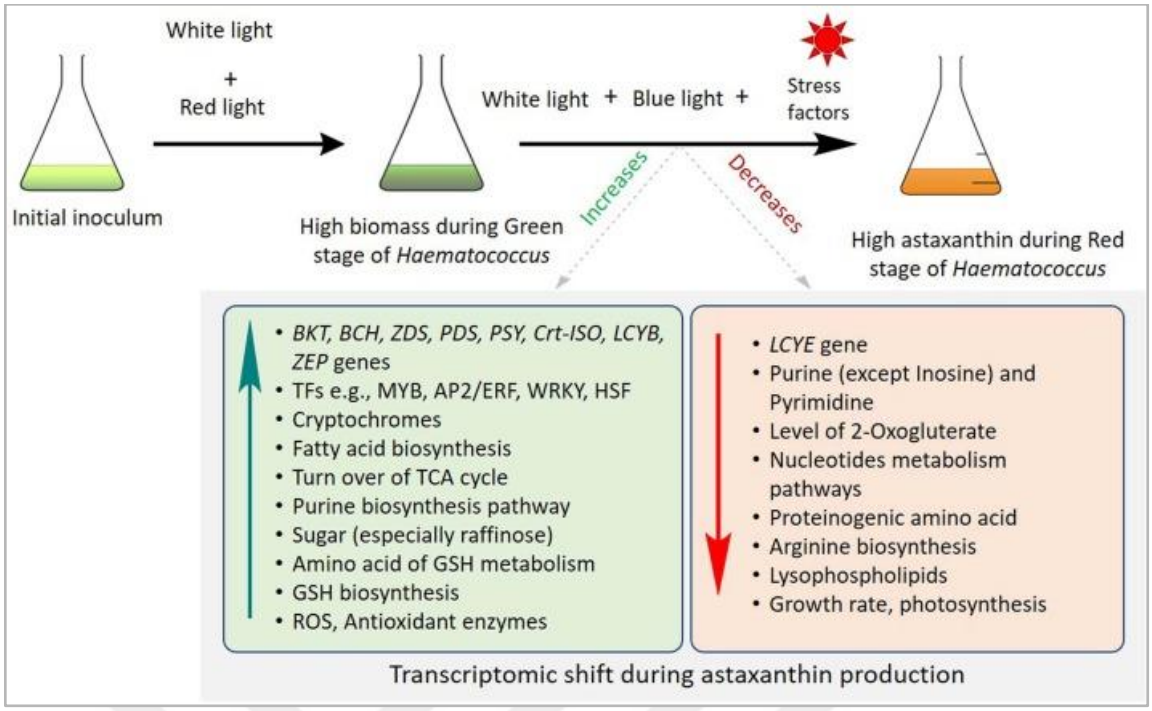


Figure 1.6. Transcriptomic shift during astaxanthin production of *Haematococcus* (Ahirwar et al., 2021)

Taking into account all of these characteristics of *Haematococcus* and presuming that the importance of its natural products is recognized and preferred by consumers, it is projected that the demand for astaxanthin that is generated by this microalga will continue to rise. Therefore, the efforts that are being put into research and development that are contributing to output in this field are of important significance.

1.5. The Objective of the Thesis

The primary motivation of this thesis is to explore all unique phases of *Haematococcus lacustris* cells, which encompass different cell cycle phases throughout their life cycle, and to ensure optimal astaxanthin production under conditions that best preserve cell viability. The purpose of this strategy is to further assist with the development of the astaxanthin molecule naturally and sustainably, which has a multitude of advantages attached to it.

Another focal point of the study is to render the astaxanthin extract obtained under optimal conditions suitable for human consumption. To achieve this, encapsulation optimization has been performed. The experimental summary of the thesis is also provided in Figure 1.7.

Another underlying motivation of the study is to establish a system that adopts an integrated biorefinery approach, aiming for environmentally friendly, sustainable, and economically efficient astaxanthin production. The comprehensive biorefinery strategy will be implemented, with a focus on producing astaxanthin in an environmentally friendly, sustainable, and economically efficient manner. This biorefinery idea seeks to develop a design for cultivating microalgae and extracting astaxanthin, where all raw materials are assessed from the initial growing stage to the production of the final product, resulting in the retrieval of several end products. As shown in Figure 1.8., the plan is to establish an integrated system that encompasses renewable energy from wind turbines in the background, ranging from small-scale cultivation to large-scale cultivation, and culminating in the final product under the human food supplements category.

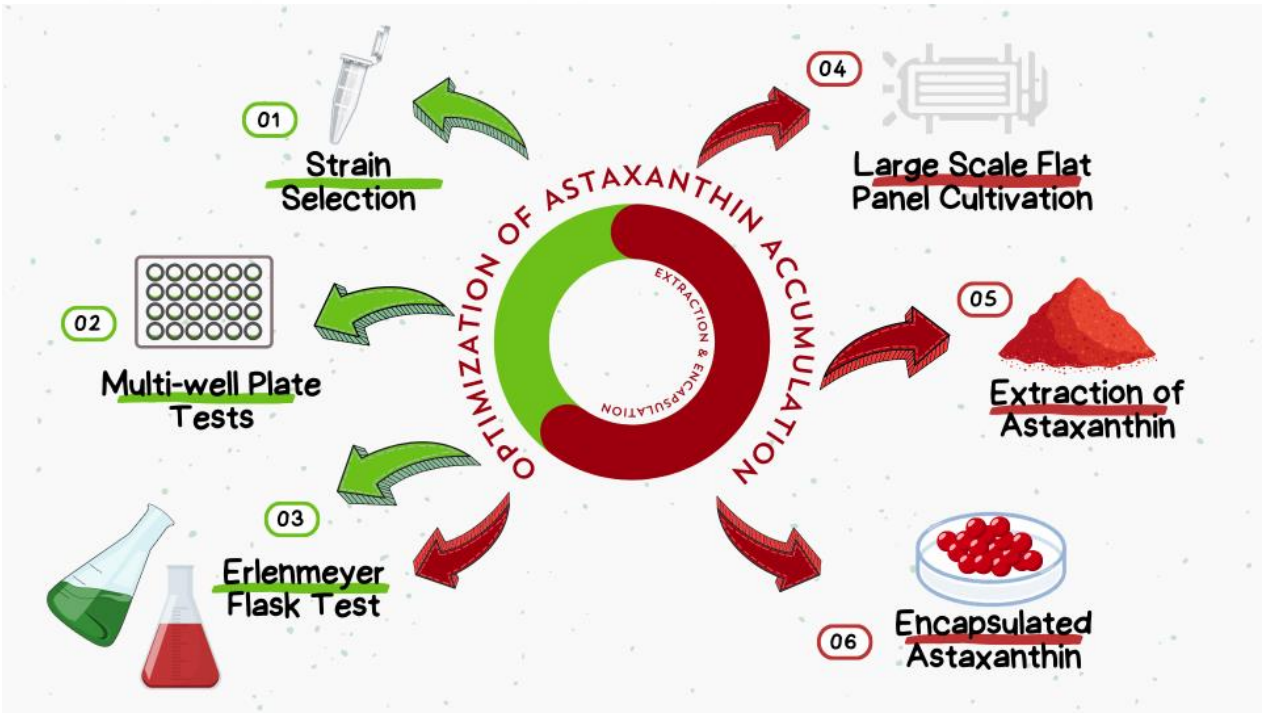


Figure 1.7. Experimental summary of the thesis from strain selection to final product

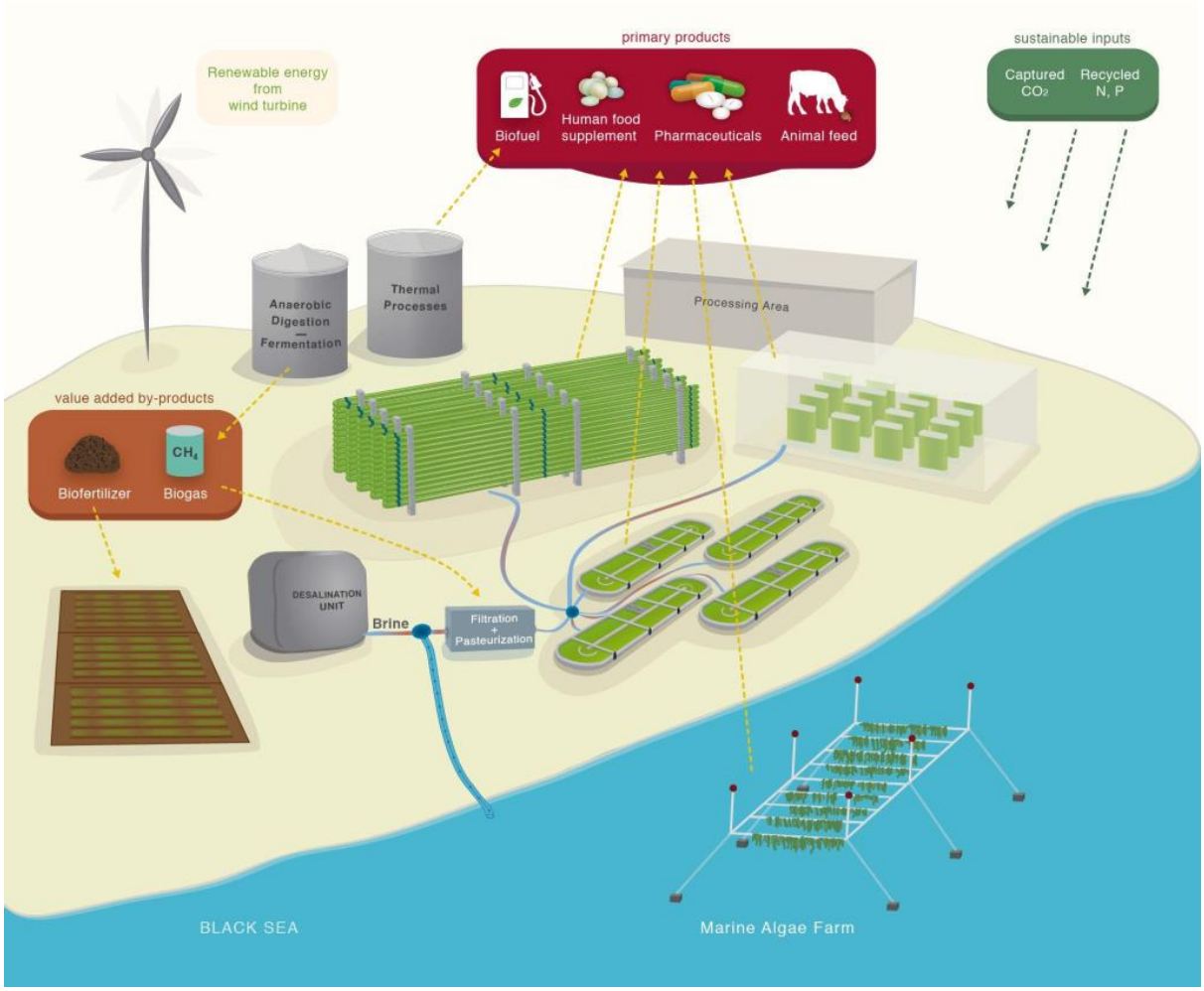


Figure 1.8. Integrated Biorefinery, İstanbul Microalgae Biotechnologies Research and Development Unit

The following chapter will concentrate on the technical intricacies of astaxanthin synthesis from microalgae and analyse the factors that establish the direction for this study.

2. LITERATURE REVIEW

2.1. Microalgae Cultivation Basics (Specific to *Haematococcus*)

Microalgae are unicellular photosynthetic microorganisms that can form filaments and colonies and have high adaptability even to extreme ecological habitats. Microalgae are generally categorized into five primary phyla: *Chlorophyta*, also known as green algae; *Rhodophyta*, or red algae; *Haptophyta*; *Stramenopiles*, which include brown algae and kelp; and *Dinophyta*, commonly referred to as dinoflagellates (Heimann et al., 2015).

These organisms can convert light and carbon dioxide into compounds such as carbohydrates, lipids, vitamins, and carotenoids as a result of photosynthetic reactions (Pulz & Gross, 2004; Eriksen, 2008; Spolaore et al., 2006). Microalgae contribute to over 50% of the world's primary photosynthesis and can thrive under various growth conditions, including autotrophic, heterotrophic, and mixotrophic environments (Jaeronsin & Pumas, 2021; Santos et al., 2019).

The appropriate conditions required for algae growth are achieved in closed or open systems called photobioreactors (PBRs). These PBR systems are complex systems that provide the necessary light source, nutrients, and carbon dioxide for photosynthetic processes, and enable the controlled growth of cell cultures. Experimental studies have demonstrated that the utilisation of closed systems in microalgae production has a positive effect on biomass productivity (Ozcelik et al., 2021). As seen in Figure 2.1. and Figure 2.2., closed tubular and flat panel systems and open raceway pools for microalgae cultivation are possible in İstanbul Microalgae Biotechnologies Research and Development Unit (IMBIYOTAB).

The selection of closed and open systems is based on the specific purpose of the end product. Both have benefits in comparison to one another. In general, open ponds are utilised for commodity items and can handle large amounts, often ranging from 100L to 15000L. Nevertheless, they are more susceptible to contamination and adverse environmental circumstances (Sato et al., 2014; Huo et al., 2017).

Open Photobioreactor Systems

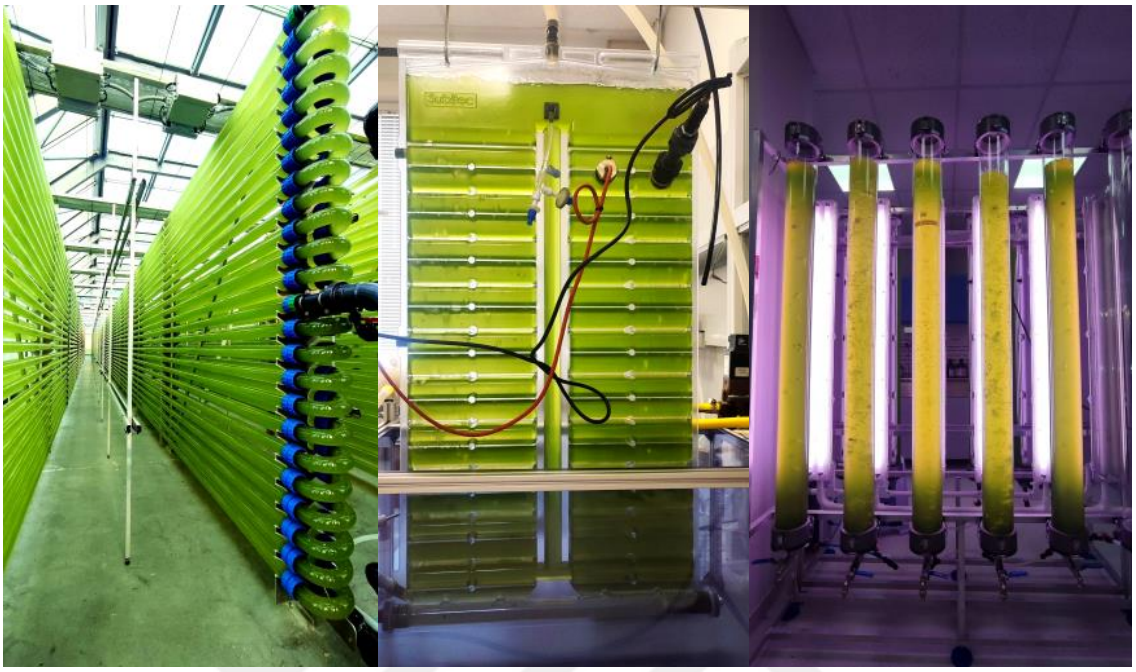


Open Raceway PBR (in volumes of 100L, 1000L, 15000L)

Figure 2.1. Open photobioreactor systems available at IMBIYOTAB

In this thesis, microalgae cultivations were grown using Erlenmeyer flask photobioreactors (PBR), vertical tubular PBR, 15 L glass PBR and flat panel PBRs in both preliminary studies and main experiments. Thus, the desired biomass was obtained from the cultures grown under controlled conditions.

Closed Photobioreactor Systems



Horizontal Tubular PBR | Flat Panel PBR | Phycobubble Vertical Tubular PBR



15 L Glass PBR | Erlenmeyer Flask PBR | Phycobubble Vertical Tubular PBR

Figure 2.2. Closed photobioreactor systems available at IMBIYOTAB

2.2. Astaxanthin Accumulation in *Haematococcus* and Its Dependence on Intracellular and Extracellular Factors

Similar to all other microalgae species, it is important to optimize the culture growth conditions of *Haematococcus.* In this section, intracellular and extracellular factors that play a role in the cultivation of *Haematococcus* and astaxanthin accumulation will be discussed under relevant headings.

2.2.1. Nutrients

The composition of the growth medium is unquestionably one of the criteria that highly influences the development of microalgae cultures. Macronutrients and micronutrients have a crucial role in the development of microalgae and promote the production of different by-products by inducing stress conditions. As fundamental substances, macronutrients like nitrogen and phosphorus directly influence the metabolic activity of cells. Within this particular framework, nitrogen holds a major role due to its involvement in vital cellular processes such as protein synthesis and energy metabolism. Similarly, phosphorus holds crucial importance as it is found in the composition of nucleic acids like deoxyribonucleic acid (DNA) and ribonucleic acid (RNA), as well as in the structure of adenosine triphosphate (ATP) (Weber and Burow, 2018; Karl, 2000).

Nutrients are major determinants of cell proliferation in *Haematococcus lacustris* (previously *Haematococcus pluvialis*) under normal circumstances (green phase) and influence the formation of astaxanthin in the red phase.

An essential constituent of the growth medium, nitrogen regulates enzymatic activity in the green phase, hence influencing growth (Zhang et al., 2018). BG11(Blue Green Medium) Medium, BBM (Bold Basal Medium) and its modified versions in terms of phosphate and nitrogen are among the most commonly used mediums for *Haematococcus*. Oslan et al., (2021) suggested that BBM medium stands out in suitable initial biomass density (IBD) when they compared these two mediums and their modified versions. In another study, Nahidian et al. (2018) reported that they obtained 86% higher growth rate than normal conditions by using a version of normal BBM medium containing 3 times more phosphate with a *Haematococcus* strain isolated from Iran.

The study conducted by Gao et al. (2015) revealed that certain *Haematococcus* species exhibited favourable growth even when exposed to salinity (NaCl) stress levels of up to 0.17M. Hence, when

subjected to the specified salinity stress, there was a decline in cell proliferation accompanied with an elevation in the carotenoid concentration within the cells. Furthermore, Mohamed et al. (2014) undertook investigations that demonstrated the impact of salinity on several strains of *Haematococcus.* The addition of NaCl to the media was found to enhance the proliferation of palmella cells and aplanospore in a separate investigation (Wan et al., 2014).

Furthermore, several investigations have documented that the accumulation of astaxanthin in *H. pluvialis* is significantly enhanced by nitrogen deprivation and prolonged exposure to intense light (Çakmak et al., 2012; Scibilia et al., 2015; Mao et al., 2018). According to Zhao et al. (2019), the cultivation of *H. pluvialis* LUGU strain in BBM medium and nitrogen-deprived BG11 medium yielded the most favourable outcomes in terms of biomass and astaxanthin accumulation.

Considering all these examples and numerous examples in the literature, in this thesis, nitrogen (N) and phosphorus (P) starvation, NaCl effect and BG11 - BBM mediums and their modified forms were included in the experimental matrix for *Haematococcus lacustris* (CCAP 34/6) strain both in green phase and red phase conditions.

2.2.2. Sonication

Given that one of the primary objectives of any new study is to enhance the accumulation of astaxanthin in *Haematococcus lacustris,* it is crucial to devise novel approaches to achieve this goal. Christwardana and Hadiyanto (2017) reported in their study that the audible sound range (20–20,000 Hz) can be effective in the growth of *H. pluvialis*. The study conducted by Ren et al. (2019) has shown that the use of low-level ultrasonic treatment resulted in an enhancement of biomass and lipid accumulation rate in *Scenedesmus* sp. In their study, Han et al., (2022) made a prediction that sonication would be efficacious in promoting microalgal development, specifically targeting *Haematococcus lacustris* cells (Figure 2.3).

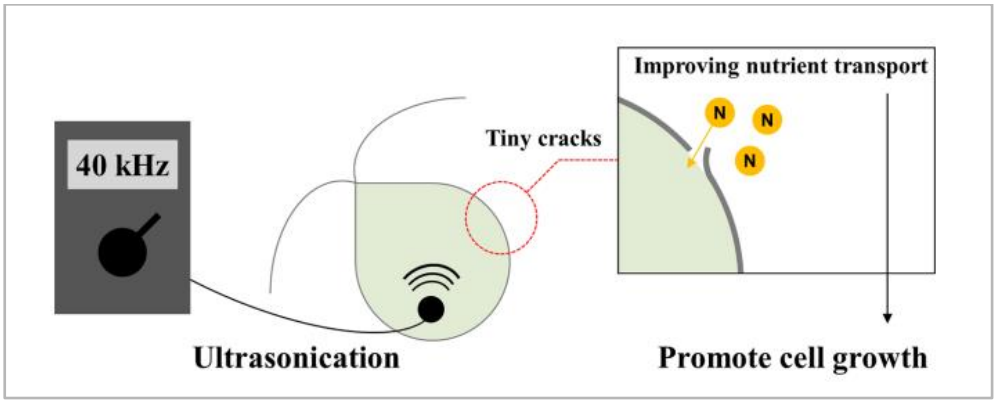


Figure 2.3. Improving nutrient transport in *H. lacustris* by ultrasonication (Han, Jeon, Ahn, & Choi, 2022)

Consequently, they conducted a comparison of the sonication procedures they experimented with at different power levels and demonstrated that a power of 20 W of ultrasonic radiation yielded the most efficient outcome in promoting cell proliferation. Following the sonication treatment, they reported the mRNA gene expression data for the nitrate/nitrite transporter, superoxide dismutase (SOD), catalase (CAT), and septal region determining protein (minD) (Figure 2.4.). Therefore, it was strongly highlighted that sonication might have a significant impact on both the proliferation of cells and the transportation of nutrients in *Haematococcus lacustris.*

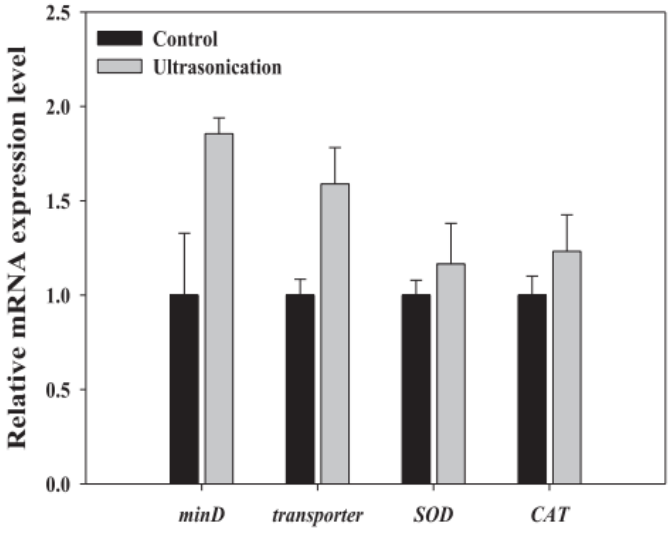


Figure 2.4. An analysis of mRNA expressions in *H. lacustris* cells under ultrasonication and non-ultrasonication conditions (Han, Jeon, Ahn, & Choi, 2022).

Considering the above-mentioned studies, the effect of sonication treatment on the *Haematococcus lacustris* (CCAP 34/6) strain was also included in the experimental matrix in this thesis.

2.2.3. Temperature

Haematococcus lacustris is a microalga found in temperate freshwater environments (Czygan, 1970). Furthermore, similar to other microalgae, *Haematococcus* is similarly responsive to fluctuations in temperature (Giannelli, Yamada, Katsuda, & Yamaji, 2015).

For *Haematococcus*, which develops in two main phases, green and red, many studies in the literature have noted that 20 to 25 ◦C is effective in the growth of cells in the green phase and that temperature values between 15-35 ◦C give optimal results depending on the strain and have a positive effect on astaxanthin accumulation (Giannelli et al., 2015; Tjahjono et al., 1994; Wan et al., 2014).

Nevertheless, the research carried out by Wan et al. (2014) reported that the highest levels of biomass and astaxanthin were achieved at a temperature of 28◦C, whereas cell death was observed at 33◦C. A further investigation conducted by Hong et al. (2015) revealed that the accumulation of astaxanthin in *H. pluvialis* was enhanced under growing conditions ranging from 25 to 28 ◦C.

Considering the studies in question, appropriate temperatures were selected for both green phase biomass production and red phase astaxanthin accumulation strategies for the *Haematococcus lacustris* (CCAP 34/6) strain in this thesis.

2.2.4. Light

Light intensity, along with additional factors, is a crucial determinant of cell development in *Haematococcus* and effectively contributes to the accumulation of astaxanthin. (Li et al., 2019). Indeed, several studies have documented that the most crucial environmental component for cells is exposure to high levels of light (Choi et al., 2002; Pang et al., 2019).

The study conducted by Zhang et al. (2018) revealed a positive correlation between the light intensity and the astaxanthin concentration in cultures exposed to light levels ranging from 50 to 400 $\mu mol/m^2/s$. Likewise, in research conducted by Fábregas et al. (2003) and Choi et al. (2015) that

compared the effects of high and low light intensities, a greater amount of zoospore production was detected under high light conditions.

It is known that *Haematococcus* cells have chlorophyll a and b. In addition to all these studies, it has been reported that intense white light damages chlorophyll-a. Cells are also sensitive to red and blue light due to their chlorophyll a and b (Singh & Singh, 2015). Both blue and red lights have been employed in several investigations involving *Haematococcus.* In a study undertaken by Ma et al. (2018), it was shown that red light had a beneficial impact on cellular proliferation, whereas blue light facilitated the accumulation of astaxanthin. A further investigation showed that red light had a 4.1 and 2.5-fold beneficial impact on cell division, while blue light-induced an increase in cell size (Mehariya et al., 2020).

Considering the above-mentioned studies, in this thesis, white, blue and red light sources were used for both green phase biomass production and red phase astaxanthin accumulation strategies for the *Haematococcus lacustris* CCAP 34/6 strain.

2.3. Downstream Processing

2.3.1. Extraction

Microalgae have complex cell wall compositions. Therefore, mechanical and/or chemical methods are used for the extraction of the desired substance. Various methods are used for astaxanthin extraction from *Haematococcus.* Examples of these methods are solvent extraction, liquid-liquid extraction, microwave-assisted extraction, supercritical carbon dioxide ($scCO_2$) extraction, sonication or high-pressure liquid extraction.

Various organic solvents (such as methanol and ethanol) that can dissolve astaxanthin are used in solvent extraction. In the liquid-liquid extraction method, the separation of dissolved components between two different liquid phases is achieved with the assistance of water and organic solvents. In microwave-assisted extraction, the entry of solvents through the cell wall is facilitated by the microwave effect. Supercritical carbon dioxide ($scCO_2$) extraction is one of the solvent-free extraction types and supercritical CO_2 is used under the effect of high pressure and low temperature and astaxanthin extraction is made possible. In the ultrasonic extraction method, cells are disrupted with ultrasonic waves, thus obtaining the desired extract. High-pressure liquid extraction (HPLS) is

carried out using solvent under high-pressure conditions (Denery et al., 2004; Kim et al., 2016; Ruen-ngam et al., 2010).

Considering the above-mentioned studies, the solvent extraction method performed by Boussiba and Vonshak (1991) and Sun et al., (2017) was used for the extraction of astaxanthin from the *Haematococcus lacustris* CCAP 34/6 strain in this thesis.

2.3.2. Encapsulation

Encapsulation is a crucial technique used in food and nutra/pharmaceutical industries to conserve different bioactive components, including enzymes and cells, or food ingredients by enclosing them in small capsules. This technique ensures the safeguarding of the intended chemical from undesired external factors, such as moisture or heat, which might potentially cause harm. Consequently, the product's stability is enhanced and its shelf life is extended. An alternative objective of this technique is to conceal the unfavourable flavours or smells of the items (Gibbs, Kermasha, Alli, & Mulligan, 1999).

As astaxanthin finds usage in sectors such as food, nutraceuticals, cosmetics, and feed industry, its inadequate stabilisation has emerged as a concerning matter that requires attention. The objective of the study performed by Lin et al. (2016) was to enhance the stability of astaxanthin. As such, spherical beads were produced by introducing the polymer solution (alginate solution) into the calcium chloride solution using the extrusion technique. In this study, factors such as needle size, calcium chloride, alginate concentrations and stirring time were compared and optimized. The stability of astaxanthin was increased by the use of calcium ions and alginate.

In another study by Cáceres et al. (2020), a similar extrusion process was performed with the addition of essential grapefruit oil. It was emphasized that the best encapsulation conditions were 7.4% w/v calcium chloride concentration and 58 minutes of crosslinking time.

Considering the above-mentioned studies, in this thesis, the conditions for encapsulating astaxanthin extract obtained from the *Haematococcus lacustris* CCAP 34/6 strain were optimized.

3. MATERIALS AND METHODS

This chapter encompasses the optimization of algal culture preparation and analysis for astaxanthin production under multiple conditions, ranging from small to large scale. To enhance traceability, the method part is subdivided into seven distinct subsections: Selection of Algae Strain, Determination of Physicochemical Conditions for Green Phase Cultivation, Determination of Physicochemical Conditions for Red Phase Cultivation, Large Scale Cultivation, Dry Weight Analysis, Astaxanthin Extraction, and Encapsulation.

3.1. Selection of Algae Strain

Haematococcus lacustris is a freshwater single-celled green algae belonging to the class Chlorophyceae, order Volvocales and family Haematococcasea. The organism goes through a life cycle that includes four clearly defined phases. During these stages, it has either stationary mature cells or mobile cells with two flagella and can reach up to a size of 30 micrometers (Figure 3.1). The model organism used in this study was, strain CCAP 34/6, and obtained from the Culture Collection of Algae and Protozoa (CCAP, Finland). All studies conducted in this study were performed at the İstanbul Microalgae Biotechnologies Research and Development Unit (IMBIYOTAB) at Boğaziçi University.

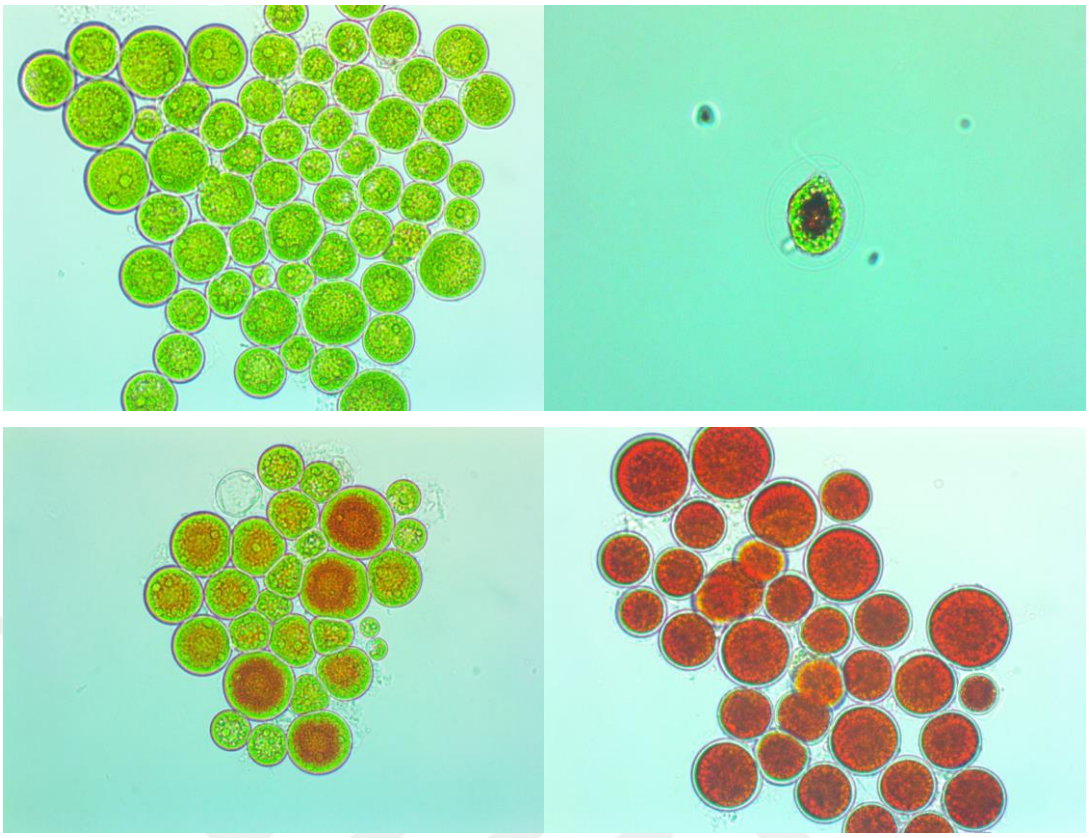


Figure 3.1. Light microscope image of *Haematococcus lacustris* CCAP 34/6 strain at different growth stages from left to right, taken at 40X. From left to right: Green Mature Coccoid Cell, Flagellated Cell, Intermediate Cell, and Red Mature Cyst (aplanospore).

3.2. Determination of Physiochemical Conditions for Green Phase Cultivation

The *Haematococcus lacustris* CCAP 34/6 strain was classified into two primary categories: green phase cultivation, which involves providing the ideal development circumstances for green cells, and red phase cultivation, which emphasizes astaxanthin production. Studies, including sonication, multiwell plate tests, and experiments conducted with 250 ml Erlenmeyer flasks, were carried out to identify the optimal physiochemical conditions for cultivating the green phase.

3.2.1. Sonication Tests

The effect of sonication on cell membrane permeability and cell growth was tested to ensure that the cells can make the most efficient use of their growth medium and uptake the nutrients in the medium at the highest rate. The cells were cultivated in BG11 Medium using self-ventilated culture flasks with a capacity of 75-500 ml (Figure 3.2.). The cultures in the flasks were maintained at a temperature of 25°C, with a light intensity of 1200 lux, and a light: dark cycle of 12 hours of light followed by 12 hours of darkness in a growth chamber (Nüve GC401, Turkey). A sufficient amount

of seed was obtained to begin the experiment. The seed was acquired with an optical density of approximately 0.1 at a wavelength of 680 nm. The culture was placed into 15 ml centrifuge tubes, with a volume of roughly 6-7 ml. The process of sonication was carried out at several power levels, specifically 20%, 30%, 40%, 50%, 60%, and 70%, for a duration of 1 minute for each condition using a sonicator (Bandelin Sonorex & Digitec DL 512 H, Germany) (Figure 3.3.). These percentage values are respectively represent 20%: 43 Hertz, 30%: 64 Hertz, 40%: 86 Hertz, 50%: 107 Hertz, 60%: 129 Hertz and 70%: 150 Hertz.

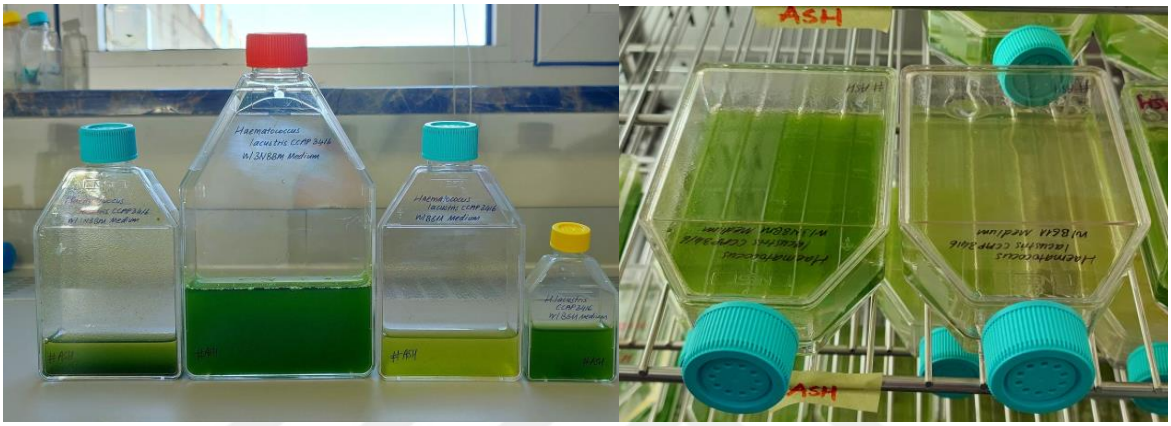


Figure 3.2. *Haematococcus lacustris* in self-ventilated culture flask.



Figure 3.3. Sonication process of *Haematococcus lacustris* culture at 20%, 30%, 40%, 50%, 60% and 70% power levels.

Following sonication, the samples became apparent confirmed with the light microscope. The lysis rates of the cells were compared. Subsequently, each sample was transferred to 12 well-plates, with a working volume of 2 ml, in 3 repetitions (Figure 3.4.). All conditions ranging from 20% to 70% were loaded onto the plate in total volumes of 6ml. Two additional conditions were included as control groups: one using only BG11 Medium and another using both BG11 Medium and culture combined. The 12 well-plates were incubated for 5-6 days at room temperature under 600 lux white

light to promote growth. The progress of cellular development was observed on a regular basis using a plate reader (SpectraMax i3, Molecular Devices, San Jose, CA, USA). The findings were assessed by comparing them to microscope images, and the ideal environment for the subsequent phase was determined.



Figure 3.4. Sonication process of *Haematococcus lacustris* culture at 20%, 30%, 40%, 50%, 60% and 70% power levels (Multiwell Plate).

3.2.2. Multi-Well Plate Study with Several Growth Media

Following sonication of the cell culture and determining the most suitable condition, a multiwell plate study was conducted to assess the impact of various media on cell proliferation. The BG11, MB3N, BBM, and 3N-BBM media, as described in Table 3.1, Table 3.2, Table 3.3, and Table 3.4, respectively, were prepared using aseptic methods. The seeds that were previously cultivated in BG11 media were subjected to centrifugation (U-320 Centrifuge, Boeco, Germany) at 4500 rpm for 5 minutes in order to separate and discard the supernatant. The samples underwent treatment using the chosen mediums. Approximately 50 ml of the culture was sonicated according to the sonication rate determined in the previous step (30%). The samples were transferred on 12-well plates with a working volume of 2 ml. Three replicates of each medium condition were applied to the plates, with a total volume of 6 ml. Plate conditions were duplicated to assess the impact of sonication on culture viability and the influence of various light sources (Table 3.4). Plate-1 and Plate-2 were examined under 600 lux white light at room temperature, whereas Plate-3 and Plate-4 were observed under 600 lux blue+red light (3 days red, 2 days blue+ red, and 4 days blue) at 23°C for 9 days (Figure 3.5). The samples were mixed by pipetting on an ongoing basis, and the data was collected daily, using a plate reader (SpectraMax i3, Molecular Devices, San Jose, CA, USA).

Table 3.1. BG11 culture medium ingredients.

#	Component	Stock solution concentration	Amount	Final concentration (mM)
1	$NaNO_3$	30 g/200mL dH_2O	10 (mL/L)	17.6
2	K_2HPO_4	0.8 g/200mL dH_2O	10 (mL/L)	0.23
3	$MgSO_4.7H_2O$	1.5 g/200mL dH_2O	10 (mL/L)	0.3
4	$CaCl_2.\ 2H_2O$	0.72 g/200mL dH_2O	10 (mL/L)	0.24
5	Citric Acid.H_2O	0.12 g/200mL dH_2O	10 (mL/L)	0.031
6	Ferric Ammonium Citrate	0.12 g/200mL dH_2O	10 (mL/L)	0.021
7	$Na_2EDTA.2H_2O$	0.02 g/200 mL dH_2O	10 (mL/L)	0.0027
8	Na_2CO_3	0.4 g/200 mL dH_2O	10 (mL/L)	0.19
9	BG-11 Trace Metals Solution		1 (mL/L)	
	H_3BO_3		2.86 (g/L)	46
	$MnCl_2.4H_2O$		1.81 (g/L)	9
	$ZnSO_4.H_2O$		0.22 (g/L)	0.77
	$Na_2MoO_4.2H_2O$		0.39 (g/L)	1.6
	$CuSO_4.5H_2O$		0.079 (g/L)	0.3
	$Co(NO_3)_2.6H_2O$		49.4 (mg/L)	0.17

Table 3.2. MB3N culture medium ingredients.

#	**Component**	**Stock solution concentration**	**Amount**	**Final concentration (mM)**
1	$NaNO_3$	10 g/400mL dH_2O	30 (mL/L)	8.82
2	$CaCl2.\ 2H_2O$	1 g/400mL dH_2O	10 (mL/L)	0.17
3	$MgSO_4.7H_2O$	3 g/400mL dH_2O	10 (mL/L)	0.3
4	K_2HPO_4	3 g/400mL dH_2O	10 (mL/L)	0.43
5	KH_2PO_4	7 g/400mL dH_2O	10 (mL/L)	1.29
6	NaCl	1 g/400mL dH_2O	10 (mL/L)	0.43
7	P-IV Metal solution		6 (mL/L)	
	$Na_2EDTA.2H_2O$		0.75 (g/L)	2
	$FeCl_3.6H_2O$		0.097 (g/L)	0.36
	$MnCl_2.4H_2O$		0.041 (g/L)	0.21
	$ZnCl_2$		0.005 (g/L)	0.037
	$CoCl_2.6H_2O$		0.002 (g/L)	0.0084
	$Na_2MoO_4.2H_2O$		0.004 (g/L)	0.017
8	Soil water: GR+ Medium		40 (mL/L)	
9	Vitamin B_{12}		1 (mL/L)	
10	Biotin Vitamin Solution		1 (mL/L)	
11	Thiamine Vitamin Solution		1 (mL/L)	

Table 3.3. BBM culture medium ingredients.

#	Component	Stock solution concentration	Amount	Final concentration (M)
1	$NaNO_3$	2.50 g/100 mL	10 (mL/L)	$2.94 . 10^{-3}$
2	$MgSO_4.7H_2O$	0.75 g/100mL	10 (mL/L)	$3.04 . 10^{-4}$
3	NaCl	0.25 g/100mL	10 (mL/L)	$4.28 . 10^{-4}$
4	K_2HPO_4	0.75 g/100mL	10 (mL/L)	$4.31 . 10^{-4}$
5	KH_2PO_4	1.75 g/100mL	10 (mL/L)	$1.29 . 10^{-3}$
6	$CaCl_2. 2H_2O$	0.25 g/100mL	10 (mL/L)	$1.70 . 10^{-3}$
7	Trace elements solution		1 (mL/L)	
	$ZnSO_4.7H_2O$	8.82 g/L		$3.07 . 10^{-5}$
	$MnCl_2.4H_2O$	1.44 g/L		$7.28 . 10^{-6}$
	MoO_3	0.71 g/L		$4.93 . 10^{-6}$
	$CuSO_4.5H_2O$	1.57 g/L		$6.29 . 10^{-6}$
	$Co(NO_3)_2.6H_2O$	0.49 g/L		$1.68 . 10^{-6}$
8	H_3BO_3	1.14 g/100 mL	1 (mL/L)	$1.85 . 10^{-4}$
9	EDTA-KOH solution		1 (mL/L)	
	$Na_2EDTA.2H_2O$	5.0 g/100 mL		$1.71 . 10^{-4}$
	KOH	3.1 g/100 mL		$5.53 . 10^{-4}$
10	Ferric solution		1 (mL/L)	
	$FeSO_4.7H_2O$	4.98 g/L		$1.79 . 10^{-5}$
	H_2SO_4 conc.	1 mL(to acidify)		
11	Soil extract		50 mL	
12	Vitamin mix		1 mL	
	Vit. B_1 (Thiamine HCl)	0.1 g/100 mL		$2.97 . 10^{-6}$
	Vit. H (Biotin)	0.025 mg/100 mL		$1.02 . 10^{-9}$
	Vit. B_{12} (Cyanocobalamin)	0.015 mg/100 mL		$1.11 . 10^{-10}$

Table 3.4. 3N-BBM culture medium ingredients.

#	Component	Stock solution concentration	Amount	Final concentration (M)
1	$NaNO_3$	2.50 g/100 mL	30 (mL/L)	$2.94 . 10^{-3}$
2	$MgSO_4.7H_2O$	0.75 g/100mL	10 (mL/L)	$3.04 . 10^{-4}$
3	NaCl	0.25 g/100mL	10 (mL/L)	$4.28 . 10^{-4}$
4	K_2HPO_4	0.75 g/100mL	10 (mL/L)	$4.31 . 10^{-4}$
5	KH_2PO_4	1.75 g/100mL	10 (mL/L)	$1.29 . 10^{-3}$
6	$CaCl_2. 2H_2O$	0.25 g/100mL	10 (mL/L)	$1.70 . 10^{-3}$
7	Trace elements solution		1 (mL/L)	
	$ZnSO_4.7H_2O$	8.82 g/L		$3.07 . 10^{-5}$
	$MnCl_2.4H_2O$	1.44 g/L		$7.28 . 10^{-6}$
	MoO_3	0.71 g/L		$4.93 . 10^{-6}$
	$CuSO_4.5H_2O$	1.57 g/L		$6.29 . 10^{-6}$
	$Co(NO3)_2.6H_2O$	0.49 g/L		$1.68 . 10^{-6}$
8	H_3BO_3	1.14 g/100 mL	1 (mL/L)	$1.85 . 10^{-4}$
9	EDTA-KOH solution		1 (mL/L)	
	$Na_2EDTA.2H_2O$	5.0 g/100 mL		$1.71 . 10^{-4}$
	KOH	3.1 g/100 mL		$5.53 . 10^{-4}$
10	Ferric solution		1 (mL/L)	
	$FeSO_4.7H_2O$	4.98 g/L		$1.79 . 10^{-5}$
	H_2SO_4 conc.	1 mL(to acidify)		
11	Soil extract		50 mL	
12	Vitamin mix		1 mL	
	Vit. B_1 (Thiamine HCl)	0.1 g/100 mL		$2.97 . 10^{-6}$
	Vit. H (Biotin)	0.025 mg/100 mL		$1.02 . 10^{-9}$
	Vit. B_{12} (Cyanocobalamin)	0.015 mg/100 mL		$1.11 . 10^{-10}$

Table 3.5. Multi-well Plate Conditions. The samples in the wells are represented by sections numbered from 1 to 12. Every triplet represents a single condition. The letter B corresponds to the BG11 Medium, the letter M corresponds to the MB3N Medium, the letter X corresponds to the BBM Medium, and the letter N corresponds to the 3N-BBM Medium.

PLATE 1			**PLATE 2**			**PLATE 3**			**PLATE 4**		
Light: White			Light: White			Light: Blue+Red			Light: Blue+Red		
Sonication: No			Sonication: Yes (30%)			Sonication: No			Sonication: Yes (30%)		
Temperature: 23°C			Temperature: 23°C			Temperature: 23°C			Temperature: 23°C		
B1	B2	B3	B4	B5	B6	B7	B8	B9	B10	B11	B12
M1	M2	M3	M4	M5	M6	M7	M8	M9	M10	M11	M12
X1	X2	X3	X4	X5	X6	X7	X8	X9	X10	X11	X12
N1	N2	N3	N4	N5	N6	N7	N8	N9	N10	N11	N12



Figure 3.5. Multiwell plate study of *Haematococcus lacustris* (CCAP 34/6) under white, blue, and red light conditions.

3.2.3. Erlenmeyer Flask Study

To validate the earlier phase of determining the optimal medium and wavelength for the species at an expanded volume, an Erlenmeyer flask study was prepared. While sonication and multiwell plate tests were in progress, the seeds grown with BG11 medium in 75 ml culture flasks were grown at room temperature under 2000 lux white light at 680 nm wavelength, reaching an optical density of 0.3 at approximately 5L (Figure 3.6). The resulting seeds were centrifuged (U-320 Centrifuge, Boeco, Germany) at 4500 rpm or 5 minutes to remove the supernatant. The seeds that were obtained were re-dissolved in BG11 and 3N-BBM mediums, as described in Table 3.1 and Table 3.4, respectively. Additionally, an alternative medium condition was added, 3P-BBM Medium, as indicated in Table 3.6.



Figure 3.6. The 5L glass bottle photobioreactor (PBR) with aeration (dry air 0.5L/min) and 2000 lux white light for *Haematococcus lacustris* CCAP 34/6 cultivation. Day zero is on the left, and day 3 is on the right.

Table 3.6. 3P-BBM culture medium ingredients.

#	Component	Stock solution concentration	Amount	Final concentration (M)
1	$NaNO_3$	2.50 g/100 mL	10 (mL/L)	$2.94 \cdot 10^{-3}$
2	$MgSO_4.7H_2O$	0.75 g/100mL	10 (mL/L)	$3.04 \cdot 10^{-4}$
3	NaCl	0.25 g/100mL	10 (mL/L)	$4.28 \cdot 10^{-4}$
4	K_2HPO_4	0.75 g/100mL	30 (mL/L)	$4.31 \cdot 10^{-4}$
5	KH_2PO_4	1.75 g/100mL	30 (mL/L)	$1.29 \cdot 10^{-3}$
6	$CaCl_2. 2H_2O$	0.25 g/100mL	10 (mL/L)	$1.70 \cdot 10^{-3}$
7	Trace elements solution		1 (mL/L)	
	$ZnSO_4.7H_2O$	8.82 g/L		$3.07 \cdot 10^{-5}$
	$MnCl_2.4H_2O$	1.44 g/L		$7.28 \cdot 10^{-6}$
	MoO_3	0.71 g/L		$4.93 \cdot 10^{-6}$
	$CuSO_4.5H_2O$	1.57 g/L		$6.29 \cdot 10^{-6}$
	$Co(NO_3)_2.6H_2O$	0.49 g/L		$1.68 \cdot 10^{-6}$
8	H_3BO_3	1.14 g/100 mL	1 (mL/L)	$1.85 \cdot 10^{-4}$
9	EDTA-KOH solution		1 (mL/L)	
	$Na_2EDTA.2H_2O$	5.0 g/100 mL		$1.71 \cdot 10^{-4}$
	KOH	3.1 g/100 mL		$5.53 \cdot 10^{-4}$
10	Ferric solution		1 (mL/L)	
	$FeSO_4.7H_2O$	4.98 g/L		$1.79 \cdot 10^{-5}$
	H_2SO_4 conc.	1 mL(to acidify)		
11	Soil extract		50 mL	
12	Vitamin mix		1 mL	
	Vit. B_1 (Thiamine HCl)	0.1 g/100 mL		$2.97 \cdot 10^{-6}$
	Vit. H (Biotin)	0.025 mg/100 mL		$1.02 \cdot 10^{-9}$
	Vit. B_{12} (Cyanocobalamin)	0.015 mg/100 mL		$1.11 \cdot 10^{-10}$

The samples were prepared in a 250 ml Erlenmeyer flask with an optical density of 0.1 at a wavelength of 680 nm, with a volume of 100 ml. Each sample condition was prepared as two replicates to be subjected to two distinct light conditions in order to observe the impact of varying light wavelengths. A total of 36 samples, each with a volume of 100 ml, were prepared including 3 identical replicates to obtain exact data and 2 replicates for 2 distinct light conditions.

Every sample was assigned a label to indicate the condition that was being examined (Table 3.7-Table 3.8.). The flasks were partitioned into 18 by 18 using a solid divider. They were then positioned in a setup that provided them with light sources and exposed them to constant shaking (3017, Lauda Gesellschaft für Labortechnik mbH, Germany) at a speed of 85-90 rpm during the experiment (Figure 3.7).

The experiment took place in an environment with a constant temperature of 23°C, which was monitored daily using a thermometer. The samples depicted on the left side in Figure 3.7 were exposed to white light at an intensity of 1500 lux, with equal periods of light and darkness (12 hours: 12 hours). The samples on the right side of the same figure were exposed to red light for 2 days, red+blue light for 2 days, and blue light for 6 days under half light-half dark (12h:12h) conditions at 1500 lux. These conditions were applied for 10 days and monitored daily by manual sampling.

In accordance with the data collected thus far, seeds were cultivated for red phase studies under optimal circumstances.

Table 3.7. Erlenmeyer flask study conditions under 1500 lux white light (the first 18 samples).

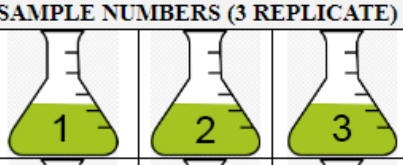
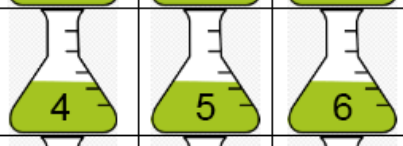
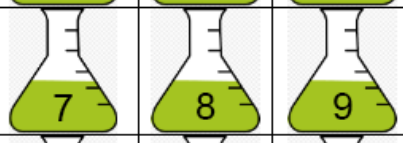
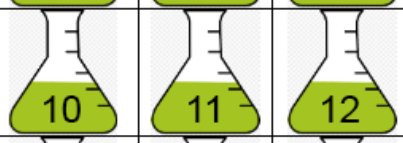
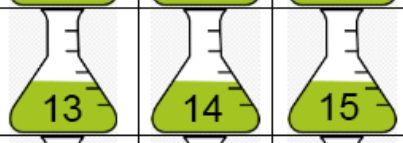
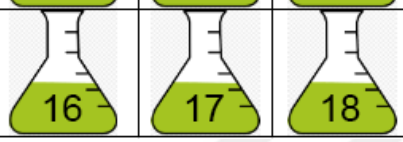
SAMPLE NUMBERS (3 REPLICATE)	CONDITIONS & PARAMETERS	SAMPLE ID
	**LIGHT:** White **SONICATION:** Non-Sonicated **MEDIUM:** BG11 Medium	**WN-BG11-01** **WN-BG11-02** **WN-BG11-03**
	**LIGHT:** White **SONICATION:** Non-Sonicated **MEDIUM:** 3N-BBM Medium	**WN-3NBBM-01** **WN-3NBBM-02** **WN-3NBBM-03**
	**LIGHT:** White **SONICATION:** Non-Sonicated **MEDIUM:** 3P-BBM Medium	**WN-3PBBM-01** **WN-3PBBM-02** **WN-3PBBM-03**
	**LIGHT:** White **SONICATION:** Sonicated (30%) **MEDIUM:** BG11 Medium	**WS-BG11-01** **WS-BG11-02** **WS-BG11-03**
	**LIGHT:** White **SONICATION:** Sonicated (30%) **MEDIUM:** 3N-BBM Medium	**WS-3NBBM-01** **WS-3NBBM-02** **WS-3NBBM-03**
	**LIGHT:** White **SONICATION:** Sonicated (30%) **MEDIUM:** 3P-BBM Medium	**WS-3PBBM-01** **WS-3PBBM-02** **WS-3PBBM-03**

Table 3.8. Erlenmeyer flask study conditions under 1500 lux blue-red light (the samples ranging 19-36).

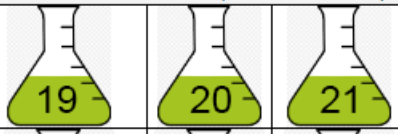
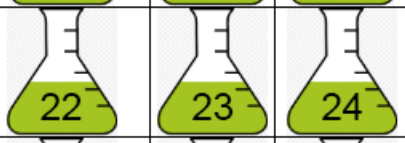
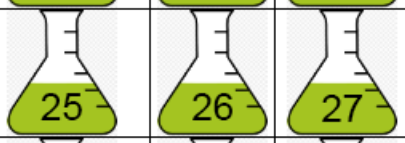
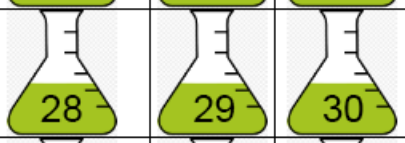
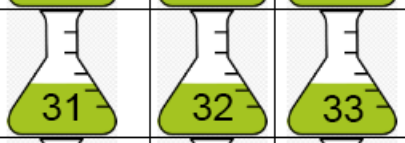
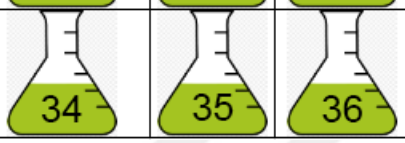
SAMPLE NUMBERS (3 REPLICATE)	CONDITIONS & PARAMETERS	SAMPLE ID
	**LIGHT:** Blue-Red **SONICATION:** Non-Sonicated **MEDIUM:** BG11 Medium	**BRN-BG11-01** **BRN-BG11-02** **BRN-BG11-03**
	**LIGHT:** Blue-Red **SONICATION:** Non-Sonicated **MEDIUM:** 3N-BBM Medium	**BRN-3NBBM-01** **BRN-3NBBM-02** **BRN-3NBBM-03**
	**LIGHT:** Blue-Red **SONICATION:** Non-Sonicated **MEDIUM:** 3P-BBM Medium	**BRN-3PBBM-01** **BRN-3PBBM-02** **BRN-3PBBM-03**
	**LIGHT:** Blue-Red **SONICATION:** Sonicated (30%) **MEDIUM:** BG11 Medium	**BRS-BG11-01** **BRS-BG11-02** **BRS-BG11-03**
	**LIGHT:** Blue-Red **SONICATION:** Sonicated (30%) **MEDIUM:** 3N-BBM Medium	**BRS-3NBBM-01** **BRS-3NBBM-02** **BRS-3NBBM-03**
	**LIGHT:** Blue-Red **SONICATION:** Sonicated (30%) **MEDIUM:** 3P-BBM Medium	**BRS-3PBBM-01** **BRS-3PBBM-02** **BRS-3PBBM-03**



Figure 3.7. Erlenmeyer Flask Study of *Haematococcus lacustris* for green phase optimization.

3.3. Determination of Physicochemical Conditions for Red Phase Cultivation

Following the completion of green phase studies in the *Haematococcus lacustris* CCAP 34/6 strain, studies were carried out to maximize astaxanthin production in the red phase. The studies were conducted under the Erlenmeyer flask study, which involved varying media, temperature, light intensity, and initial biomass density.

3.3.1. Erlenmeyer Flask Study

In order to be utilized in the red phase study, the seeds were initially cultivated in a 5L glass bottle photobioreactor (PBR) under the most favourable conditions determined during the green phase experiments (Figure 3.8.). To enhance the formation of astaxanthin in the red phase, stress conditions were induced by manipulating the media composition, ambient temperature, and light intensity.

BG11 medium with salinity stress (BG11+ 0.17 M NaCl), BG11-N and BBM-N with nitrogen stress, and BBM-P with phosphorus stress were prepared under aseptic conditions. Using media mentioned in Table 3.9, Table 3.10, Table 3.11, and Table 3.12, each sample was prepared in a 250 ml Erlenmeyer in a volume of 100 ml and at a wavelength of 680 nm so that the initial biomass density would be 0.5. Each sample was prepared in 3 replicates and labelled according to the conditions it represented (Table 3.13.). A total of 12 samples, each with a volume of 100 ml, were prepared.



Figure 3.8. The 5L glass bottle photobioreactor (PBR) with aeration for *Haematococcus lacustris* red phase cultivation.

The flasks were subsequently positioned in an arrangement where they were exposed to light sources and consistently shaken (3017, Lauda Gesellschaft für Labortechnik mbH, Germany) at a speed of 85 rpm during the whole period of the experiment (Figure 3.9). The 3500 lux white and blue

light sources were progressively switched and remained on constantly. The first 3 days consisted of white and blue light, whereas the next days consisted of blue light solely.

The experimental setup was gradually acclimated from 23°C to 28°C at one-day intervals and then maintained at a constant temperature of 28°C for the duration of the experiment. The study was conducted over a duration of 20 days, including daily taking of manual samples. The samples were observed using a light microscope, and the rate at which cells changed colour from green to red was monitored on a hemocytometer (0.0025m^2-100mm, Counting Chamber, ISOLAB, Germany). Cells were categorised and counted as green mature cells, transition cells (green+red), and red mature cells. The counted and categorised cells were allocated a cell score, wherein transitional cells received a value at least twice that of green cells, and red cells were assigned a value at least 1.5 times that of transitional cells. The culture exhibiting the most rapid red colouration was identified based on the scores obtained.



Figure 3.9. Erlenmeyer Flask Study of *Haematococcus lacustris* CCAP 34/6 for red phase optimization.

Table 3.9. BG11+NaCl culture medium ingredients.

#	**Component**	**Stock solution concentration**	**Amount**	**Final concentration (mM)**
1	$NaNO_3$	30 g/200mL dH_2O	10 (mL/L)	17.6
2	K_2HPO_4	0.8 g/200mL dH_2O	10 (mL/L)	0.23
3	$MgSO_4.7H_2O$	1.5 g/200mL dH_2O	10 (mL/L)	0.3
4	$CaCl_2.\ 2H_2O$	0.72 g/200mL dH_2O	10 (mL/L)	0.24
5	Citric Acid.H_2O	0.12 g/200mL dH_2O	10 (mL/L)	0.031
6	Ferric Ammonium Citrate	0.12 g/200mL dH_2O	10 (mL/L)	0.021
7	$Na_2EDTA.2H_2O$	0.02 g/200 mL dH_2O	10 (mL/L)	0.0027
8	Na_2CO_3	0.4 g/200 mL dH_2O	10 (mL/L)	0.19
9	NaCl	20 g/ 200 ml	99.4(ml/L)	0.17
10	BG-11 Trace Metals Solution		1 (mL/L)	
	H_3BO_3		2.86 (g/L)	46
	$MnCl_2.4H_2O$		1.81 (g/L)	9
	$ZnSO_4.H_2O$		0.22 (g/L)	0.77
	$Na_2MoO_4.2H_2O$		0.39 (g/L)	1.6
	$CuSO_4.5H_2O$		0.079 (g/L)	0.3
	$Co(NO_3)_2.6H_2O$		49.4 (mg/L)	0.17

Table 3.10. BG11-N culture medium ingredients.

#	**Component**	**Stock solution concentration**	**Amount**	**Final concentration (mM)**
1	K_2HPO_4	0.8 g/200mL dH_2O	10 (mL/L)	0.23
2	$MgSO_4.7H_2O$	1.5 g/200mL dH_2O	10 (mL/L)	0.3
3	$CaCl_2.\ 2H_2O$	0.72 g/200mL dH_2O	10 (mL/L)	0.24
4	Citric Acid.H_2O	0.12 g/200mL dH_2O	10 (mL/L)	0.031
5	Ferric Ammonium Citrate	0.12 g/200mL dH_2O	10 (mL/L)	0.021
6	$Na_2EDTA.2H_2O$	0.02 g/200 mL dH_2O	10 (mL/L)	0.0027
7	Na_2CO_3	0.4 g/200 mL dH_2O	10 (mL/L)	0.19
8	BG-11 Trace Metals Solution		1 (mL/L)	
	H_3BO_3		2.86 (g/L)	46
	$MnCl_2.4H_2O$		1.81 (g/L)	9
	$ZnSO_4.H_2O$		0.22 (g/L)	0.77
	$Na_2MoO_4.2H_2O$		0.39 (g/L)	1.6
	$CuSO_4.5H_2O$		0.079 (g/L)	0.3
	$Co(NO_3)_2.6H_2O$		49.4 (mg/L)	0.17

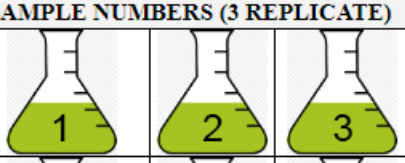
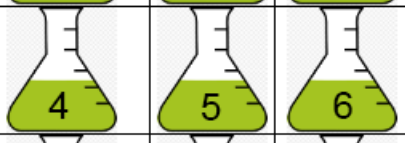
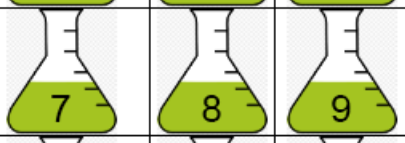
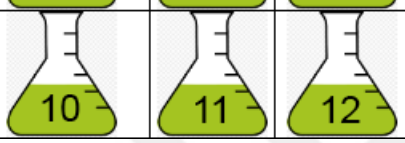
Table 3.11. BBM-N culture medium ingredients.

#	Component	Stock solution concentration	Amount	Final concentration (M)
1	$MgSO_4.7H_2O$	0.75 g/100mL	10 (mL/L)	$3.04 . 10^{-4}$
2	NaCl	0.25 g/100mL	10 (mL/L)	$4.28 . 10^{-4}$
3	K_2HPO_4	0.75 g/100mL	10 (mL/L)	$4.31 . 10^{-4}$
4	KH_2PO_4	1.75 g/100mL	10 (mL/L)	$1.29 . 10^{-3}$
5	$CaCl_2. 2H_2O$	0.25 g/100mL	10 (mL/L)	$1.70 . 10^{-3}$
6	Trace elements solution		1 (mL/L)	
	$ZnSO_4.7H_2O$	8.82 g/L		$3.07 . 10^{-5}$
	$MnCl_2.4H_2O$	1.44 g/L		$7.28 . 10^{-6}$
	MoO_3	0.71 g/L		$4.93 . 10^{-6}$
	$CuSO_4.5H_2O$	1.57 g/L		$6.29 . 10^{-6}$
	$Co(NO_3)_2.6H_2O$	0.49 g/L		$1.68 . 10^{-6}$
7	H_3BO_3	1.14 g/100 mL	1 (mL/L)	$1.85 . 10^{-4}$
8	EDTA-KOH solution		1 (mL/L)	
	$Na_2EDTA.2H_2O$	5.0 g/100 mL		$1.71 . 10^{-4}$
	KOH	3.1 g/100 mL		$5.53 . 10^{-4}$
9	Ferric solution		1 (mL/L)	
	$FeSO_4.7H_2O$	4.98 g/L		$1.79 . 10^{-5}$
	H_2SO_4 conc.	1 mL(to acidify)		
10	Soil extract		50 mL	
11	Vitamin mix		1 mL	
	Vit. B_1 (Thiamine HCl)	0.1 g/100 mL		$2.97 . 10^{-6}$
	Vit. H (Biotin)	0.025 mg/100 mL		$1.02 . 10^{-9}$
	Vit. B_{12} (Cyanocobalamin)	0.015 mg/100 mL		$1.11 . 10^{-10}$

Table 3.12. BBM-P culture medium ingredients.

#	Component	Stock solution concentration	Amount	Final concentration (M)
1	$NaNO_3$	2.50 g/100 mL	10 (mL/L)	$2.94 . 10^{-3}$
2	$MgSO_4.7H_2O$	0.75 g/100mL	10 (mL/L)	$3.04 . 10^{-4}$
3	NaCl	0.25 g/100mL	10 (mL/L)	$4.28 . 10^{-4}$
4	$CaCl_2. 2H_2O$	0.25 g/100mL	10 (mL/L)	$1.70 . 10^{-3}$
5	Trace elements solution		1 (mL/L)	
	$ZnSO_4.7H_2O$	8.82 g/L		$3.07 . 10^{-5}$
	$MnCl_2.4H_2O$	1.44 g/L		$7.28 . 10^{-6}$
	MoO_3	0.71 g/L		$4.93 . 10^{-6}$
	$CuSO_4.5H_2O$	1.57 g/L		$6.29 . 10^{-6}$
	$Co(NO_3)_2.6H_2O$	0.49 g/L		$1.68 . 10^{-6}$
6	H_3BO_3	1.14 g/100 mL	1 (mL/L)	$1.85 . 10^{-4}$
7	EDTA-KOH solution		1 (mL/L)	
	$Na_2EDTA.2H_2O$	5.0 g/100 mL		$1.71 . 10^{-4}$
	KOH	3.1 g/100 mL		$5.53 . 10^{-4}$
8	Ferric solution		1 (mL/L)	
	$FeSO_4.7H_2O$	4.98 g/L		$1.79 . 10^{-5}$
	H_2SO_4 conc.	1 mL(to acidify)		
9	Soil extract		50 mL	
10	Vitamin mix		1 mL	
	Vit. B_1 (Thiamine HCl)	0.1 g/100 mL		$2.97 . 10^{-6}$
	Vit. H (Biotin)	0.025 mg/100 mL		$1.02 . 10^{-9}$
	Vit. B_{12} (Cyanocobalamin)	0.015 mg/100 mL		$1.11 . 10^{-10}$

Table 3.13. Erlenmeyer flask study conditions under 3500 lux blue light (the samples ranging from 01 to 12).

SAMPLE NUMBERS (3 REPLICATE)	CONDITIONS & PARAMETERS	SAMPLE ID
	**LIGHT:** Blue **SONICATION:** Non-Sonicated **MEDIUM:** BG11+NaCl Medium	**MBW- NS-BG11+NaCl-01** **MBW-NS-BG11+NaCl-02** **MBW-NS-BG11+NaCl-03**
	**LIGHT:** Blue **SONICATION:** Non-Sonicated **MEDIUM:** BG11-N Medium	**MBW-NS-BG11-N-01** **MBW-NS-BG11-N-02** **MBW-NS-BG11-N-03**
	**LIGHT:** Blue **SONICATION:** Non-Sonicated **MEDIUM:** BBM-N Medium	**MBW-NS-BBM-N-01** **MBW-NS-BBM-N-02** **MBW-NS-BBM-N-03**
	**LIGHT:** Blue **SONICATION:** Non-Sonicated **MEDIUM:** BBM-P Medium	**MBW-NS-BBM-P-01** **MBW-NS-BBM-P-02** **MBW-NS-BBM-P-03**

3.4. Large Scale Cultivation

Following the experiments conducted in the green and red stages, the most optimal circumstances were determined for each phase. Simultaneously with the ongoing red phase research, a culture grown in the background in a 6L volume glass bottle PBR according to the most suitable green phase conditions was prepared to obtain the final product (astaxanthin) on a large scale. The cells in the culture were subjected to centrifugation for 20 min using a large-scale centrifuge (8KS Refrigerated Centrifuge, Sigma, Germany) operating at 4500 rpm. This process was carried out when the cells were in the mature green phase, and it resulted in their separation from the supernatant. The seed that was obtained was dissolved again in BG11-N media, the details of which are given in Table 3.10.

The 6L flat panel photobioreactor (6L FPA Photobioreactor Laboratory Unit, Subitec, Germany) was prepared for the purpose of cultivating large scale. A solution of hydrogen peroxide with a concentration of 3% was prepared with 18.2 MΩ ultra-pure water. The mixture was then pumped over the inner surface of the PBR using a peristaltic pump. The aeration system was initiated, and the mixture was efficiently distributed throughout the entire surface of the PBR for 48 hours. The peristaltic pump hose, PBR connecting hoses, aeration parts, and other systems utilized during the inoculation phase were sterilized using hydrogen peroxide.

Following the treatment of the PBR with hydrogen peroxide, it was subsequently washed with autoclaved 18.2 MΩ ultrapure water to eliminate any remaining residue. Following the washing process, any outward-opening components of the PBR were extracted and subjected to autoclaving (for 1 hour at 121°C), without compromising the sterilization of the remaining fixed parts. Once the sterilization process for the entire system was concluded, the culture that had been prepared in the BG11-N medium was transferred to the system using a peristaltic pump. The light systems were connected to cages on both sides of the photobioreactor.

The culture was produced on day zero with a wavelength of 680 nm, an optical density of 0.5, and a pH of 7.5. Aeration with dry air (0.5L/min) was implemented to ensure consistent agitation of the culture throughout the duration of the experiment. During day zero, a 2000 lux white light was administered continuously for a period of 24 hours, with alternating intervals of 12 hours of darkness and 12 hours of light. During the first day, a 2500 lux red light was used continuously for 24 hours, with alternating periods of 12 hours of darkness and 12 hours of light. The determination of light transitions was made by taking daily samples and taking into account the phases in which the cells were seen under the light microscope. Subsequently, following the exposure to white light, the blue light (12h/12h) was adjusted to an intensity of 3000 lux on Day 3. On the fifth day, the luminosity of the blue light source, capable of emitting light across a large region of the PBR, was raised from 3000 lux to 5000 lux. To illuminate the slightly dim sections, two 1000 lux blue light sources were positioned on opposite sides of the PBR. Continuous illumination was provided using all light sources (Figure 3.10). The ambient temperature of the experimental setup was incrementally raised and then maintained at the desired temperature. The initial temperature on day zero was 24°C. It was then raised to 25°C on Day 3 and further increased to 28°C on Day 5, remaining constant at this amount thereafter.

Microscopic images of the cells were snapped daily, and the progression of their colour change from green to red was seen over a period of 16 days. The culture, which transitioned from a green to a more diverse brownish shade between days 10 and 12, underwent a complete transformation to a red colour by day 14, indicating its readiness for harvest by day 16 (Figure 3.11.).

The samples collected from the final culture and the samples collected on day zero during the green phase were examined using a stereo microscope (Axio Zoom.V16, Zeiss, Germany) (Figure 3.12).

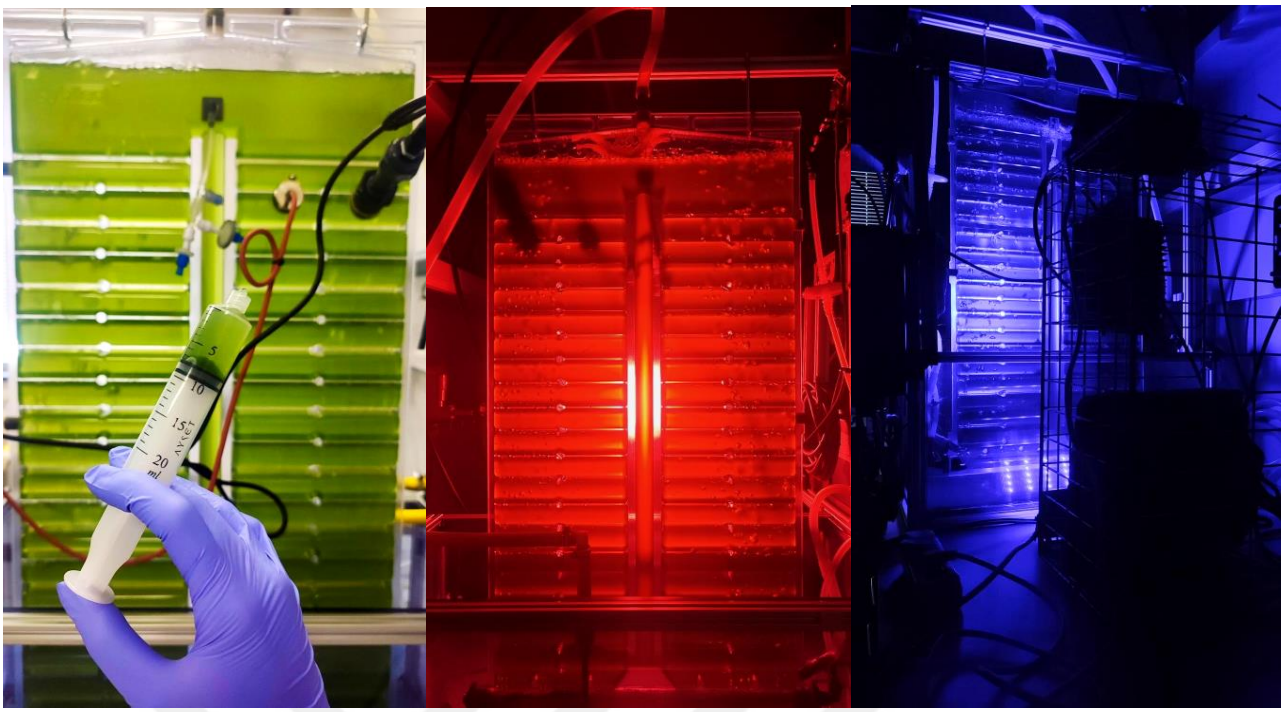


Figure 3.10. *Haematococcus lacustris* CCAP 34/6 culture images in 6L Flat Panel PBR. From left to right: illuminated by white, red, and blue light during the green phase.

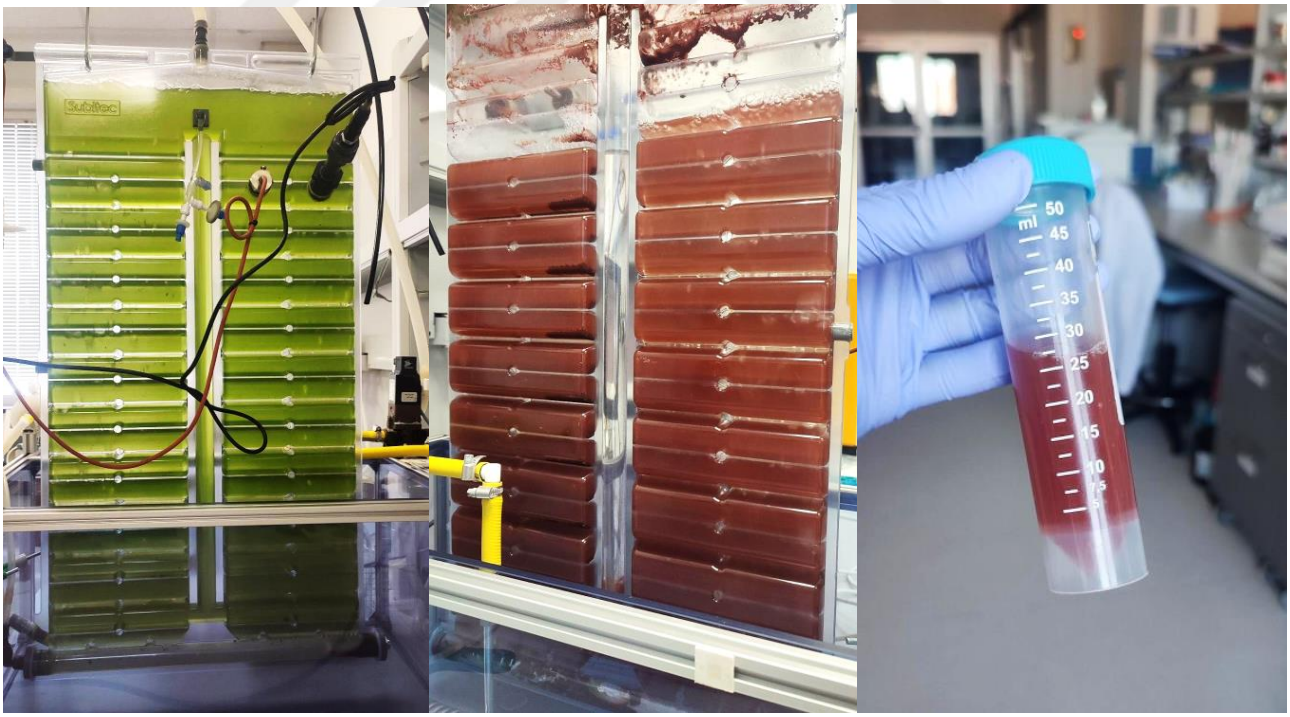


Figure 3.11. 6L Flat Panel PBR and sample images of *Haematococcus lacustris* CCAP 34/6. From left to right: green phase, red phase, and 16th day (the last day) sample of red phase.

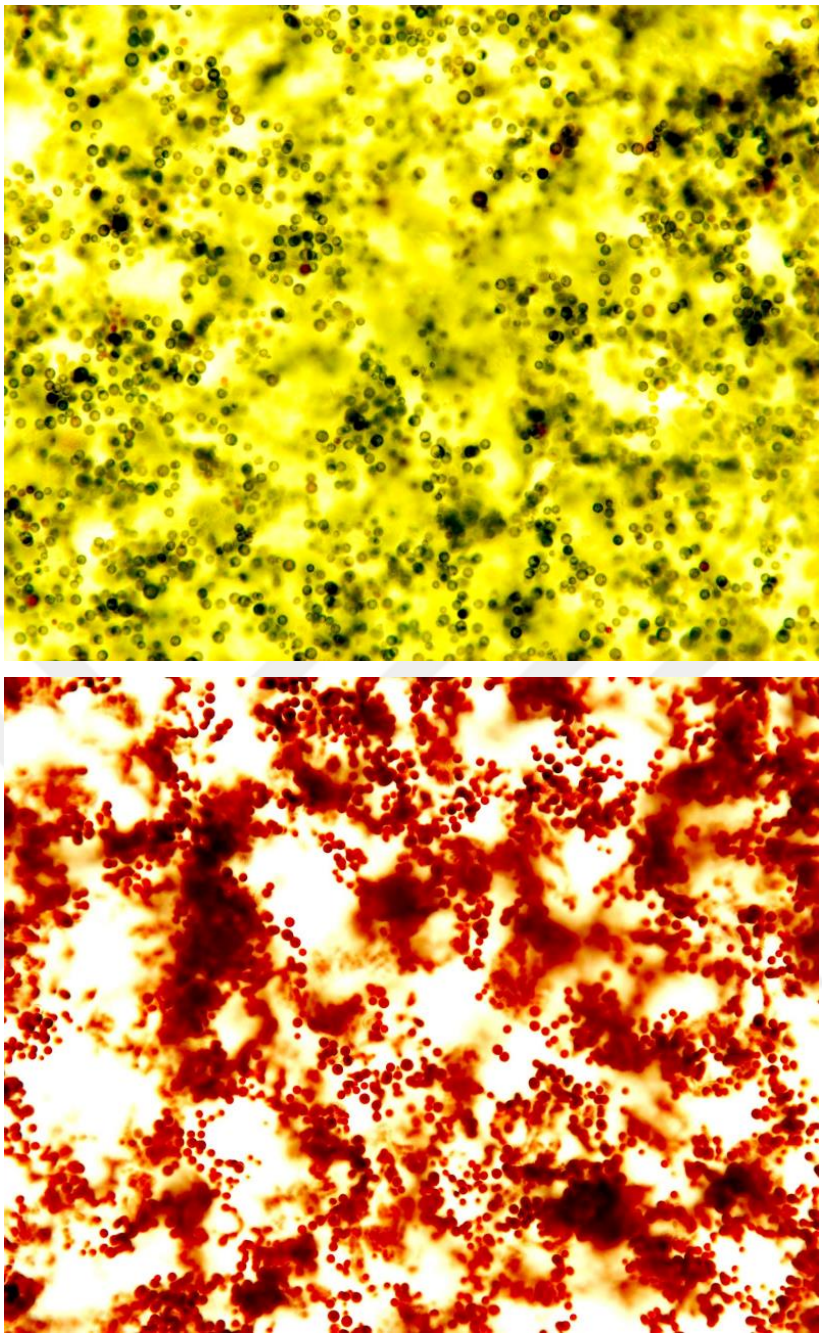


Figure 3.12. Stereo Microscope images of *Haematococcus lacustris* CCAP 34/6 in green and red phases (10X).

3.5. Dry Weight Analyses

The culture produced from a large-scale red phase cultivation in a 6-litre volume was transferred from a photobioreactor (PBR) to a 5L glass bottle using the peristaltic pump. Following that, three 15 ml samples were homogeneously taken from the culture (Figure 3.13) for the purpose of performing dry weight analysis by using the method of Zhu et al. (Zhu & Lee, 1997).



Figure 3.13. *Haematococcus lacustris* CCAP 34/6 harvested culture in the red phase.

Whatman GF/A 47mm, 0.7µm diameter microfiber filters placed in aluminium weighing dishes were prepared for each sample. Prepared filters were combusted in the muffle furnace (Daihan Scientific, South Korea) at 450°C for 2 hours. The filters taken out of the muffle furnace were allowed to cool outside for a duration of 5 minutes, after which they were transferred to a desiccator till the subsequent stage.

The filters removed from the desiccator were assigned numbers and measured using an analytical balance to determine their weight, which includes both the filter and the aluminium dish. This weight is denoted as W1 (W1 = Filter + Aluminium dish). The filter was positioned on the porous filter stone of the vacuum filtration unit. The vacuum was activated, and 5 ml of 18 MΩ ultra-pure water (UPW) was dispensed from a 5 ml serological pipette to wash the filter. During the operation of the vacuum, 10 ml of the sample was extracted from the 15 ml centrifuge tube using a serological pipette and transferred onto the filter for a duration of roughly 1-2 minutes, ensuring that it passed through the filter (Figure 3.14). Following that, an additional 5 ml of ultrapure water was put onto the filter and rinsed one more. Using a tweezer, the filter was extracted from the vacuum unit and repositioned inside the aluminium dish.



Figure 3.14. Dry weight determination of *Haematococcus lacustris* CCAP 34/6 harvested culture in the red phase. From left to right: Vacuum filtration unit, a vacuumed sample, filters in an aluminium dish left in the desiccator.

The filters in the dish containing the sample were maintained at a temperature of 105°C for a duration of 2 hours using a drying oven. Afterwards, they were let to reach the ambient temperature for 5 minutes and then stored in the desiccator for a minimum of 30 minutes. The filters were taken out from the desiccator and reweighed using the analytical balance, resulting in the acquisition of the W2 value, which represents the combined weight of the aluminium dish, filter, and biomass. The dry weight of the sample (g/L) was determined using Equation 3.1 given below:

$$W2(g) - W1(g) \times 100 = M\ (biomass) \quad (3.1)$$

W1= Filter + Aluminum Dish

W2= Filter+Aluminum Dish+Biomass

M (biomass) = Dry weight of the algae in culture

3.6. Astaxanthin Extraction

The *Haematococcus lacustris* CCAP 34/6 strain was subjected to astaxanthin extraction after cultivation in the red phase. To perform the extraction, the method introduced to the literature by Boussiba and Vonshak (1991) and Sun et al., (2017) was used.

Firstly, three 10 ml cultures were transferred from a homogenous culture into 15 ml centrifuge tubes. The samples were subjected to centrifugation at a speed of 3000 rpm for a duration of 2 minutes at the ambient temperature, and separated from the supernatant. The cell pellet was rinsed twice with 18 MΩ ultra-pure water (UPW). The centrifugation procedure was conducted under identical circumstances as the previous washing process. The pellet formed after the washing process was dissolved in a solution of 10 ml KOH and methanol (5% KOH in 30% methanol) to eliminate the chlorophyll present in it. The sample was subjected to incubation at a temperature of 65°C in a water bath (MaxTurdy-30, Daihan Scientific, Wonju, South Korea) for a duration of 15 minutes. Following the incubation period, the sample, which had been treated to remove chlorophyll, was subjected to centrifugation at a speed of 4500 rpm for a duration of 2 minutes, under room temperature. The pellet was isolated from the supernatant that included residual chlorophyll (Figure 3.14).

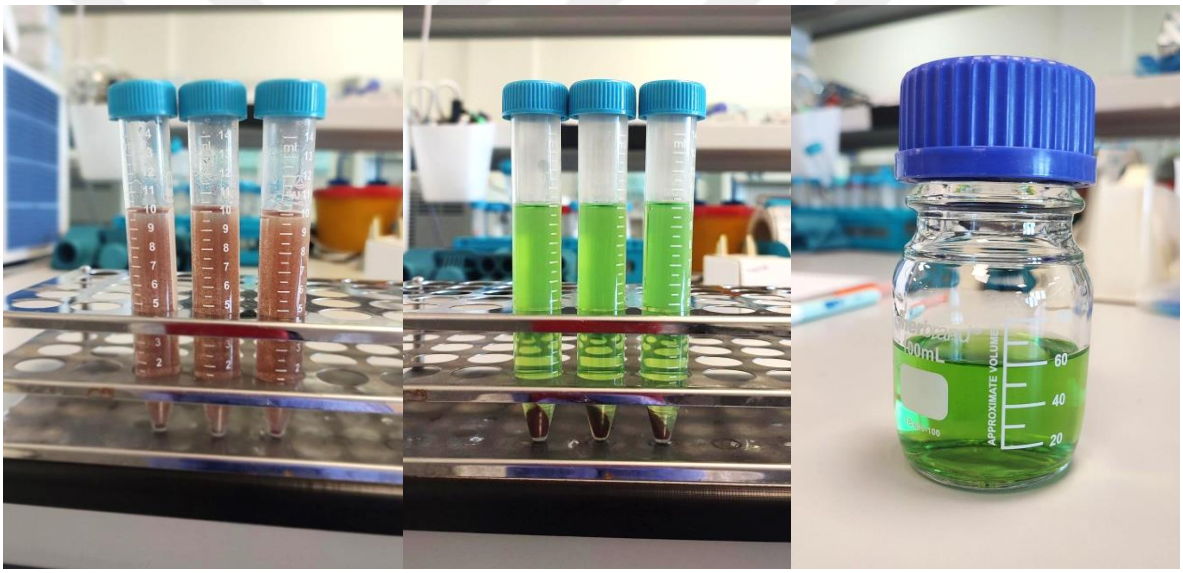


Figure 3.15. Chlorophyll removal from *Haematococcus lacustris* CCAP 34/6 culture by KOH+Methanol solution treatment.

The collected pellet was rinsed twice with 18 MΩ ultrapure water. Following the final washing step, 5 ml of DMSO was introduced to each pellet and exposed to ultrasonication at a power of 200W for a duration of 10 minutes. Following that, the samples were placed in a water bath (MaxTurdy-30, Daihan Scientific, Wonju, South Korea) and subjected to incubation at a temperature of 45°C for 20 minutes. The supernatant containing astaxanthin was collected in a glass container. The operations were repeated until the supernatant achieved transparency, with a total of 5 iterations performed (Figure 3.15.). The obtained mixture of astaxanthin (Figure 3.16) was measured using a spectrophotometer (DR 3900, Hach, Colorado, USA) at a wavelength of 490 nm. Each step was performed three times in three identical triplets, resulting in a total of nine samples. Determination of

astaxanthin from the extract obtained was carried out according to Equation 3.2 and Equation 3.3 (Davines, 1976) given below:

$$c\ (\text{mg/L}) = 4.5 \times A_{490nm} \times V_a \times V_b \quad (3.2)$$

$$\text{Astaxanthin content (\%, w/w): } C = C_t / m \quad (3.3)$$

c: per unit volume astaxanthin concentration

V_a (L): Volume of extract

V_b (L): Volume of culture sample

c_t (mg/L): Astaxanthin concentration



Figure 3.16. Extraction of astaxanthin from *Haematococcus lacustris* CCAP 34/6 culture by DMSO treatment.

3.7. Encapsulation

3.7.1. Optimization of Encapsulation

In order to encapsulate the obtained extract, the encapsulation conditions have been optimized. Astaxanthin extract mixed with 1.5%, 2% and 3% sodium alginate was dripped into $CaCl_2$ prepared at 0.15 M, 0.3 M and 0.5 M concentrations, respectively, and the loading efficiency values were compared. In the next step, the sample treated with 3% sodium alginate was formed into beads in 0.3 M $CaCl_2$ and the stability of the beads was compared at room temperature and +4°C. In the next step of the experiment, in the determination of the amount of astaxanthin to be loaded into the beads, three conditions, 10 mg/L, 25 mg/L, and 50 mg/L, were compared. Equation 3.4-6 was used in the C_{C-PC} loading efficiency calculations.

$$C_{C-PC}\ \left(\frac{mg}{mL}\right) = \frac{OD_{615} - 0.474 * OD_{652}}{5.34} \tag{3.4}$$

$$C_{Asta}\ \left(\frac{mg}{mL}\right) = OD_{480} * 0.750 \tag{3.5}$$

$$Loading\ efficiency\ (LE, \%) = \frac{C_{in\ alginate} * V_{alginate} - C_{in\ CaCl_2} * V_{CaCl_2}}{C_{in\ alginate} * V_{alginate}} \tag{3.6}$$

3.7.2. Encapsulation of Astaxanthin

Initially, the solution consisting of DMSO and astaxanthin extract was separated from each other by the process of lyophilization (HC4110, GYROZEN, Korea) at -110°C. The procedure yielded a pure and dry extract of astaxanthin (Figure 3.17).

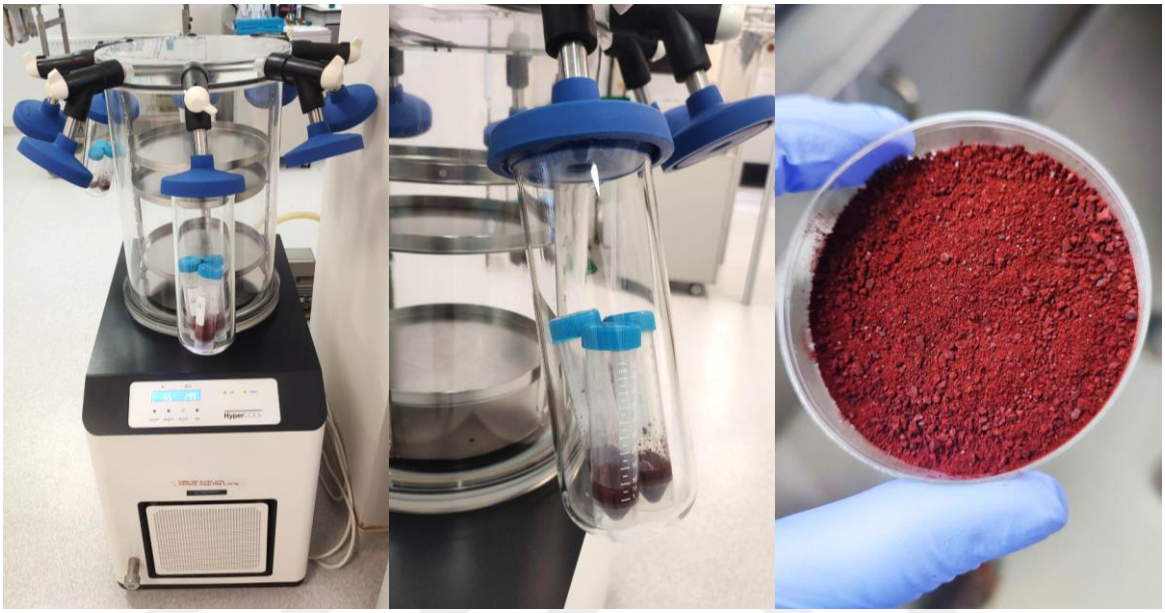


Figure 3.17. Astaxanthin + DMSO mixture subjected to lyophilization process (left and middle). Lyophilized astaxanthin powder (right).

A 3% solution of sodium alginate was prepared using a hotplate stirrer. Once the alginate solution had cooled to the temperature of the surrounding room, 1 mg of pure astaxanthin extract was dissolved in 20 ml of sodium alginate using a stirrer and fish. The homogenous liquid was divided into 60 ml and 20 ml syringes to generate particles of varying sizes (Figure 3.18).



Figure 3.18. Sodium alginate + astaxanthin mixture

A 0.3 M $CaCl_2$ solution was prepared. After obtaining a homogeneous $CaCl_2$ solution, it was placed in a beaker and continuously mixed with the help of a stirrer and fish. As the stirring process persisted, the syringe containing the alginate+astaxanthin mixture was released into the $CaCl_2$ solution. The resultant combination was allowed to undergo a process of particle formation inside the solution, resulting in the production of particles measuring 4 mm and 8 mm in diameter (Figure 3.19.).

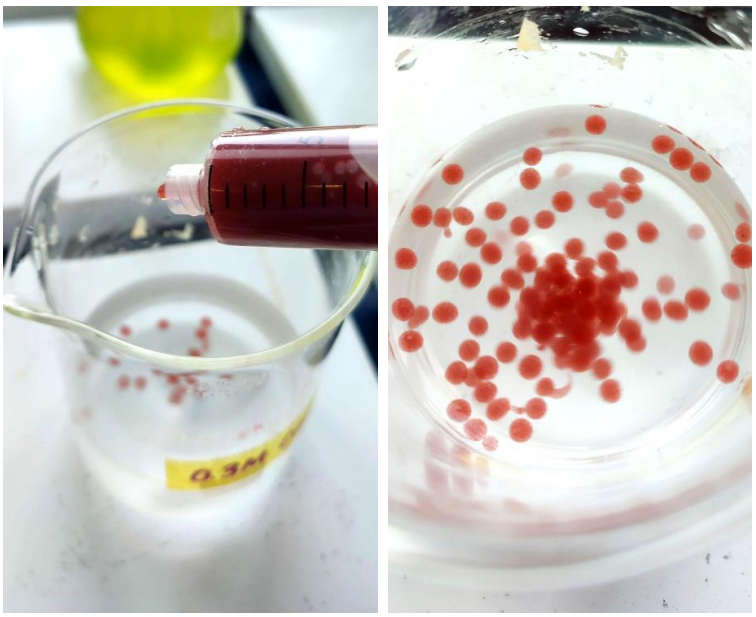


Figure 3.19. Astaxanthin+sodium alginate particles formed in 0.3 M $CaCl_2$ solution

The obtained particles were separated from the solution they were in with the help of a filter. The encapsulated astaxanthin extract obtained as 4 mm and 8 mm diameter, shown in Figure 3.20., was presented as the final product.

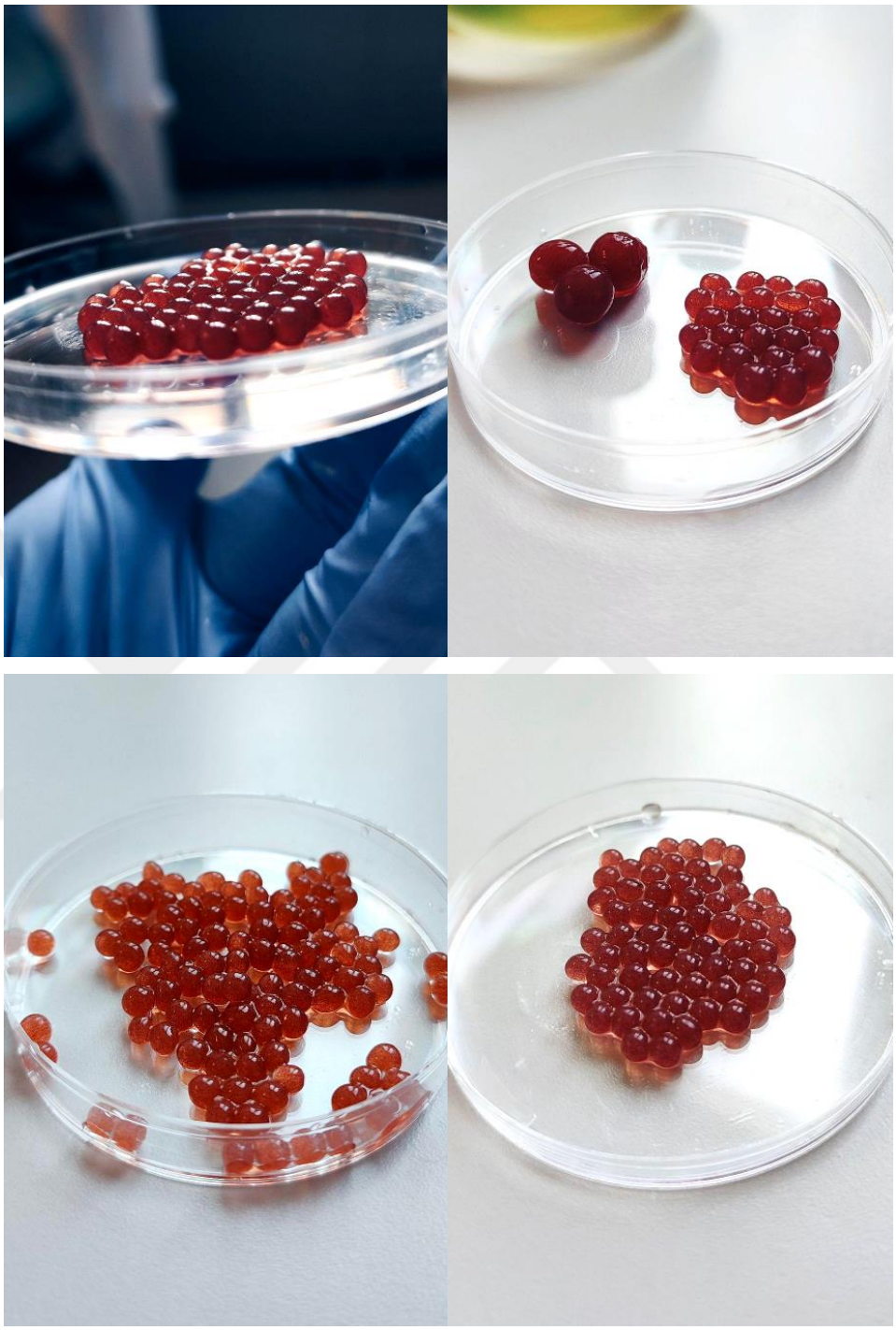


Figure 3.20. Encapsulated astaxanthin extract in 4 mm and 8 mm diameters.

4. RESULTS AND DISCUSSION

The results and discussion part are structured into seven primary categories, each representing a significant aspect of the experiments conducted in the methodology. The headings are divided into two main sections, the green and red stages, indicating the two main stages of the life cycle of *Haematococcus lacustris* CCAP 34/6 strain.

The title "Determination of Physicochemical Conditions for Green Phase Cultivation" presents the findings from experiments involving sonication, multiwell plate, and Erlenmeyer flask. On the other hand, "Determination of Physicochemical Conditions for Red Phase Cultivation" encompasses the results of the Erlenmeyer flask study, large-scale cultivation, dry weight analysis, astaxanthin extraction, and encapsulation experiments.

4.1. Determination of Physicochemical Conditions for Green Phase Cultivation

4.1.1. Sonication Tests

The sonication test, the details of which are mentioned in Section 3.2.1, was performed to investigate whether the cells uptake the essential substances in their medium better concerning the study Han et al., (2022). The cells were exposed to sonication, and their rates of growth were monitored in multiwell plates for 5 days. The collected findings are presented in Table 4.1, Figure 4.1, and Figure 4.2. Furthermore, images of the cells before being subjected to sonication and the images taken on Day 0 after being subjected to each sonication condition were captured using a light microscope (Figure 4.3.). The images were compared to the findings obtained in Table 4.1, Figure 4.1-2, and the optimal growing environment for the cells was determined.

Upon examining the microscope images on Day 0, it was observed that the cells in the 40% condition exhibited a higher degree of lysis compared to the other two prior observations. This trend continued to develop progressively in the subsequent 50%, 60%, and 70% conditions (Figure 4.3.). Therefore, the assessment was restricted to a range of 20% to 50%.

Based on the data collected, it is evident that the samples subjected to 30% sonication exhibited the greatest growth compared to other conditions, with a growth rate of 153.24% from Day 0 to Day 5. The 40% and 50% conditions exhibited a respective rise of 32.14% and 32.55%, whereas

the 20% condition demonstrated an average increase of 40.50% when assuming an average cell density of 0.11. Upon comparing the acquired data with the microscope images, it was apparent that the cells exposed to 20% and 30% sonication had the highest growth rate without experiencing any cell fragmentation. The data shown in Table 4.1 were acquired in an experimental setting where both growth medium and medium+nonsonicated culture conditions were included as a control group. This was done to assess the impact of cell fragmentation on the optical density measurements obtained on Day 0. However, despite having a cell density of 40% and 50% on Day 0, the final two conditions failed to show adequate development due to fragmentation. This position is further corroborated by the microscopic images displayed in Figure 4.3.

The conditions of 20% and 30% sonication providing the best results were evaluated individually on a separate graph in Figure 4.2. It was determined that the 30% sonication condition offered the best results in the test.

In addition, the condition of 30% sonication exhibited 84.23% more growth compared to the non-sonicated culture condition, which showed a growth rate of 69.01%, as shown in Table 4.1. The acquired information has provided insight into the "Sonicated Culture" condition, which will be utilized in the following multi-well and Erlenmeyer tests.

Table 4.1. Optical density over time table of *H. lacustris* CCAP 34/6 for five different conditions.

Time (Days)	**Non-sonicated Control Group (OD at 680 nm)**	**Sonicated Groups (OD at 680 nm)**			
		%20 (1min)	**%30 (1min)**	**%40 (1min)**	**%50 (1min)**
Day 0	0.071	0.079	0.077	0.084	0.086
Day 1	0.083	0.112	0.103	0.096	0.096
Day 2	0.098	0.115	0.116	0.097	0.099
Day 3	0.1	0.112	0.12	0.099	0.1
Day 4	0.11	0.11	0.15	0.1	0.1
Day 5	0.12	0.096	0.195	0.111	0.114

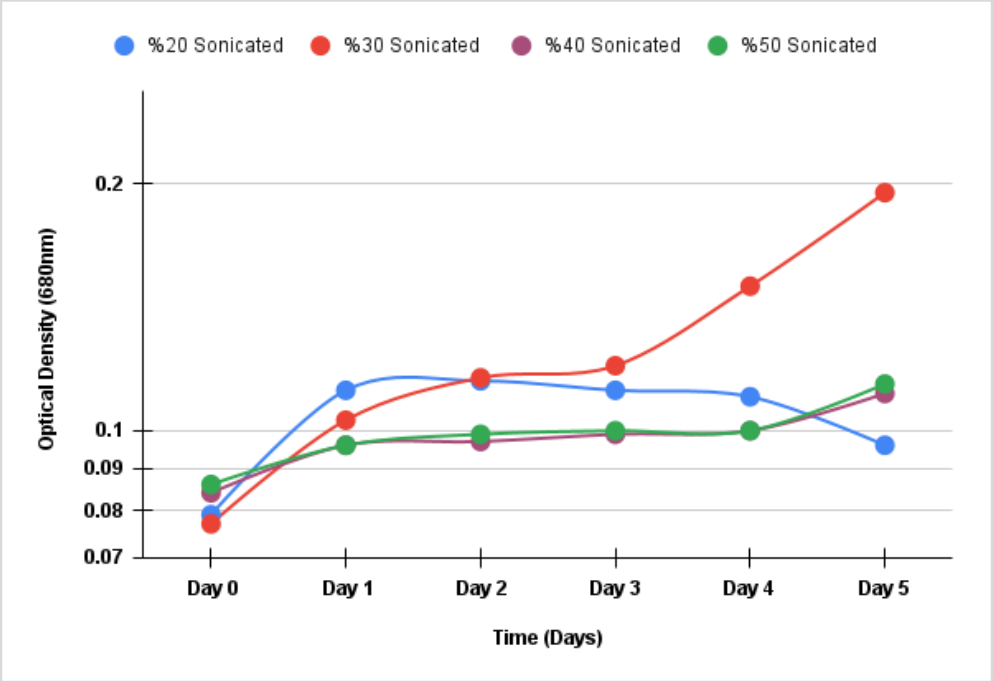


Figure 4.1. Optical density over time graph of *H. lacustris* CCAP 34/6 for four different sonication conditions.

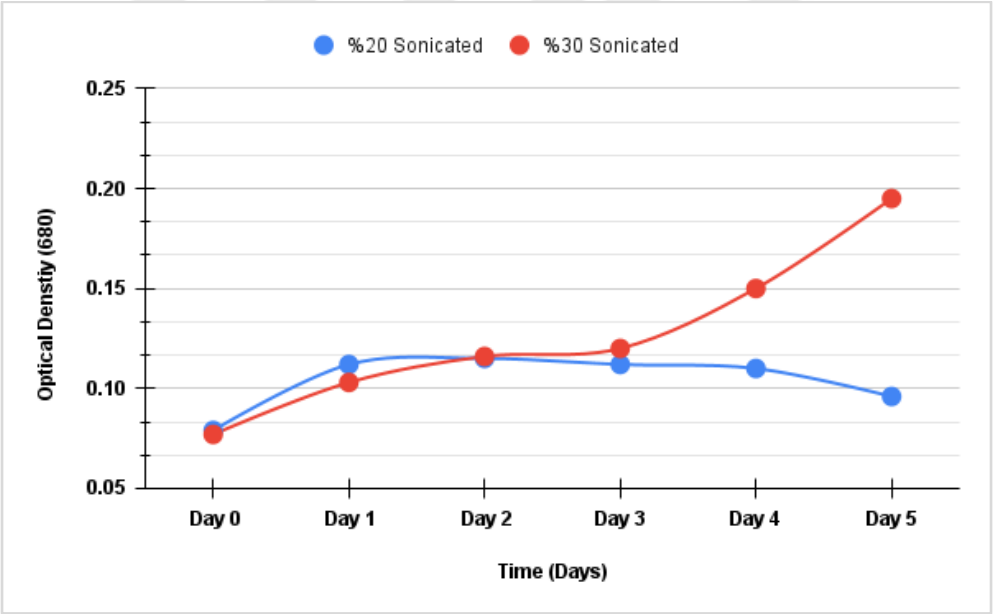


Figure 4.2. Optical density over time graph of *H. lacustris* CCAP 34/6 for the conditions 20% and 30%.

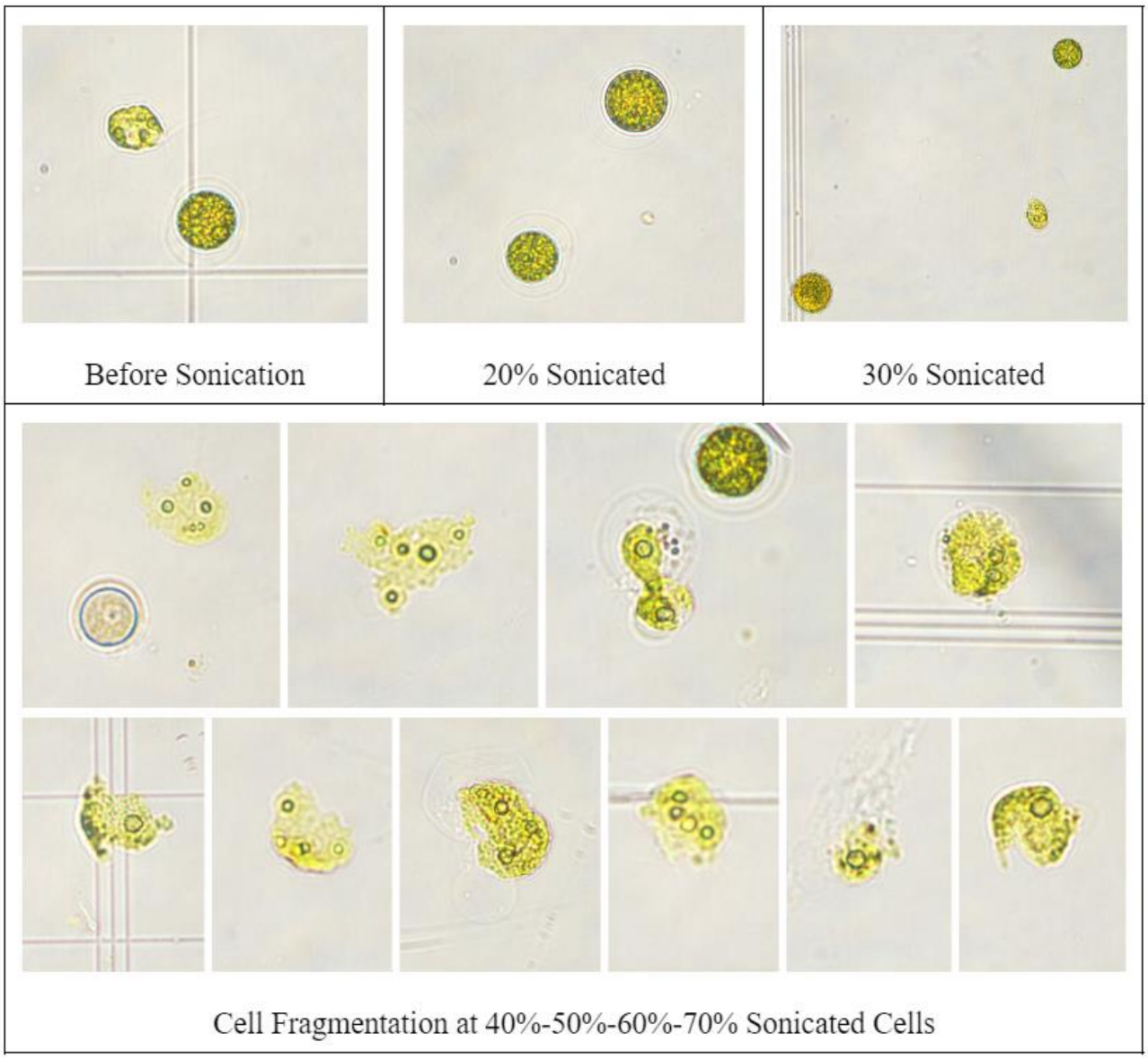


Figure 4.3. Microscopic images of *H. lacustris* CCAP 34/6 taken at different degrees of sonication. The initial three photos in the initial row, arranged from left to right, depict the culture before sonication (at 40x magnification), the culture subjected to 20% sonication (at 40x magnification), and the culture subjected to 30% sonication (at 10x magnification). The subsequent photos in the second row depict cell bursts occurring in 40%, 50%, 60%, and 70% sonicated cultures (taken 40x) and are given out of order.

4.1.2. Multi-Well Plate Study with Several Growth Media

The multiwell plate test was conducted to investigate the effects of four different growth media conditions, two different sonication conditions, and two different light combinations on cell growth, as detailed in Section 3.2.2. The growth media conditions consist of BG11, MB3N, BBM, and 3N:BBM recipes.

The sonication conditions comprise two states: 30% sonication and the absence of sonication, referred to as "sonicated" and "non-sonicated" respectively. The 30% sonication condition was chosen based on the findings from Section 4.2.1. In this part, the tests were conducted to ensure the consistency and validity of the previous results. Both sonicated and non-sonicated conditions were tested using various media and light sources. The results obtained are provided in detail in Table 4.2-5 and Figure 4.4-7.

The results indicate that cells treated with blue+red light and 30% sonication demonstrated a superior outcome compared to the other conditions. When comparing the initial and final day densities, these cells exhibited a cell growth of 1,058.33% in the 3N:BBM medium (Table 4.2). Cells exposed to Blue+Red light, without sonication, demonstrated a significant rise of 991.89% and 756.41% in BG11 and 3N:BBM medium, respectively, under comparable circumstances. These findings surpassed the outcomes of other conditions, as shown in Table 4.3.

Upon examination of the circumstances exposed to white light, it was found that there was no notable enhancement in the sonication (30%) condition compared to the other tables (Table 4.4). However, cells cultivated in BG11 medium without sonication had a substantial rise of 772.97% (Table 4.5). The conditions indicated in the last row of the tables are denoted with an asterisk (*). The aforementioned marked circumstances served as crucial contextual information for the next part of the investigation, including larger volume cultures in Erlenmeyer flasks.

Table 4.2. Time-dependent optical density values of *H. lacustris* CCAP 34/6 strain under sonication (30%), blue+red light, and different growth media conditions.

Conditions			
Sonication: Yes (30%)		Light: Blue+Red	
Temperature: 23°C		Plate No: #4	
Time (Days)	**Optical Density at 680 nm**		
	BG11	**MB3N**	**BBM**	**3N:BBM**
Day 0	0.036	0.038	0.033	0.036
Day 1	0.049	0.042	0.042	0.046
Day 2	0.075	0.076	0.072	0.059
Day 3	0.095	0.08	0.062	0.061
Day 4	0.09	0.097	0.086	0.066
Day 5	0.102	0.112	0.109	0.121
Day 6	0.253	0.107	0.105	0.162
Day 7	0.27	0.11	0.11	0.176
Day 8	0.288	0.126	0.11	0.23
Day 9	0.285	0.132	0.122	0.417
Increase (%)	691,66%	247,36%	269,69%	1.058,33%
	-	-	-	*

Table 4.3. Time-dependent optical density values of *H. lacustris* CCAP 34/6 strain under blue+red light and different growth media conditions.

Conditions			
Sonication: No (Non-sonicated)		Light: Blue+Red	
Temperature: 23°C		Plate No: #3	
Time (Days)	**Optical Density at 680 nm**		
	BG11	**MB3N**	**BBM**	**3N:BBM**
Day 0	0.037	0.034	0.03	0.039
Day 1	0.047	0.053	0.05	0.05
Day 2	0.089	0.05	0.063	0.056
Day 3	0.091	0.06	0.062	0.06
Day 4	0.178	0.072	0.059	0.072
Day 5	0.147	0.077	0.081	0.121
Day 6	0.271	0.097	0.11	0.192
Day 7	0.331	0.103	0.112	0.223
Day 8	0.349	0.177	0.129	0.327
Day 9	0.404	0.194	0.127	0.334
Increase (%)	991,89%	470,58%	323,33%	756,41%
	*	-	-	*

Table 4.4. Time-dependent optical density values of *H. lacustris* CCAP 34/6 strain under sonication (30%), white light, and different growth media conditions.

Conditions			
Sonication: Yes (30%)		Light: White	
Temperature: 23°C		Plate No: #2	
Time (Days)	**Optical Density at 680 nm**		
	BG11	**MB3N**	**BBM**	**3N:BBM**
Day 0	0.036	0.039	0.053	0.038
Day 1	0.045	0.037	0.043	0.036
Day 2	0.06	0.05	0.055	0.051
Day 3	0.062	0.042	0.059	0.049
Day 4	0.068	0.045	0.077	0.047
Day 5	0.094	0.051	0.086	0.056
Day 6	0.135	0.052	0.099	0.072
Day 7	0.176	0.071	0.127	0.089
Day 8	0.196	0.067	0.127	0.108
Day 9	0.223	0.05	0.049	0.139
Increase (%)	519,44%	79,48%	139,62%	265,78%
	-	-	-	-

Table 4.5. Time-dependent optical density values of *H. lacustris* CCAP 34/6 strain under white light, and different growth media conditions.

Conditions			
Sonication: No (Non-sonicated)		Light: White	
Temperature: 23°C		Plate No: #1	
Time (Days)	**Optical Density at 680 nm**		
	BG11	**MB3N**	**BBM**	**3N:BBM**
Day 0	0.037	0.038	0.04	0.04
Day 1	0.042	0.038	0.035	0.039
Day 2	0.061	0.055	0.053	0.057
Day 3	0.078	0.047	0.046	0.06
Day 4	0.08	0.06	0.068	0.08
Day 5	0.108	0.065	0.068	0.09
Day 6	0.194	0.082	0.081	0.125
Day 7	0.279	0.088	0.089	0.169
Day 8	0.318	0.093	0.089	0.142
Day 9	0.323	0.076	0.09	0.21
Increase (%)	772,97%	144,73%	125,0%	425,0%
	*	-	-	-

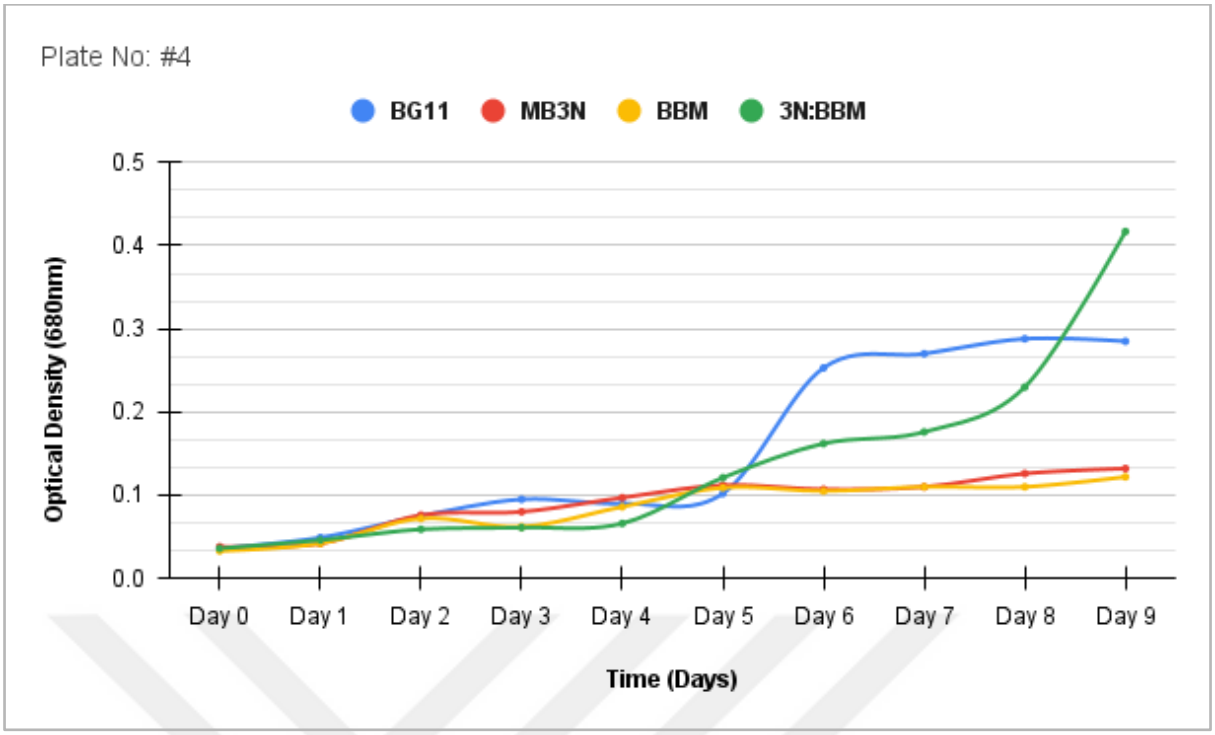


Figure 4.4. Time-dependent optical density graph of *H. lacustri*s CCAP 34/6 strain under sonication (30%), blue+red light, and different growth media conditions.

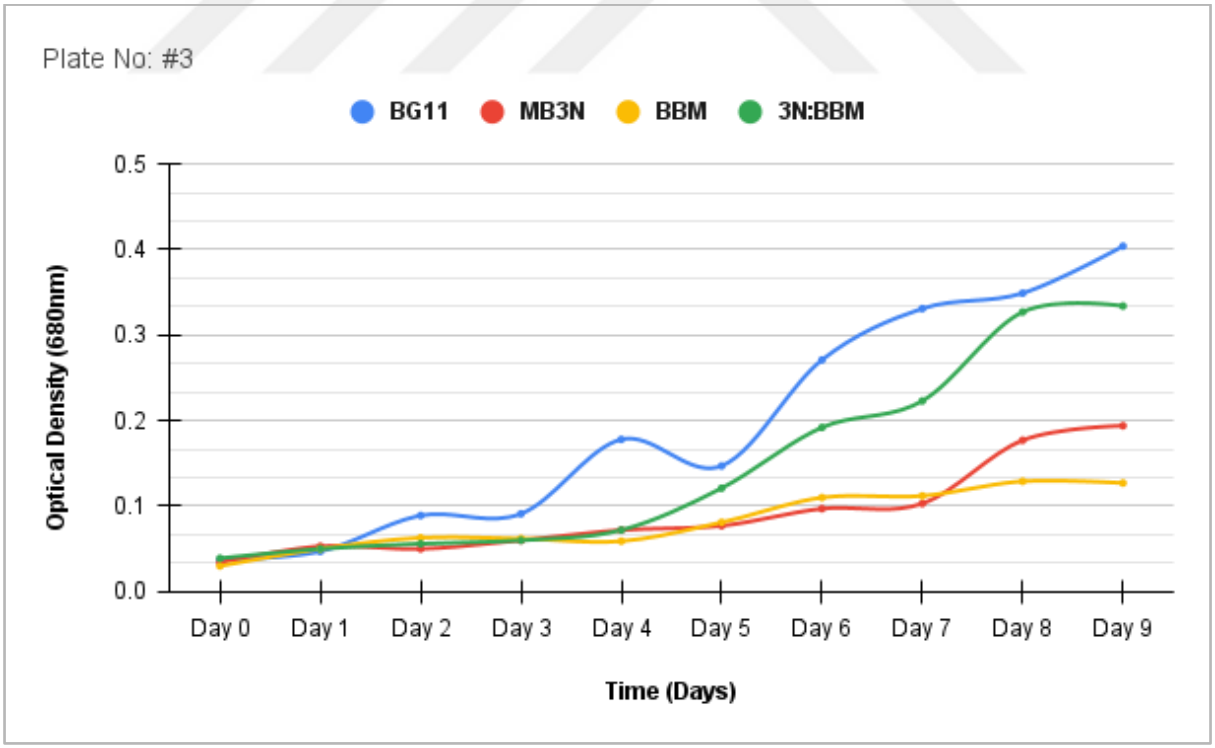


Figure 4.5. Time-dependent optical density graph of *H. lacustris* CCAP 34/6 strain under blue+red light and different growth media conditions.

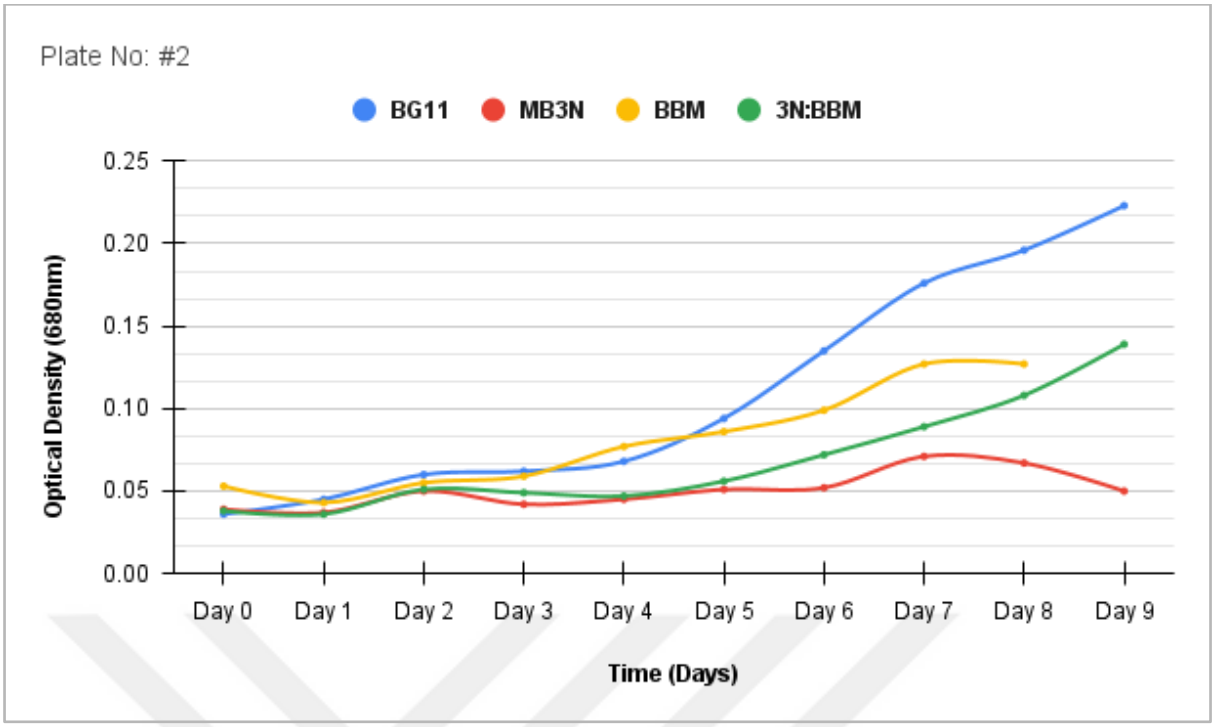


Figure 4.6. Time-dependent optical density graph of *H. lacustris* CCAP 34/6 strain under sonication (30%), white light, and different growth media conditions.

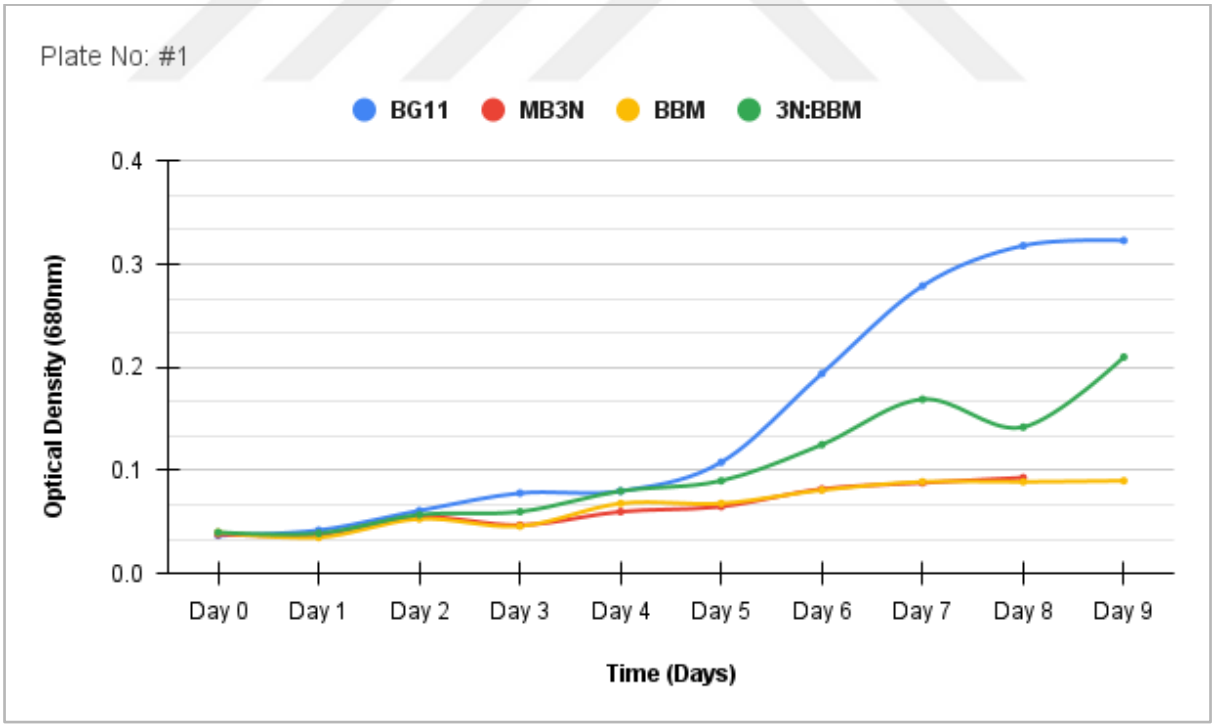


Figure 4.7. Time-dependent optical density graph of *H. lacustris* CCAP 34/6 strain under white light, and different growth media conditions.

4.1.3. Erlenmeyer Flask Study

The Erlenmeyer flask test was performed to investigate the effects of three different media conditions, two different sonication conditions, and two different light combinations on cell growth at 23°C in the green phase, as detailed in Section 3.2.3. The media conditions included BG11, 3N:BBM and 3P:BBM media. The selection of BG11 and 3N:BBM media was based on the best circumstances (BRS-3NBBM, BRN-BG11, WN-BG11, and BRN-3NBBM) obtained from the multiwell plate test conducted in the previous step (Section 4.2.2). In addition, as shown in the study of Nahidian et al. (2018), it was revealed that the 3P:BBM medium exhibited beneficial outcomes in the growth of *Haematococcus* species. For this reason, this medium was also included as the third medium condition in the Erlenmeyer test, which both confirmed the multiwell plate test and provided the opportunity to work in higher volumes compared to the multiwell plate.

The data is shown in Table 4.6. indicate that the BRN-3N:BBM condition had the greatest increase. This condition is characterized by the absence of sonication, exposure to blue+red light, and the presence of a 3N:BBM medium. As seen in the table, the initial three optimal circumstances emphasize the beneficial impacts of non-sonicated and blue+red light conditions on the proliferation of cells.

After evaluating the data while maintaining consistent sonication, media, and light conditions individually, the following results were obtained:

When the media and light conditions remained at a constant level, it was noted that the WN-BG11 condition achieved higher values compared to WS-BG11 (165.75%); the WN-3NBBM achieved higher values compared to WS-3NBBM (164.47%); and the WN-3PBBM achieved higher values compared to WS-3PBBM (182.66%). In a comparable way, the percentage of BRN-BG11 (301.6%) exceeded that of BRS-BG11 (147.99%), BRN-3NBBM (308.2%) surpassed BRS 3NBBM (213.04%), and BRN-3PBBM (290.78%) exceeding BRS-3PBBM (268.42%). Therefore, it was noted that the *H. lacustris* CCAP 34/6 strain had a superior growth pattern when not subjected to sonication.

When sonication and media conditions were kept constant, the BRN-BG11 condition exhibited superior growth compared to WN-BG11 (238.59%), BRN-3NBBM (308.21%) surpassed WN-3NBBM (212.5%), and BRN-3PBBM (290.78%) improved growth profile compared to WN-3PBBM (272.13%). Hence, it was noted that the *H. lacustris* CCAP 34/6 strain had a more favourable growth pattern under blue+red light circumstances.

When an evaluation is made by keeping the sonication and light conditions constant in addition to the best conditions obtained above, it was observed that BRN-3NBBM (308.21%), BRN-BG11 (301.63%), and BRN-3PBBM (290.78%) provide the best value, respectively.

As the Erlenmeyer flask test also confirmed the multiwell plate test conducted in the previous stage, the comparison of these two tests provided further results: The three optimal conditions achieved in the multiwell-plate test are known as BRS-3NBBM, BRN-BG11, and BRN-3NBBM (Table 4.2-5.). Similarly, in the Erlenmeyer flask test, the three optimal conditions were identified as BRN-3NBBM, BRN-BG11, and BRN-3PBBM. Although the findings were similar, the superior performance of BRS-3NBBM (Blue+red light, sonicated, 3NBBM medium) in the multiwell plate test may be attributed to the mixing difficulty during plate readings and the comparatively small working volume (2ml). Such findings exposed the limitations of the multiwell plate test and highlighted the necessity of the Erlenmeyer test for confirming the outcomes.

These studies also presented findings from the standpoint of sonication application: Christwardana and Hadiyanto (2017) proposed that audible sound (20-20,000 Hz) positively influences the proliferation of *Haematococcus* cells, whereas Han et al. (2022) demonstrated favourable outcomes from ultrasonication testing. In contrast to the findings of earlier research, this thesis demonstrates that non-sonicated circumstances are more effective for the *Haematococcus lacustris* CCAP 34/6 strain.

In light of these results, in this section, the first of the growth stages (green) of the *H. lacustris* CCAP 34/6 strain, which is divided into two main headings, the green phase and the red phase, has been completed. The best condition has been shown to be “BRN-3NBBM” (under blue+red light, non-sonicated, in 3N:BBM medium). This result reiterated the beneficial impact of nitrogen in the media on microalgae growth, as shown in the research of Zhang et al. (2018).

Consequently, the culture intended for use in large-scale operations was prepared based on the optimal conditions identified, and the volume was increased to 5L.

Table 4.6. Time-dependent optical density values of *H. lacustris* CCAP 34/6 strain for the green phase study.

Conditions				Optical Density (at 680 nm)	Time (Days)										% Increase
Light	Sonication	Medium	Sample Name		Day 1	Day 2	Day 3	Day 4	Day 5	Day 6	Day 7	Day 8	Day 9	Day10	
White	Nonsonicated	BG11	WN-BG11		0.057	0.055	0.063	0.125	0.151	0.131	0.146	0.164	0.193	0.193	238.59
	Nonsonicated	3N:BBM	WN-3NBBM		0.064	0.070	0.072	0.117	0.125	0.130	0.167	0.192	0.225	0.200	212.5
	Nonsonicated	3P:BBM	WN-3PBBM		0.061	0.081	0.087	0.110	0.116	0.134	0.116	0.149	0.214	0.227	272.13
	30%	BG11	WS-BG11		0.073	0.075	0.090	0.092	0.115	0.108	0.140	0.143	0.148	0.194	165.75
	30%	3N:BBM	WS-3NBBM		0.076	0.076	0.351	0.097	0.119	0.141	0.155	0.220	0.180	0.201	164.47
	30%	3P:BBM	WS-3PBBM		0.075	0.100	0.099	0.101	0.120	0.111	0.146	0.206	0.151	0.212	182.66
Blue + Red	Nonsonicated	BG11	BRN-BG11		0.061	0.070	0.087	0.098	0.121	0.166	0.177	0.193	0.230	0.245	301.63
	Nonsonicated	3N:BBM	BRN-3NBBM		0.073	0.068	0.064	0.120	0.116	0.148	0.148	0.234	0.203	0.298	308.21
	Nonsonicated	3P:BBM	BRN-3PBBM		0.076	0.099	0.111	0.109	0.130	0.179	0.228	0.201	0.248	0.297	290.78
	30%	BG11	BRS-BG11		0.075	0.061	0.070	0.093	0.124	0.172	0.169	0.162	0.203	0.186	147.99
	30%	3N:BBM	BRS-3NBBM		0.069	0.325	0.084	0.101	0.122	0.141	0.182	0.216	0.187	0.216	213.04
	30%	3P:BBM	BRS-3PBBM		0.057	0.068	0.115	0.109	0.130	0.168	0.170	0.169	0.194	0.210	268.42

4.2. Determination of Physicochemical Conditions for Red Phase Cultivation

4.2.1. Erlenmeyer Flask Study

This section was conducted to see the effects of 4 different media conditions, namely BG11+NaCl, BG11-N, BBM-N, and BBM-P, on non-sonicated *H. lacustris* CCAP 34/6 strains and to determine the optimal red phase conditions. Accordingly, daily microscope images were taken for 20 days, and the progression of cell phases was monitored (Figure 4.8-10.). The cells were labelled as mature green, transition, and mature red, and corresponding cell scores were given.

The cell score comparison is summarised in Table 4.7 revealed that the samples cultured in BG11-N medium exhibited the most optimal condition. The comparison in the table is based on colours to make the result more understandable. Accordingly, the culture growing in BBM-P medium with still green cell density at the end of the 20th day is shown in green colour. BG11-N, which gave the best result, was represented with an intense red colour to differentiate it from the others. The comparison of the conditions is also given in Figure 4.9. In addition, Figure 4.9 provides a comparison of the conditions at the Erlenmeyer flask level. The contrast between the culture exposed to BG11-N medium (front) and the culture exposed to BBM-P (back) becomes evident on Day 20.

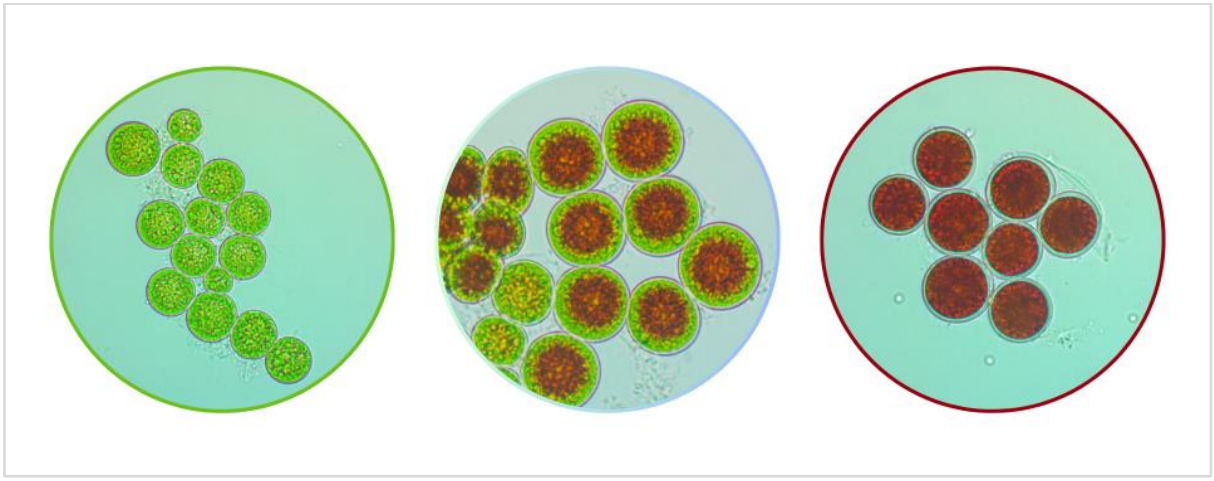


Figure 4.8. Light microscope image of *Haematococcus lacustris* CCAP 34/6 taken at 40x. From left to right: Green Mature Coccoid Cell, Intermediate Cell (transitional cells), and Red Mature Cells.

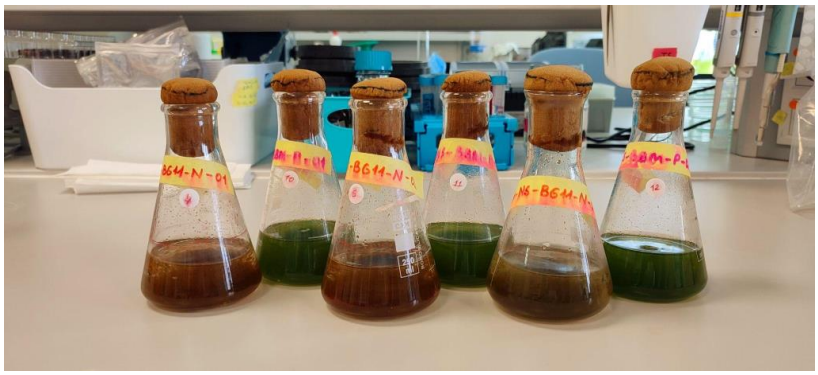


Figure 4.9. Comparison of *H. lacustris* CCAP 34/6 cultures growing in BG11-N medium (front) and BBM-P medium under red phase conditions (back) on day 20.

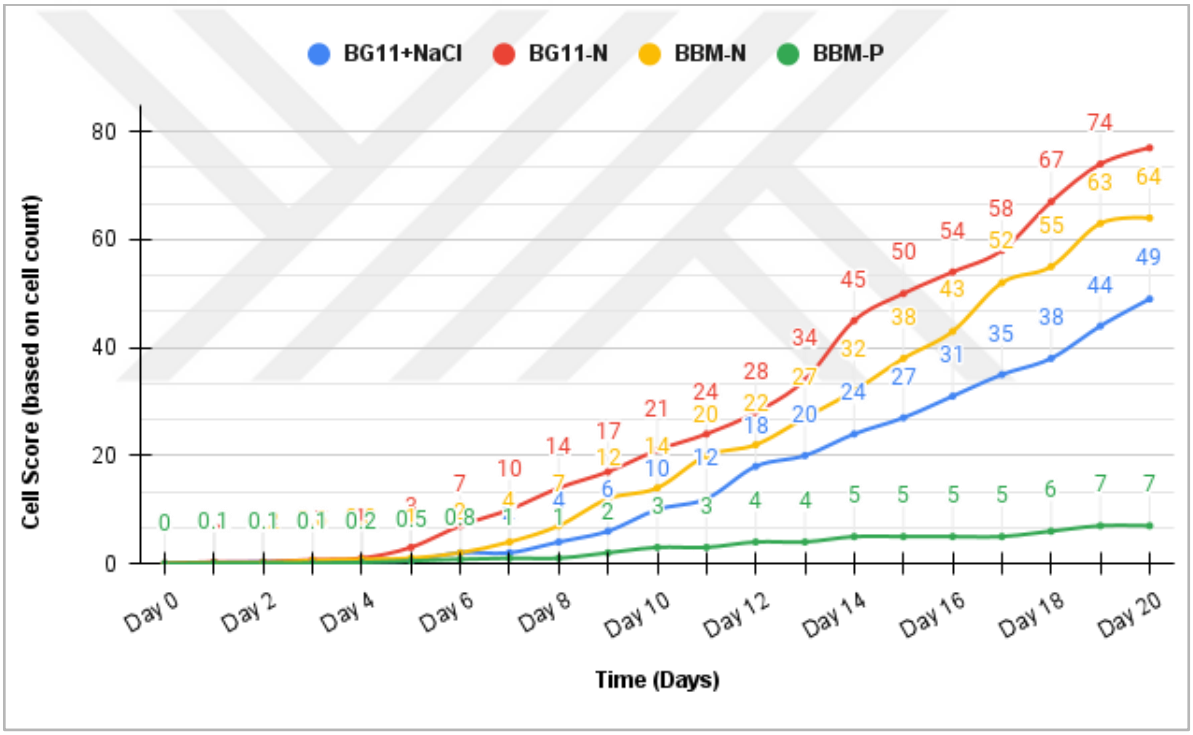


Figure 4.10. Time-dependent red mature cell score graph of *H. lacustris* CCAP 34/6 strain grown under red phase conditions.

Table 4.7. Summary of red phase transformation of *H. lacustris* CCAP 34/6 strain grown under red phase conditions in different growth media conditions

Conditions	Sample ID	20th day
LIGHT: Blue SONICATION: Non-Sonicated MEDIUM: BG11+NaCl Medium	MBW- NS-BG11+NaCl-01	*
	MBW-NS-BG11+NaCl-02	*
	MBW-NS-BG11+NaCl-03	*
LIGHT: Blue SONICATION: Non-Sonicated MEDIUM: BG11-N Medium	MBW-NS-BG11-N-01	***
	MBW-NS-BG11-N-02	***
	MBW-NS-BG11-N-03	***
LIGHT: Blue SONICATION: Non-Sonicated MEDIUM: BBM-N Medium	MBW-NS-BBM-N-01	**
	MBW-NS-BBM-N-02	**
	MBW-NS-BBM-N-03	**
LIGHT: Blue SONICATION: Non-Sonicated MEDIUM: BBM-P Medium	MBW-NS-BBM-P-01	-
	MBW-NS-BBM-P-02	-
	MBW-NS-BBM-P-03	-

The findings shown in Table 4.7 corroborate the conclusions drawn in other research (Çakmak et al., 2012; Scibilia et al., 2015; Mao et al., 2018) indicating that nitrogen deficiency in the media induces stress conditions. While not as significant as nitrogen deficiency in the present study, salinity stress emerged as the third most impactful stress condition, corroborating the findings of Gao et al. (2015). Considering that temperature fluctuations are also accepted as a stress factor in the literature (Giannelli, Yamada, Katsuda, & Yamaji, 2015), it is seen in the results obtained that temperature changes cause cells to respond as stress conditions. Consequently, factors classified as stressors regarding light, temperature, and medium composition that favourably influence astaxanthin accumulation were identified.

4.3. Large Scale Cultivation

The Large Scale Cultivation section involves growing the *H. lacustris* CCAP 34/6 strain on a large scale (6L) using the optimal conditions developed in the previous sections and making it ready for harvesting and extraction. *H. lacustris* CCAP 34/6 strain cultivated under specified green phase

conditions was introduced into the flat panel PBR system in 6L volume. Astaxanthin accumulation in the culture inoculated in the BG11-N medium was monitored from Day 0 to Day 16. Images of cells before and following inoculation are provided in Figure 4.11., and data collected throughout the sixteen-day follow-up period are presented in Figure 4.12.

From the first day of inoculation, the physical conditions determined for the red phase (temperature, light) were gradually applied in a room isolated from the external conditions where the PBR was installed. Although the cells were harvested and inoculated in the green mature coccoid cell phase (Figure 4.12., Day 1-2), the cells exhibited a tendency to undergo division when exposed to new media upon being moved to the flat panel PBR. The existence of flagellated cells in the Day 2 segment (left) in Figure 4.12 more clearly demonstrates this situation. As a result of this prediction obtained by considering the microscope images in the previous studies, the temperature was incrementally raised from 24°C to 28°C to prevent the loss of the culture. Similarly, light sources were systematically modified and augmented throughout time intervals of 1-2-2 and 3-days for a comparable purpose. Therefore, the specified stress conditions for the red phase were possible to apply under a controlled environment.

The cellular condition was investigated by observing microscope images of samples taken daily. The cells under monitoring were assessed based on their susceptibility to contamination, cell growth phases, pH levels, and optical density measurements. Since suitable aseptic conditions were maintained, the culture transferred from bottle glass PBR to flat panel PBR did not provide a substantial risk of contamination. Hence, it was evident that the three-stage cleaning carried out during the sterilization of the flat panel PBR system achieved successful outcomes. Optical density values were initiated with 0.5 (680 nm) and 7.5 pH as predicted in the study of Oslan et al., (2021) and the culture was followed to reach the mid-exponential phase for the first 3-4 days. Accordingly, it was exposed to white, red, and blue light lights, respectively, and fixed to blue light after the third day.

The transition of the cells from the green mature coccoid cell phase to the mature red phase was also followed with daily microscope images. As detailed in the figures divided into days in Figure 4.12, the cells were inoculated in the mature green phase, but in the following days, they consumed the contents of the medium they were in and transitioned into the division phase. Following that, on the second day, the fully developed green cells started to be substituted by mobile flagellated cells. Commencing on the fifth day, the cells returned to the fully developed green phase and later transformed into intermediate cells on the tenth day, initiating the accumulation of astaxanthin.

During this phase, the culture harbours green mature cells, intermediate cells, and red cells simultaneously (Days 10-13). The transition stage is represented by a brownish culture imagined in a photobioreactor (PBR), as seen in Figure 4.13 (in the middle).

On Day 13, the accumulation of astaxanthin continued to rise steadily. Meanwhile, the microscope images were analysed by considering the accumulation of astaxanthin, which began in the center of the cells and extended over the whole surface. By the conclusion of the sixteenth day, the cells that had fully transitioned into the red phase had achieved the red colouration seen in Figure 4.12. Day 16. This colour change corresponds to the image seen on the right side of Figure 4.13. Thus, the culture was ready to be harvested for astaxanthin extraction.

In light of these results, it is possible to make the following comments about the PBR systems used: During the studies, different PBR systems were used at various stages including preliminary and main experiments. Tubular PBR systems, Flat Panel PBR systems, Erlenmeyer flask PBR systems and glass bottle PBR systems are among them. As highlighted by Ozcelik et al. (2021) and considering the conditions in the Istanbul Microalgae Biotechnologies Research and Development Unit (IMBIYOTAB) where the experiments were carried out, closed systems create positive effects in terms of parameters such as contamination, light, and temperature control. Considering how important the healthy growth of cells is for a microalgae strain like *Haematococcus lacustris*, which is unique and undergoes major changes in the cell cycle, it is seen that the choice of PBR system has significant positive effects on the overall experimental results.

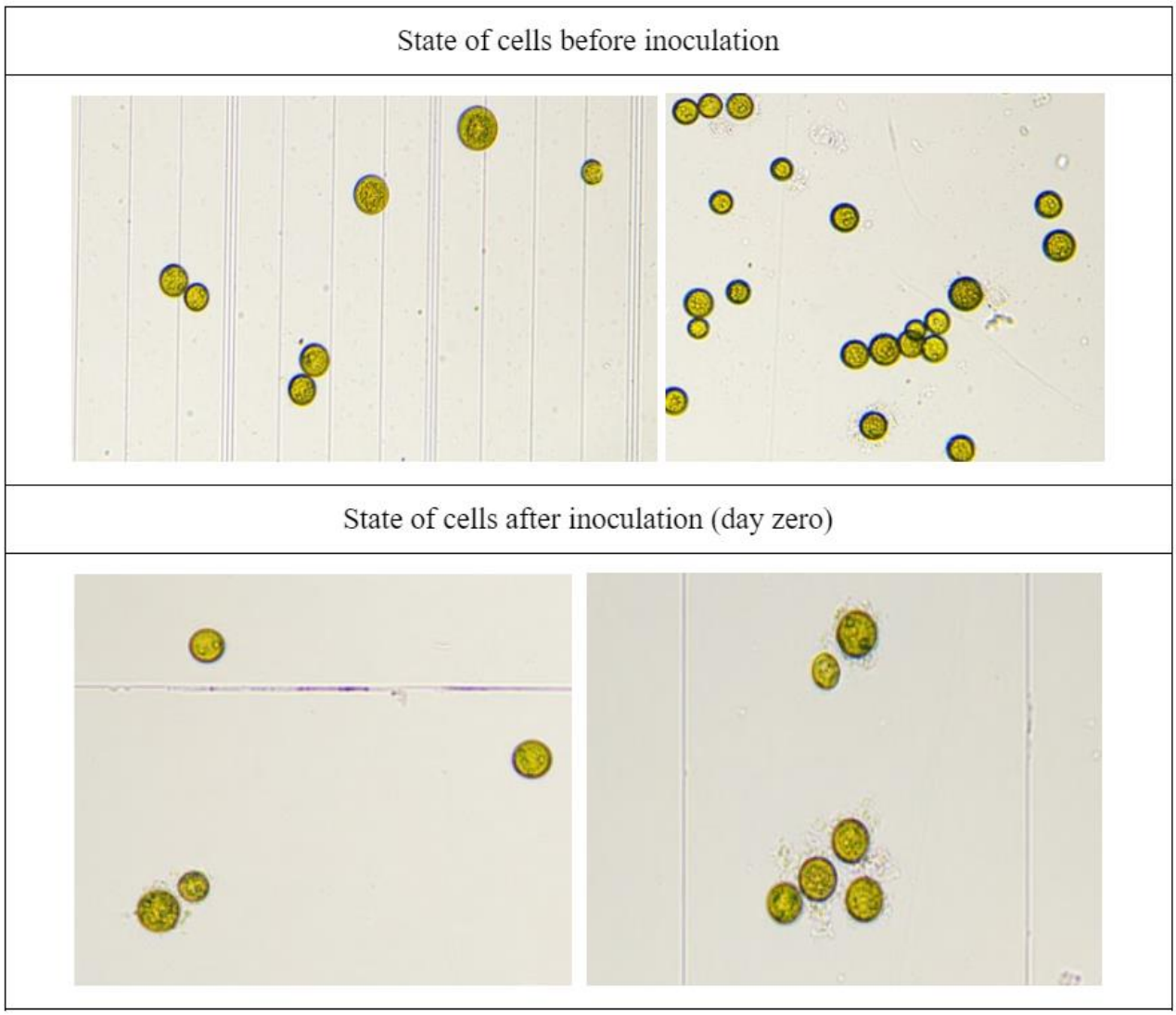
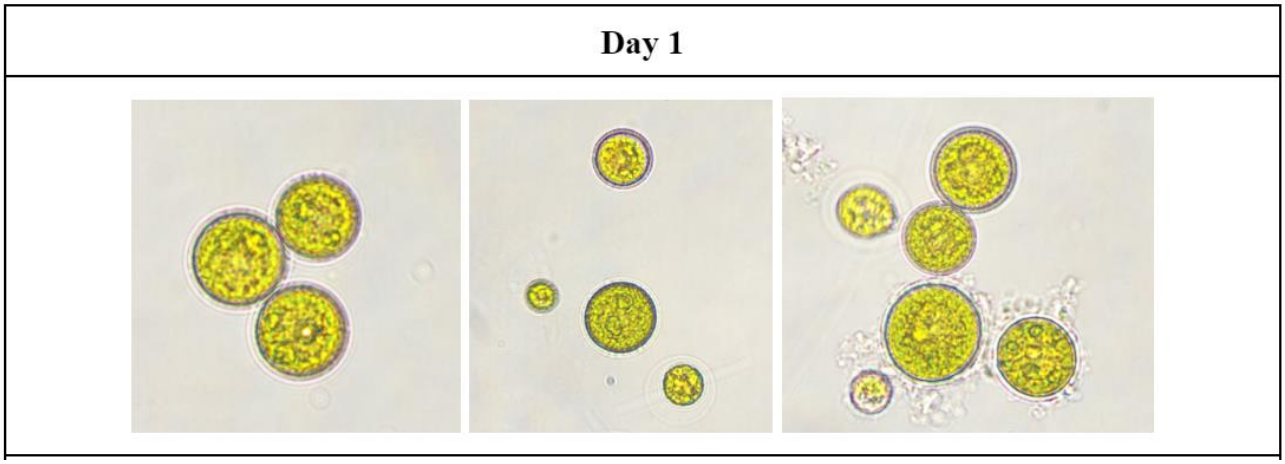
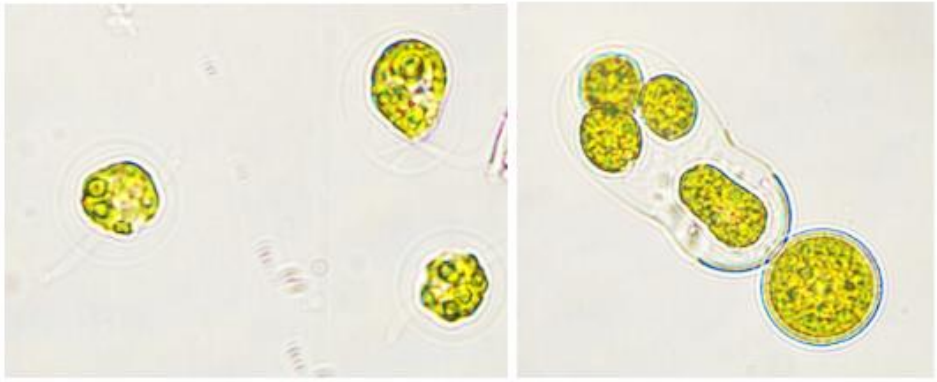


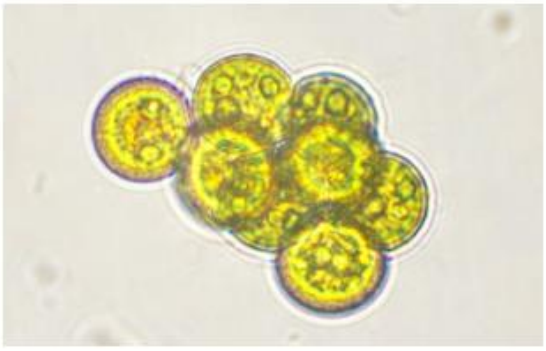
Figure 4.11. *H. lacustris* CCAP 34/6 strain in the green mature coccoid cell phase before and after large-scale (6L) inoculation.



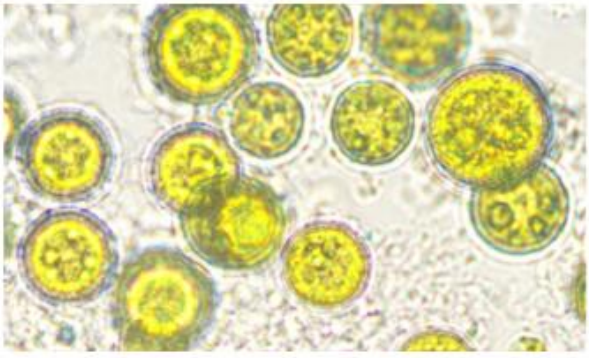
Day 2



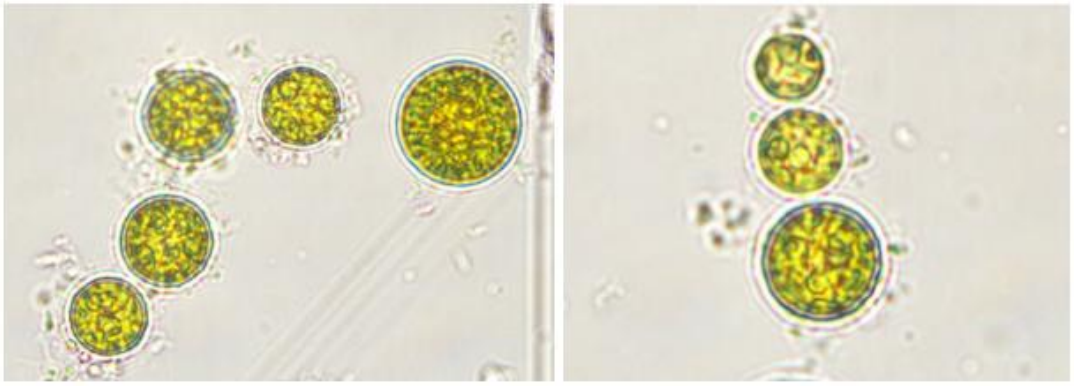
Day 5



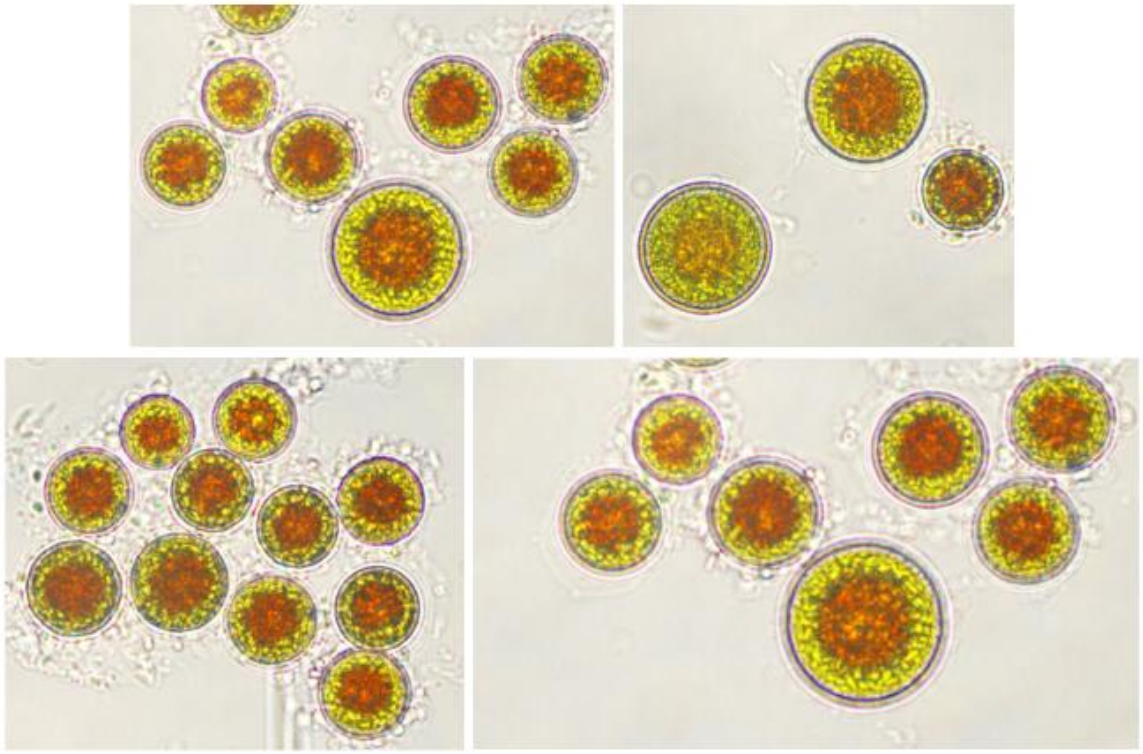
Day 7



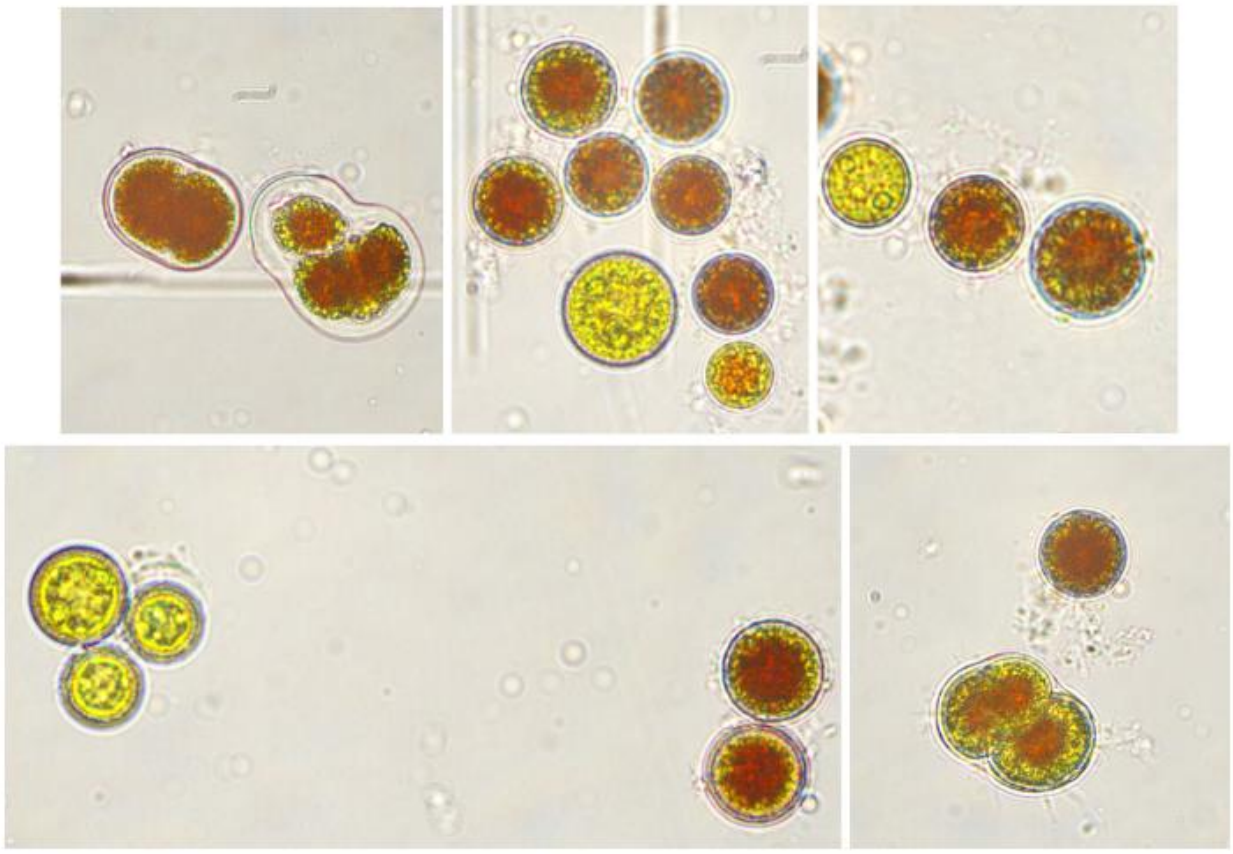
Day 8



Day 10



Day 12



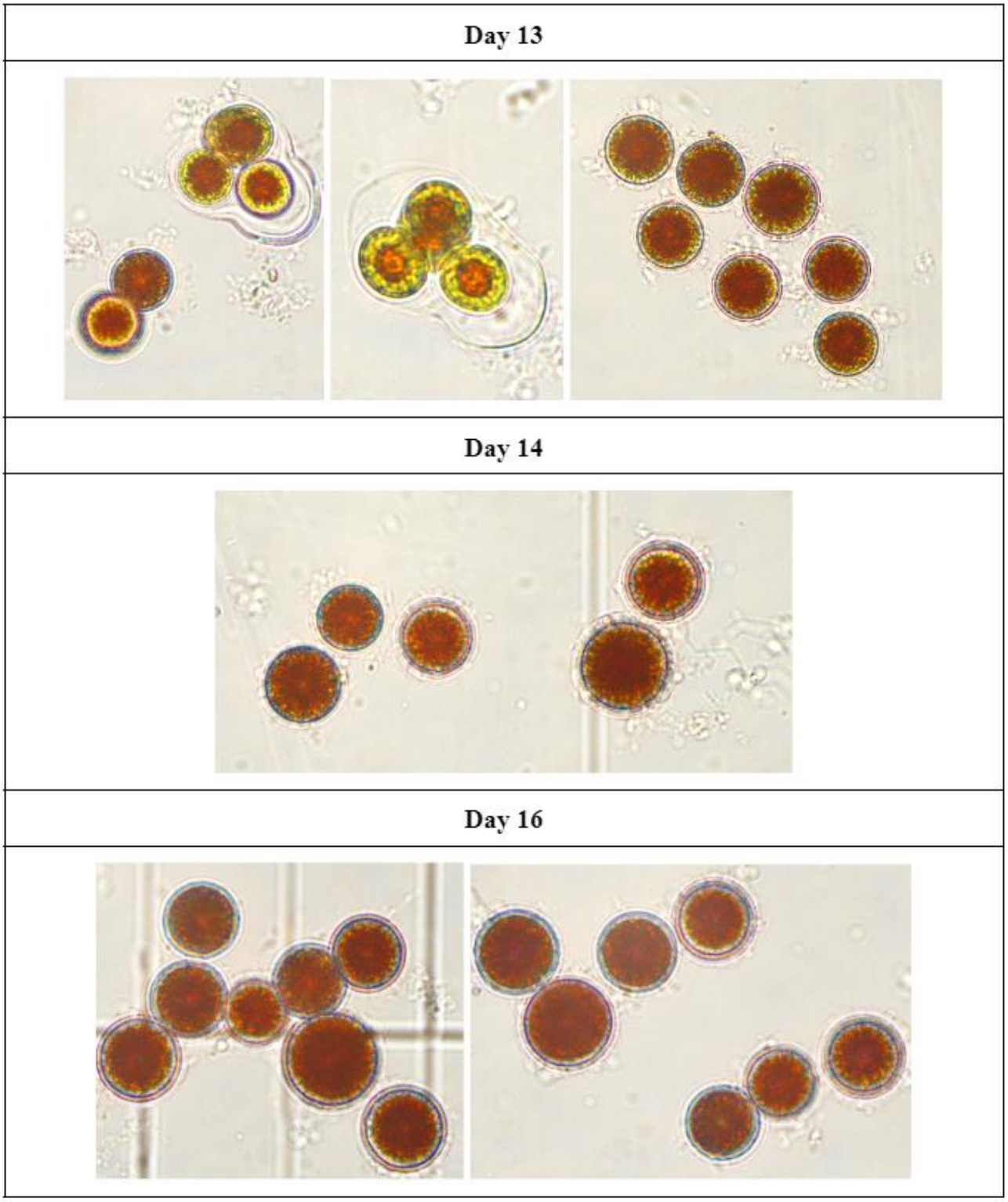


Figure 4.12. Cell phase status of *H. lacustris* CCAP 34/6 strain under red phase stress conditions.

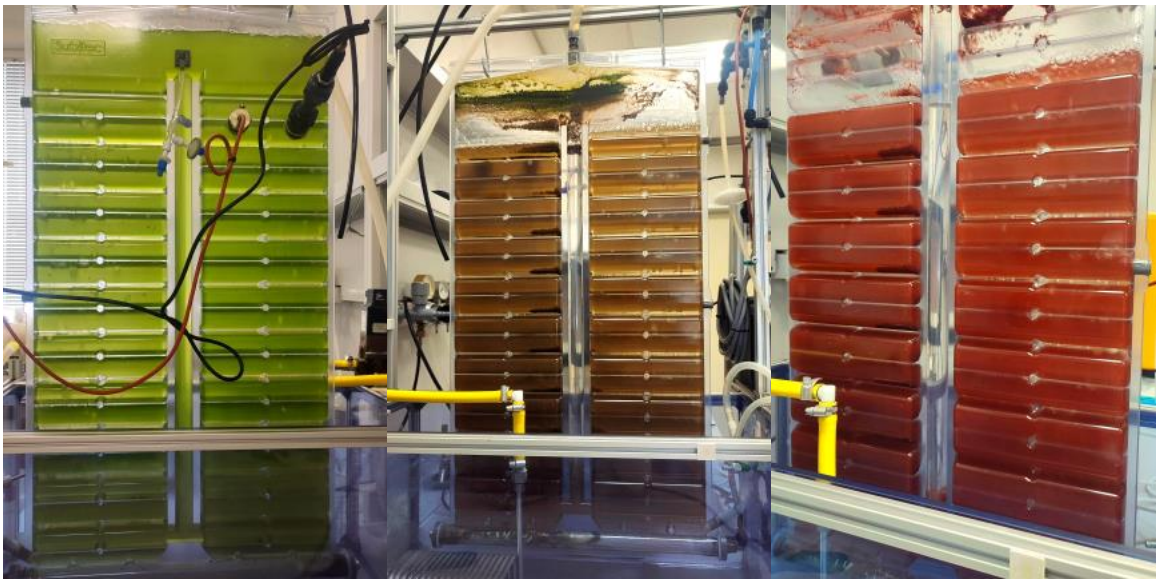


Figure 4.13. Change from Day 1 to Day 16 and astaxanthin accumulation of *Haematococcus lacustris* CCAP 34/6 strain in 6L Flat Panel PBR under red phase conditions.

4.4. Dry Weight Analyses

This section includes the dry weight analyses of the *H. lacustris* CCAP 34/6 strain harvested in the red phase in the previous step. Comprehensive information on these analyses are given in Table 4.8.

The calculations were performed using 9 homogeneous samples taken from the culture in 3 repetitions, and the findings were derived from the mean values. Accordingly, the biomass harvested in the red phase of the culture was 2.02 g/L.

Table 4.8. Dry weight analysis of *H. lacustris* CCAP 34/6 harvested in the red phase.

Dry weight analysis				
W1: Filter + Aluminum Weighing Dish **W2:** Filter + Aluminum Weighing Dish + Sample				
Equations: W2(g) -W1(g) x 100 = M (biomass) M (biomass) = Dry weight of the algae in culture				
Measurement				
Samples	**W2 (g)**	**W1 (g)**	**W2-W1(g)**	Average value W2-W1 = 0.0202 g/10 ml **= 2.02 g/L**
Sample 1	1.09	1.0699	0.0201	
Sample 2	1.0964	1.0763	0.0201	
Sample 3	1.0951	1.0747	0.0204	

4.5. Astaxanthin Extraction

This section focuses on the extraction of astaxanthin from the *H. lacustris* CCAP 34/6 strain obtained in the red phase. The extraction procedure was conducted following the methodology outlined by Boussiba et al., (1991), Sun et al., (2017), and Davines et al. (Davines, 1976). The achieved results are presented in Table 4.9.

Upon comparison with the dry weight data of the culture, the concentration of astaxanthin was determined to be 0.021 (%, w/w). When compared to existing literature, a result within the range of 1%-5% was achieved (Molino et al., 2018; Shah, Liang, Cheng, & Daroch, 2016).

Table 4.9. Astaxanthin concentration analysis of *H. lacustris* CCAP 34/6 harvested in the red phase.

Astaxanthin concentration analysis
Equations: c (mg/L)= 4.5 x A_{490nm} x V_a x V_b Astaxanthin content (%, w/w) : $C = C_t / m_t$ *c:* per unit volume astaxanthin concentration V_a (L): Volume of extract V_b (L): Volume of culture sample c_t (mg/L): Astaxanthin concentration
Measurement
Astaxanthin content (%, w/w) : $C = C_t / m_t$ **= 0.021**

It has been reported in the literature that *Haematococcus* can generally produce 1-3% of the dry biomass amount of astaxanthin and this amount can be up to 5% (Molino et al., 2018; Shah, Liang, Cheng, & Daroch, 2016). When the data obtained as a result of this study are evaluated, it is seen that 2.1% astaxanthin accumulation in *Haematococcus lacustris* CCAP 34/6 strain was obtained in an acceptable range in accordance with the literature.

4.6. Encapsulation

4.6.1. Optimization of Encapsulation

In this section, astaxanthin optimization was performed by evaluating the alginate and $CaCl_2$ concentration, ambient temperature, and the amount of astaxanthin loaded into the beads. The results obtained are detailed in Tables 4.10-12.

The concentrations of alginate were examined under three different conditions: 1.5%, 2%, and 3%. Table 4.10 revealed that the optimal alginate concentration was 3%. The analyses of $CaCl_2$ concentrations (0.15M, 0.3M, and 0.5M) show that the optimal condition was established at 0.3 M. Temperature testing conducted with 3% alginate and 0.3 M $CaCl_2$ conditions indicated that ambient temperature outperforms +4°C in terms of loading efficiency. In the determination of the amount of astaxanthin to be loaded into the beads, three conditions, 10 mg/L, 25 mg/L, and 50 mg/L, were compared, and it was observed that the 50 mg/L condition gave the best result.

Table 4.10. Alginate and $CaCl_2$ optimization

Sample	C-PC mass in supernatant (mg)	C-PC mass in beads	Loading efficiency (%)
1,5% Alginate 0,15 M $CaCl_2$	1.679	0.458	21.4
	1.561	0.576	27.0
	1.333	0.804	37.6
1,5% Alginate 0,3 M $CaCl_2$	1.389	0.749	35.0
	1.505	0.633	29.6
	1.407	0.730	34.2
1,5% Alginate 0,5 M $CaCl_2$	1.641	0.497	23.2
	1.531	0.606	28.4
	1.538	0.599	28.0
2% Alginate 0,15 M $CaCl_2$	1.744	0.821	32.0
	1.597	0.968	37.7
	1.607	0.958	37.3
2% Alginate 0,3 M $CaCl_2$	1.624	0.941	36.7
	1.614	0.951	37.1
	1.644	0.921	35.9
2% Alginate 0,5 M CaCl2	1.664	0.901	35.1
	1.575	0.990	38.6
	1.567	0.998	38.9
3% Alginate 0,15 M $CaCl_2$	1.724	1.839	**51.6**
	1.715	1.848	**51.9**
	1.674	1.888	**53.0**
3% Alginate 0,3 M $CaCl_2$	1.702	1.860	**52.4**
	1.653	1.910	**53.6**
	1.700	1.862	**52.3**
3%Alginate 0,5 M $CaCl_2$	1.519	2.044	**57.4**
	1.789	1.774	**49.8**
	1.739	1.823	**51.0**

Table 4.11. Encapsulation temperature optimization

Sample	Temperature	Total C-PC mass (mg)	C-PC mass in beads	Loading efficiency (%)
3% Alginate 0,3 M $CaCl_2$	Room	0.864	0.637	**73.8**
		0.864	0.587	**67.9**
		0.864	0.675	**78.2**
	+4°C	0.864	0.431	**49.9**
		0.864	0.474	**54.9**
		0.864	0.474	**54.9**

Table 4.12. Astaxanthin amount optimization

Astaxanthin Amount (mg/L)	Temperature	Loading efficiency (%)
10 mg/L	Room	94.8
		88.8
		90.3
25 mg/ L		91.9
		89.8
		88
50 mg/L		**94.4**
		95.1
		95.7

4.6.2. Encapsulation of Astaxanthin

The astaxanthin extract produced in section 4.5 underwent encapsulation using the optimized protocols outlined in section 4.6.1. Therefore, beads were synthesized by combining 3% alginate with 50 mg/L astaxanthin extract in a 0.3 M $CaCl_2$ solution at ambient temperature.

As presented in Figure 4.14., accompanied by stereo microscope images, edible beads sized 4 mm and 8 mm in diameter, within a total volume of 20 ml, provide the consumer with a final product containing 1 mg of pure astaxanthin.

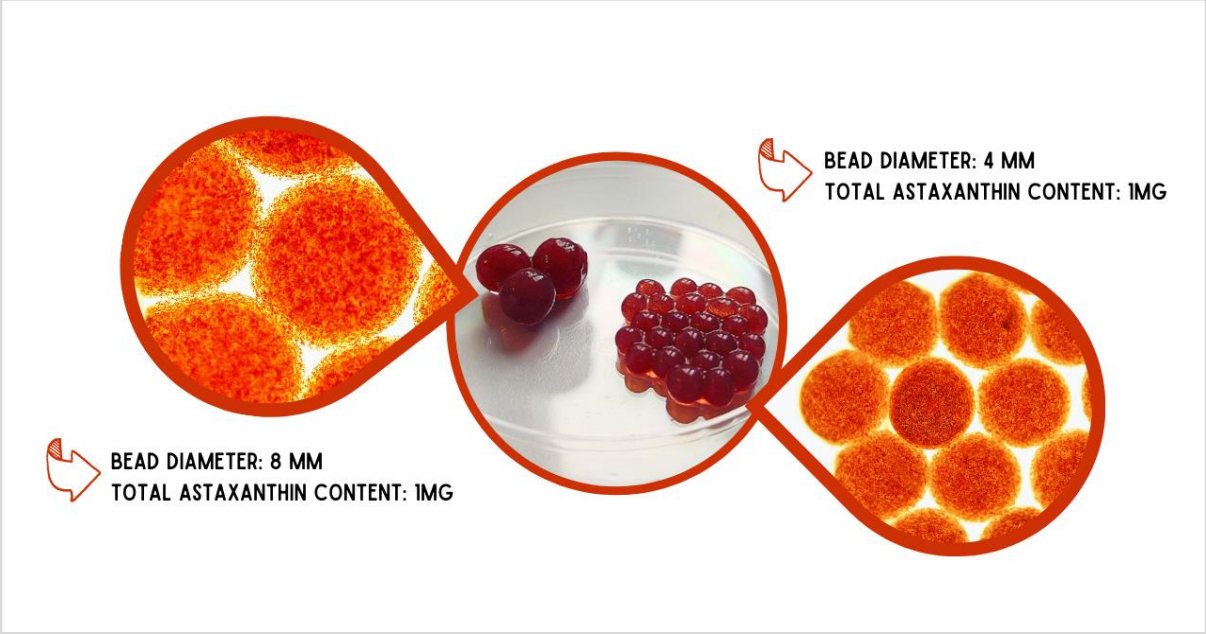


Figure 4. 14. Encapsulated form of astaxanthin extracted from *Haematococcus lacustris* CCAP 34/6 strain in 4 mm and 8 mm diameter form.

When the final product is evaluated both in terms of research-development studies and what it offers to the end consumer, the following results emerge: Astaxanthin derived from natural sources seems to be advantageous in all aspects, in contrast to a compound that constitutes 97% of the market as a commercial product with its synthetic counterpart (Schmidt et al., 2011). Moreover, it is a natural product that is not only derived from a natural source, but also sustainably produced until it is combined with sodium alginate, also derived from microalgae, and encapsulated in the final product form. Considering how natural astaxanthin compound has shown beneficial results for human health in various studies, the fact that its synthetic alternative by-products (Nair et al., 2023) are not suitable for human use (Gateau et al., 2017) once again highlights the difference between the two. In addition, considering that natural astaxanthin is 50 times more effective antioxidant than synthetic (Capelli et

al., 2013), it is clear that the contributions to the literature on the natural production of this important compound are very important.

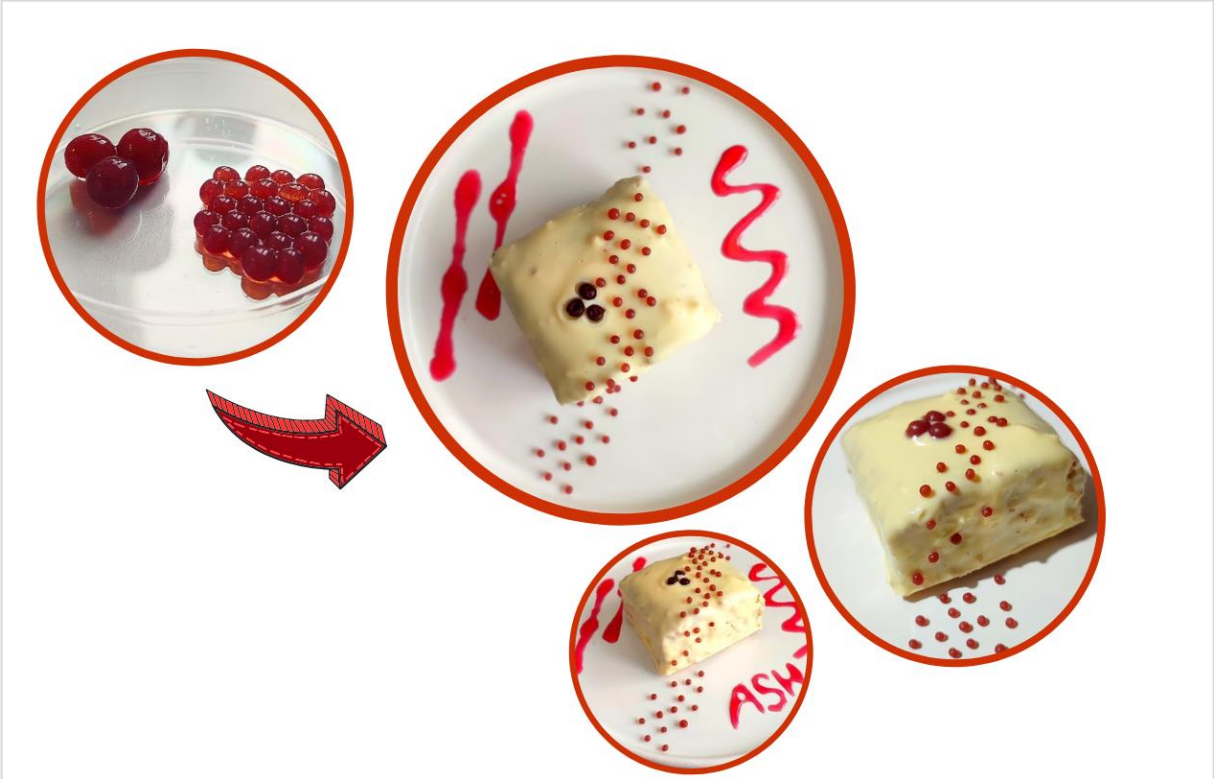


Figure 4.15. Instances of alternate plates using encapsulated astaxanthin beads.

The primary underlying motives of the research may be succinctly summarised as follows: The principal objective of the research was to investigate the distinct phases of *Haematococcus lacustris* CCAP 34/6 strains and to optimise conditions for astaxanthin synthesis while maintaining cell viability. Optimal circumstances were achieved after meticulous research.

Another underlying objective of this thesis is to render the astaxanthin extract appropriate for human consumption. An improved encapsulation technique using sodium alginate, a microalgal product, has been optimized to accomplish this. Consequently, in the future, food consumption will be feasible, as seen in Figure 4.15.

From a sustainability perspective, the final product, which creates a positive ground in terms of both method and resource utilization, is also an important product when evaluated in terms of its potential to be used as food supply or alternative food content, as it is among the alternatives that can be a solution to the food crisis. In Figure 4.15, a plate was prepared using the beads obtained as a

concrete example of alternative food. In the near future, it is possible to see foods with high nutritional content and positive effects on human health.

Another background motivation of the study is to contribute to an integrated biorefinery system aiming at environmentally friendly, sustainable and economically efficient astaxanthin production. The synthesis of astaxanthin seems feasible within the framework of biorefinery, characterised by the simultaneous generation of several compounds in a unified system, hence optimising advantages and minimising expenses. The astaxanthin compound adheres to the "high value first" idea used in biorefinery concepts and merits attention. Nonetheless, it seems amenable to an exhaustive analysis owing to the systematic methodologies and rigorous operational conditions necessitated by the manufacturing environment. Furthermore, a comprehensive study of other by-products, including oil extraction from *Haematococcus*, may be more appropriate for the biorefinery idea and seems to need further investigation before a conclusive choice is made.

5. CONCLUSIONS AND RECOMMENDATIONS

Astaxanthin has become a value-added biocompound in high demand for its many health benefits, especially antioxidant properties. The synthesis of astaxanthin can be achieved using either natural or synthetic methods. Nevertheless, natural astaxanthin outperforms the synthetic alternative in some aspects and assumes its position in the industry in a form applicable for human use.

Haematococcus one of the most prominent microalgae species, among natural options with its ability to accumulate high astaxanthin. In this study, one of the less-studied *Haematococcus lacustris* CCAP 34/6 strain was evaluated in terms of optimal astaxanthin accumulation conditions and the obtained extract was presented as the final product in encapsulated edible form. For this purpose, the relevant strain was subjected to various processes in stages under the studies divided into two main headings: green phase and red phase. Suitable growth medium, sonication option and white-blue-red light sources were evaluated with multiwell plate tests. Light, temperature, growth medium and sonication conditions were evaluated in the study carried to a higher volume with Erlenmeyer flask tests. Based on the acquired information on the optimal conditions, astaxanthin was synthesised from the culture cultivated in a 6L volume. It was subsequently extracted and encapsulated under the optimal encapsulation conditions and obtained in an edible form.

This study showed that non-sonicated culture in the green phase at 23°C provided the most optimal growth conditions by showing 308.21%, 301.63% and 290.78% biomass increases in 3N:BBM, BG11 and 3P:BBM media under gradual blue-red light treatment, respectively. The highest astaxanthin accumulation in the red phase was obtained in BG11-N medium under gradual blue light and at 28°C. After large-scale cultivation, 2.02 g/L biomass was produced as dry weight and 2.1% astaxanthin was obtained. In the encapsulation process, the most optimal conditions were obtained with 0.3M $CaCl_2$, 3% sodium alginate and 50 mg/L pure astaxanthin extract at room temperature, and according to these conditions, edible beads with 4mm and 8mm diameters containing 1 mg pure astaxanthin (in a total volume of 20 ml) were produced. Overall, this thesis study provided valuable information to the literature as the findings of a comprehensive study that starts at the cellular level and extends to the final encapsulated product by creating the most suitable growth conditions for one of the most potent known antioxidant astaxanthin production in *Haematococcus lacustris* CCAP 34/6 strain.

REFERENCES

Ahirwar, A., Meignen, G., Khan, M. J., Sirotiya, V., Scarsini, M., Roux, S., Marchand, J., Schoefs, B., & Vinayak, V. (2021). Light modulates transcriptomic dynamics upregulating astaxanthin accumulation in *Haematococcus*: A review. *Bioresource Technology, 340*, 125707. https://doi.org/10.1016/j.biortech.2021.125707

Becker, E. W. (2013). Microalgae for human and animal nutrition. In A. Richmond & Q. Hu (Eds.), *Handbook of microalgal culture: Applied phycology and biotechnology* (2nd ed., pp. 461–503). Wiley Blackwell.

Bhuvaneswari, S., Yogalakshmi, B., Sreeja, S., & Anuradha, C. V. (2014). Astaxanthin reduces hepatic endoplasmic reticulum stress and nuclear factor-κB-mediated inflammation in high fructose and high fat diet-fed mice. *Cell Stress & Chaperones, 19*(2), 183–191. https://doi.org/10.1007/s12192-013-0465-2

Boussiba, S., & Vonshak, A. (1991). Astaxanthin accumulation in the green alga *Haematococcus pluvialis*. *Plant Cell Physiology, 32*(8), 1077–1082. https://doi.org/10.1093/oxfordjournals.pcp.a078477

Cáceres, L. M., Velasco, G. A., Dagnino, E. P., & Chamorro, E. R. (2020). Microencapsulation of grapefruit oil with sodium alginate by gelation and ionic extrusion: Optimization and modeling of crosslinking and study of controlled release kinetics. *Journal of Microencapsulation, 37*(3), 203–216. https://doi.org/10.1080/02652048.2020.1752293

Capelli, B., Bagchi, D., & Cysewski, G. R. (2013). Synthetic astaxanthin is significantly inferior to algal-based astaxanthin as an antioxidant and may not be suitable as a human nutraceutical supplement. *Nutrafoods, 12*, 145–152.

Capelli, B., Talbott, S., & Ding, L. (2019). Astaxanthin sources: Suitability for human health and nutrition. *Functional Foods in Health and Disease, 9*, 430–445.

Chew, B. P., Wong, M. W., Park, J. S., & Wong, T. S. (1999). Dietary beta-carotene and astaxanthin but not canthaxanthin stimulate splenocyte function in mice. *Anticancer Research, 19*(6B), 5223–5227.

Choi, H. D., Kim, J. H., Chang, M. J., Kyu-Youn, Y., & Shin, W. G. (2011). Effects of astaxanthin on oxidative stress in overweight and obese adults. *Phytotherapy Research, 25*(12), 1813–1818. https://doi.org/10.1002/ptr.3533

Choi, Y. E., Yun, Y.-S., & Park, J. M. (2002). Evaluation of factors promoting astaxanthin production by a unicellular green alga, *Haematococcus pluvialis*, with fractional factorial design. *Biotechnology Progress, 18*(6), 1170–1175.

Choi, Y. Y., Hong, M.-E., & Sim, S. J. (2015). Enhanced astaxanthin extraction efficiency from *Haematococcus pluvialis* via the cyst germination in outdoor culture systems. *Process Biochemistry, 50*(12), 2275–2280. https://doi.org/10.1016/j.procbio.2015.09.015

Christwardana, M., & Hadiyanto, H. (2017). The effects of audible sound for enhancing the growth rate of microalgae *Haematococcus pluvialis* in vegetative stage. *HAYATI Journal of Biosciences, 24*(3), 149–155. https://doi.org/10.1016/j.hjb.2017.10.001

Coral-Hinostroza, G. N., Ytrestøyl, T., Ruyter, B., & Bjerkeng, B. (2004). Plasma appearance of unesterified astaxanthin geometrical E/Z and optical R/S isomers in men given single doses of a mixture of optical 3 and 3'R/S isomers of astaxanthin fatty acyl diesters. *Comparative Biochemistry and Physiology Part C: Toxicology & Pharmacology, 139*(1-3), 99–110. https://doi.org/10.1016/j.cca.2004.09.011

Cunningham, F. X., & Gantt, E. (2005). A study in scarlet: Enzymes of ketocarotenoid biosynthesis in the flowers of *Adonis aestivalis*: Adonis β-ring oxygenases. *Plant Journal, 41*, 478–492. https://doi.org/10.1111/j.1365-313X.2004.02255.x

Czygan, F. C. (1970). Blood-rain and blood-snow: Nitrogen-deficient cells of *Haematococcus pluvialis* and *Chlamydomonas nivalis*. *Archiv für Mikrobiologie, 74*(1), 69–76.

Çakmak, T., Angun, P., Demiray, Y. E., Özkan, A. D., Elibol, Z., & Tekinay, T. (2012). Differential effects of nitrogen and sulfur deprivation on growth and biodiesel feedstock production of

Chlamydomonas reinhardtii. *Biotechnology and Bioengineering*, *109*(8), 1947–1957. https://doi.org/10.1002/bit.24464

Davinelli, S., Nielsen, M. E., & Scapagnini, G. (2018). Astaxanthin in skin health, repair, and disease: A comprehensive review. *Nutrients*, *10*(4), Article 522. https://doi.org/10.3390/nu10040522

Denery, J. R., Dragull, K., Tang, C. S., & Li, Q. X. (2004). Pressurized fluid extraction of carotenoids from *Haematococcus pluvialis* and *Dunaliella salina* and kavalactones from *Piper methysticum*. *Analytica Chimica Acta*, *501*, 175–181. https://doi.org/10.1016/j.aca.2003.09.026

Domínguez-Bocanegra, A. R., Ponce-Noyola, T., & Torres-Muñoz, J. A. (2007). Astaxanthin production by *Phaffia rhodozyma* and *Haematococcus pluvialis*: A comparative study. *Applied Microbiology and Biotechnology*, *75*(4), 783–791. https://doi.org/10.1007/s00253-007-0889-9

EFSA FEEDAP Panel. (2005). Opinion of the Scientific Panel on Additives and Products or Substances used in Animal Feed on the request from the European Commission on the safety of use of colouring agents in animal nutrition: Part I. General principles and astaxanthin. *EFSA Journal*, *291*, 1–40. https://doi.org/10.2903/j.efsa.2005.291

Eriksen, N. T. (2008). The technology of microalgal culturing. *Biotechnology Letters*, *30*(12), 1525–1536. https://doi.org/10.1007/s10529-008-9812-8

Fábregas, J., Domínguez, A., Maseda, A., & Otero, A. (2003). Interactions between irradiance and nutrient availability during astaxanthin accumulation and degradation in *Haematococcus pluvialis*. *Applied Microbiology and Biotechnology*, *61*(5), 545–551. https://doi.org/10.1007/s00253-002-1207-0

Ferrante, R. J., Browne, S. E., Shinobu, L. A., Bowling, A. C., Baik, M. J., MacGarvey, U., et al. (1997). Evidence of increased oxidative damage in both sporadic and familial amyotrophic lateral sclerosis. *Journal of Neurochemistry*, *69*(5), 2064–2074. https://doi.org/10.1046/j.1471-4159.1997.69052064.x

Gao, Z., Meng, C., Zhang, X., Xu, D., Miao, X., Wang, Y., & others. (2012). Induction of salicylic acid (SA) on transcriptional expression of eight carotenoid genes and astaxanthin accumulation in

Haematococcus pluvialis. *Enzyme and Microbial Technology*, *51*, 225–230. https://doi.org/10.1016/j.enzmictec.2012.07.001

Gateau, H., Solymosi, K., Marchand, J., & Schoefs, B. (2017). Carotenoids of microalgae used in food industry and medicine. *Mini-Reviews in Medicinal Chemistry*, *17*(12), 1140–1172.

Giannelli, L., Yamada, H., Katsuda, T., & Yamaji, H. (2015). Effects of temperature on the astaxanthin productivity and light harvesting characteristics of the green alga *Haematococcus pluvialis*. *Journal of Bioscience and Bioengineering*, *119*(3), 345–350. https://doi.org/10.1016/j.jbiosc.2014.10.008

Gibbs, B. F., Kermasha, S., Alli, I., & Mulligan, C. N. (1999). Encapsulation in the food industry: A review. *International Journal of Food Sciences and Nutrition*, *50*(3), 213–224. https://doi.org/10.1080/096374899101256

Han, D., Li, Y., & Hu, Q. (2013). Biology and commercial aspects of *Haematococcus pluvialis*. In A. Richmond & Q. Hu (Eds.), *Handbook of Microalgal Culture: Applied Phycology and Biotechnology* (2nd ed., pp. 388–405). Wiley Blackwell.

Han, S., Jeon, M. S., Ahn, J., & Choi, Y. (2022). Establishment of ultrasonic stimulation to enhance growth of *Haematococcus lacustris*. *Bioresource Technology*, *360*, 127525. https://doi.org/10.1016/j.biortech.2022.127525

Hazen, T. E. (1899). The life history of *Sphaerella lacustris*. *Memoirs of the Torrey Botanical Club*, *6*, 211–244.

Heimann, K., & Huerlimann, R. (2015). Microalgal classification: Major classes and genera of commercial microalgal species. In *Handbook of Marine Microalgae* (p. 25). Elsevier.

Higuera-Ciapara, I., Félix-Valenzuela, L., & Goycoolea, F. M. (2006). Astaxanthin: A review of its chemistry and applications. *Critical Reviews in Food Science and Nutrition*, *46*(2), 185–196. https://doi.org/10.1080/10408690590957188

Hong, M. E., Hwang, S. K., Chang, W. S., Kim, B. W., Lee, J., & Sim, S. J. (2015). Enhanced autotrophic astaxanthin production from *Haematococcus pluvialis* under high temperature via heat

stress-driven Haber–Weiss reaction. *Applied Microbiology and Biotechnology*, *99*(13), 5203–5215. https://doi.org/10.1007/s00253-015-6600-2

Huo, S., Shang, C., Wang, Z., Zhou, W., Cui, F., Zhu, F., Yuan, Z., & Dong, R. (2017). Outdoor growth characterization of an unknown microalga screened from contaminated *Chlorella* culture. *Biomedical Research International*, *2017*, 5681617. https://doi.org/10.1155/2017/5681617

Iwamoto, T., Hosoda, K., Hirano, R., Kurata, H., Matsumoto, A., Miki, W., et al. (2000). Inhibition of low-density lipoprotein oxidation by astaxanthin. *Journal of Atherosclerosis and Thrombosis*, *7*(3), 216–222. https://doi.org/10.5551/jat1994.7.216

Jannel, S., Caro, Y., Bermudes, M., & Petit, T. (2020). Novel insights into the biotechnological production of *Haematococcus pluvialis*-derived astaxanthin: Advances and key challenges to allow its industrial use as a novel food ingredient. *Journal of Marine Science and Engineering*, *8*(10), 789. https://doi.org/10.3390/jmse8100789

Jareonsin, S., & Pumas, C. (2021). Advantages of heterotrophic microalgae as a host for phytochemicals production. *Frontiers in Bioengineering and Biotechnology*, *9*. https://doi.org/10.3389/fbioe.2021.741276

Kang, C. D., & Sim, S. J. (2008). Direct extraction of astaxanthin from *Haematococcus* culture using vegetable oils. *Biotechnology Letters*, *30*(3), 441–444. https://doi.org/10.1007/s10529-007-9578-0

Karppi, J., Rissanen, T. H., Nyyssönen, K., Kaikkonen, J., Olsson, A. G., Voutilainen, S., et al. (2007). Effects of astaxanthin supplementation on lipid peroxidation. *International Journal for Vitamin and Nutrition Research*, *77*(1), 3–11. https://doi.org/10.1024/0300-9831.77.1.3

Khan, H. (2020). Astaxanthin anticancer effects are mediated through multiple molecular mechanisms: A systematic review. *Pharmacological Research*, *155*, 104689. https://doi.org/10.1016/j.phrs.2020.104689

Kim, D. Y., Vijayan, D., Praveenkumar, R., Han, J. I., Lee, K., Park, J. Y., Chang, W. S., Lee, J. S., & Oh, Y. K. (2016). Cell-wall disruption and lipid/astaxanthin extraction from microalgae: *Chlorella* and *Haematococcus*. *Bioresource Technology*, *199*, 300–310. https://doi.org/10.1016/j.biortech.2015.08.107

Kim, J. H., Chang, M. J., Choi, H. D., Youn, Y.-K., Kim, J. T., Oh, J. M., & Shin, W. G. (2011). Protective effects of *Haematococcus* astaxanthin on oxidative stress in healthy smokers. *Journal of Medicinal Food, 14*(12), 1469–1475. https://doi.org/10.1089/jmf.2010.0168

Kishimoto, Y., Yoshida, H., & Kondo, K. (2016). Potential anti-atherosclerotic properties of astaxanthin. *Marine Drugs, 14*(35). https://doi.org/10.3390/md14010035

Kuhn, R., & Sörensen, N. A. (1938). Über astaxanthin und ovoverdin. *Berichte der Deutschen Chemischen Gesellschaft A/B Series, 71*, 1879–1888. https://doi.org/10.1002/cber.19380710918

Leonardi, P. I., Popovich, C. A., & Damiani, M. C. (2011). Feedstocks for second-generation biodiesel: Microalgae's biology and oil composition. In M. A. d. S. Bernardes (Ed.), *Economic effects of biofuel production* (pp. 317–347). InTech. https://doi.org/10.5772/23125

Li, F., Cai, M., Lin, M., Huang, X., Wang, J., Zheng, X., Wu, S., & An, Y. (2019). Accumulation of astaxanthin was improved by the nonmotile cells of *Haematococcus pluvialis*. *BioMed Research International, 2019*, 8101762. https://doi.org/10.1155/2019/8101762

Li, J., Zhu, D., Niu, J., Shen, S., & Wang, G. (2011). An economic assessment of astaxanthin production by large scale cultivation of *Haematococcus pluvialis*. *Biotechnology Advances, 29*(6), 568–574.

Lin, S.-F., Chen, Y.-C., Chen, R.-N., Chen, L.-C., Ho, H.-O., Tsung, Y.-H., & et al. (2016). Improving the stability of astaxanthin by microencapsulation in calcium alginate beads. *PLoS ONE, 11*(4), e0153685. https://doi.org/10.1371/journal.pone.0153685

Ma, R., Thomas-Hall, S. R., Chua, E. T., Eltanahy, E., Netzel, M. E., Netzel, G., Lu, Y., & Schenk, P. M. (2018). Blue light enhances astaxanthin biosynthesis metabolism and extraction efficiency in *Haematococcus pluvialis* by inducing haematocyst germination. *Algal Research, 35*, 215–222. https://doi.org/10.1016/j.algal.2018.09.020

Mao, X. M., Wu, T., Sun, D. Z., Zhang, Z., & Chen, F. (2018). Differential responses of the green microalga *Chlorella zofingiensis* to the starvation of various nutrients for oil and astaxanthin production. *Bioresource Technology, 249*, 791–798. https://doi.org/10.1016/j.biortech.2017.10.097

Markou, G., & Nerantzis, E. (2013). Microalgae for high-value compounds and biofuels production: A review with focus on cultivation under stress conditions. *Biotechnology Advances, 31*(8), 1532–1542.

McNulty, H. P., Byun, J., Lockwood, S. F., Jacob, R. F., & Mason, R. P. (2007). Differential effects of carotenoids on lipid peroxidation due to membrane interactions: X-ray diffraction analysis. *Biochimica et Biophysica Acta, 1768*(1), 167–174. https://doi.org/10.1016/j.bbamem.2006.09.010

McNulty, H., Jacob, R. F., & Mason, R. P. (2008). Biologic activity of carotenoids related to distinct membrane physicochemical interactions. *The American Journal of Cardiology, 101*(10A), 20D–29D. https://doi.org/10.1016/j.amjcard.2008.02.004

Mehariya, S., Sharma, N., Iovine, A., Casella, P., Marino, T., Larocca, V., Molino, A., & Musmarra, D. (2020). An integrated strategy for nutraceuticals from *Haematococcus pluvialis*: From cultivation to extraction. *Antioxidants, 9*(9), 825. https://doi.org/10.3390/antiox9090825

Miki, W. (1991). Biological functions and activities of animal carotenoids. *Pure and Applied Chemistry, 63*(1), 141–146. https://doi.org/10.1351/pac199163010141

Miyawaki, H., Takahashi, J., Tsukahara, H., & Takehara, I. (2008). Effects of astaxanthin on human blood rheology. *Journal of Clinical Biochemistry and Nutrition, 43*(1), 69–74. https://doi.org/10.3164/jcbn.2008048

Mohamed, H., & Al-Kahtani, H. (2014). Bioprocessing of microalgae for the production of biodiesel: A review. *Journal of Applied Phycology, 26*(6), 2227–2236. https://doi.org/10.1007/s10811-014-0491-3

Molino, A., Iovine, A., Casella, P., Mehariya, S., Chianese, S., Cerbone, A., Rimauro, J., & Musmarra, D. (2018). Microalgae characterization for consolidated and new applications in human food, animal feed, and nutraceuticals. *International Journal of Environmental Research and Public Health, 15*(11), 2436. https://doi.org/10.3390/ijerph15112436

Naguib, Y. M. A. (2000). Antioxidant activities of astaxanthin and related carotenoids. *Journal of Agricultural and Food Chemistry, 48*(4), 1150–1154. https://doi.org/10.1021/jf990960n

Nahidian, B., Ghanati, F., Shahbazi, M., & Soltani, N. (2018). Effect of nutrients on the growth and physiological features of newly isolated *Haematococcus pluvialis* TMU. *Bioresource Technology*, *255*, 229–237. https://doi.org/10.1016/j.biortech.2018.01.045

Naito, Y., Uchiyama, K., Aoi, W., Hasegawa, G., Nakamura, N., Yoshida, N., Maoka, T., Takahashi, J., & Yoshikawa, T. (2004). Prevention of diabetic nephropathy by treatment with astaxanthin in diabetic db/db mice. *BioFactors*, *20*(1), 49–59. https://doi.org/10.1002/biof.5520200108

Nakada, T., & Ota, S. (2016). What is the correct name for the type of *Haematococcus* Flot. (Volvocales, Chlorophyceae)? *TAXON*, *65*(2), 343-348. https://doi.org/10.12705/652.11

Nakajima, Y., Inokuchi, Y., Shimazawa, M., Otsubo, K., Ishibashi, T., & Hara, H. (2008). Astaxanthin, a dietary carotenoid, protects retinal cells against oxidative stress in vitro and in mice in vivo. *Journal of Pharmacy and Pharmacology*, *60*(10), 1365–1374. https://doi.org/10.1211/jpp.60.10.0001

Niizawa, I., Espinaco, B. Y., Leonardi, J. R., Heinrich, J. M., & Sihufe, G. A. (2018). Enhancement of astaxanthin production from *Haematococcus pluvialis* under autotrophic growth conditions by a sequential stress strategy. *Preparative Biochemistry & Biotechnology*, *48*(6), 528–534. https://doi.org/10.1080/10826068.2018.1495091

Oslan, S. N. H., Shoparwe, N. F., Yusoff, A. H., Rahim, A. A., Chang, C. S., Tan, J. S., Oslan, S. N., Arumugam, K., Ariff, A. B., Sulaiman, A. Z., & Mohamed, M. S. (2021). A review on *Haematococcus pluvialis* bioprocess optimization of green and red stage culture conditions for the production of natural astaxanthin. *Biomolecules*, *11*(2), 256. https://doi.org/10.3390/biom11020256

Ozcelik, D., Sakarya, F. K., Erdinçler, B., Yılmaz, A., Avcı, S., Borhan, E., & Haznedaroğlu, B. Z. (2021). Recent advancements in algal biorefineries. In A. Shekh & R. Sarada (Eds.), *Microalgal Biotechnology: Recent advances, market potential, and sustainability* (p. 77). The Royal Society of Chemistry.

Pang, N., Gu, X., Fu, X., & Chen, S. (2019). Effects of gluconate on biomass improvement and light stress tolerance of *Haematococcus pluvialis* in mixotrophic culture. *Algal Research*, *43*, 101647. https://doi.org/10.1016/j.algal.2019.101647

Pan-utai, W., Parakulsuksatid, P., & Phomkaivon, N. (2017). Effect of inducing agents on growth and astaxanthin production in *Haematococcus pluvialis*: Organic and inorganic. *Biocatalysis and Agricultural Biotechnology, 12*, 152–158. https://doi.org/10.1016/j.bcab.2017.10.004

Park, J., Chyun, J., Kim, Y., Line, L. L., & Chew, B. P. (2010). Astaxanthin decreased oxidative stress and inflammation and enhanced immune response in humans. *Nutrition & Metabolism, 7*, 18. https://doi.org/10.1186/1743-7075-7-18

Peng, J., Xiang, W., Tang, Q., Sun, N., Chen, F., & Yuan, J. (2008). Comparative analysis of astaxanthin and its esters in the mutant E1 of *Haematococcus pluvialis* and other green algae by HPLC with a C30 column. *Science in China Series C: Life Sciences, 51*, 1108–1115.

Pulz, O., & Gross, W. (2004). Valuable products from biotechnology of microalgae. *Applied Microbiology and Biotechnology*, *65*(6), 635–648. https://doi.org/10.1007/s00253-004-1527-4

Ren, H.-Y., Xiao, R.-N., Kong, F., Zhao, L., Xing, D., Ma, J., Ren, N.-Q., & Liu, B.-F. (2019). Enhanced biomass and lipid accumulation of mixotrophic microalgae by using low-strength ultrasonic stimulation. *Bioresource Technology, 272*, 606–610. https://doi.org/10.1016/j.biortech.2018.10.065

Ruen-ngam, D., Shotipruk, A., & Pavasant, P. (2010). Comparison of extraction methods for recovery of astaxanthin from *Haematococcus pluvialis*. *Separation Science and Technology, 46*, 64–70. https://doi.org/10.1080/01496395.2010.493546

Santos, A., Janssen, M., Lamers, P., Evers, W., & Wijffels, R. (2012). Growth of oil-accumulating microalga *Neochloris oleoabundans* under alkaline–saline conditions. *Bioresource Technology, 104*, 593–599. https://doi.org/10.1016/j.biortech.2011.11.079

Sato, R., Maeda, Y., Yoshino, T., Tanaka, T., & Matsumoto, M. (2014). Seasonal variation of biomass and oil production of the oleaginous diatom *Fistulifera* sp. in outdoor vertical bubble column and raceway-type bioreactors. *Journal of Bioscience and Bioengineering, 117*(6), 720–724. https://doi.org/10.1016/j.jbiosc.2013.12.012

Schmidt, I., Schewe, H., Gassel, S., Jin, C., Buckingham, J., Hümbelin, M., Sandmann, G., & Schrader, J. (2011). Biotechnological production of astaxanthin with Phaffia

rhodozyma/Xanthophyllomyces dendrorhous. Applied microbiology and biotechnology, 89(3), 555–571. https://doi.org/10.1007/s00253-010-2976-6

Scibilia, L., Girolomoni, L., Berteotti, S., Alboresi, A., & Ballottari, M. (2015). Photosynthetic response to nitrogen starvation and high light in *Haematococcus pluvialis*. *Algal Research, 12*, 170–181. https://doi.org/10.1016/j.algal.2015.08.003

Shah, M. M. R., Liang, Y., Cheng, J. J., & Daroch, M. (2016). Astaxanthin-producing green microalga *Haematococcus pluvialis*: From single cell to high value commercial products. *Frontiers in Plant Science, 7*, 531.

Singh, S. P., & Singh, P. (2015). Effect of temperature and light on the growth of algae species: A review. *Renewable and Sustainable Energy Reviews, 50*, 431–444. https://doi.org/10.1016/j.rser.2015.05.024

Spolaore, P., Cassan, C. J., Duran, E., & Isambert, A. (2006). Commercial applications of microalgae. *Journal of Bioscience and Bioengineering, 101*(2), 87–96. https://doi.org/10.1263/jbb.101.87

Sun, H., Liu, B., Lu, X., Cheng, K. W., & Chen, F. (2017). Staged cultivation enhances biomass accumulation in the green growth phase of *Haematococcus pluvialis*. *Bioresource Technology, 233*, 326–331. https://doi.org/10.1016/j.biortech.2017.03.011

Tanaka, T., Kawamori, T., Ohnishi, M., Makita, H., Mori, H., Satoh, K., & Hara, A. (1995). Suppression of azoxymethane-induced rat colon carcinogenesis by dietary administration of naturally occurring xanthophylls astaxanthin and canthaxanthin during the postinitiation phase. *Carcinogenesis, 16*(12), 2957–2963. https://doi.org/10.1093/carcin/16.12.2957

Tanaka, T., Morishita, Y., Suzui, M., Kojima, T., Okumura, A., & Mori, H. (1994). Chemoprevention of mouse urinary bladder carcinogenesis by the naturally occurring carotenoid astaxanthin. *Carcinogenesis, 15*(1), 15–19. https://doi.org/10.1093/carcin/15.1.15

Tjahjono, A. E., Hayama, Y., Kakizono, T., Terada, Y., Nishio, N., & Nagai, S. (1994). Hyper-accumulation of astaxanthin in a green alga *Haematococcus pluvialis* at elevated temperatures. *Biotechnology Letters, 16*(2), 133–138. https://doi.org/10.1007/BF00132241

Turkez, H., Geyikoglu, F., Yousef, M. I., Togar, B., Gürbüz, H., Celik, K., Akbaba, G. B., & Polat, Z. (2014). Hepatoprotective potential of astaxanthin against 2,3,7,8-tetrachlorodibenzo-p-dioxin in cultured rat hepatocytes. *Toxicology and Industrial Health*, *30*(1), 101–112. https://doi.org/10.1177/0748233712459631

Uchiyama, K., Naito, Y., Hasegawa, G., Nakamura, N., Takahashi, J., & Yoshikawa, T. (2002). Astaxanthin protects β-cells against glucose toxicity in diabetic db/db mice. *Redox Reports*, *7*(5), 290–293.

Wan, M., Zhang, J., Hou, D., Fan, J., Li, Y., Huang, J., & Wang, J. (2014). The effect of temperature on cell growth and astaxanthin accumulation of *Haematococcus pluvialis* during a light–dark cyclic cultivation. *Bioresource Technology*, *167*, 276–283. https://doi.org/10.1016/j.biortech.2014.06.044

Wang, J., Chen, Z., & Lu, W. (2012). Hypoglycemic effect of astaxanthin from shrimp waste in alloxan-induced diabetic mice. *Medicinal Chemistry Research*, *21*(11), 2363–2367. https://doi.org/10.1007/s00044-011-9727-4

Wayama, M., Ota, S., Matsuura, H., Nango, N., Hirata, A., & Kawano, S. (2013). Three-dimensional ultrastructural study of oil and astaxanthin accumulation during encystment in the green alga *Haematococcus pluvialis*. *PLoS ONE*, *8*(12), e53618. https://doi.org/10.1371/journal.pone.0053618

Xue, L., Han, D., Li, Y., Chu, F., Miao, M., Zhang, L., & Fan, J. (2017). Astaxanthin attenuates total body irradiation-induced hematopoietic system injury in mice via inhibition of oxidative stress and apoptosis. *Stem Cell Research & Therapy*, *8*. https://doi.org/10.1186/s13287-016-0464-3

Yang, L., Qiao, X., Liu, J., Wu, L., Cao, Y., Xu, J., & Xue, C. (2021). Preparation, characterization and antioxidant activity of astaxanthin esters with different molecular structures. *Journal of the Science of Food and Agriculture*, *101*(6), 2576–2583. https://doi.org/10.1002/jsfa.10887

Yang, Y., Seo, J. M., Nguyen, A., Pham, T. X., Park, H. J., Park, Y., Kim, B., Bruno, R. S., & Lee, J. (2011). Astaxanthin-rich extract from the green alga *Haematococcus pluvialis* lowers plasma lipid concentrations and enhances antioxidant defense in apolipoprotein E knockout mice. *Journal of Nutrition*, *141*(9), 1611–1617. https://doi.org/10.3945/jn.110.136510

Yuan, J.-P., Peng, J., Yin, K., & Wang, J.-H. (2011). Potential health-promoting effects of astaxanthin: A high-value carotenoid mostly from microalgae. *Molecular Nutrition & Food Research*, *55*, 150–165. https://doi.org/10.1002/mnfr.201000361

Zhang, C., Chen, X., & Too, H. P. (2020). Microbial astaxanthin biosynthesis: Recent achievements, challenges, and commercialization outlook. *Applied Microbiology and Biotechnology*, *104*(13), 5725–5737. https://doi.org/10.1007/s00253-020-10648-2

Zhang, W. W., Zhou, X. F., Zhang, Y. L., Cheng, P. F., Ma, R., Cheng, W. L., & Chu, H. Q. (2018). Enhancing astaxanthin accumulation in *Haematococcus pluvialis* by coupled light intensity and nitrogen starvation in column photobioreactors. *Journal of Microbiology and Biotechnology*, *28*(12), 2019–2028. https://doi.org/10.4014/jmb.1807.07008

Zhao, Y., Yue, C., Geng, S., Ning, D., Ma, T., & Yu, X. (2019). Role of media composition in biomass and astaxanthin production of *Haematococcus pluvialis* under two-stage cultivation. *Bioprocess and Biosystems Engineering*, *42*(4), 593–602. https://doi.org/10.1007/s00449-018-02064-8